論文 / 著書情報
Article / Book Information

題目(和文)	水溶液プロセスで作製した高い透明性および導電性を持つ酸化亜鉛膜
Title(English)	Solution-Processed Zinc Oxide Films Having High Transparency and Conductivity
著者(和文)	HongJeongSoo
Author(English)	Jeongsoo Hong
出典(和文)	学位:博士（工学）, 学位授与機関:東京工業大学, 報告番号:甲第9641号, 授与年月日:2014年9月25日, 学位の種別:課程博士, 審査員:松下　伸広,大坂　武男,川路　均,尾笹　一成,脇　慶子
Citation(English)	Degree:Doctor (Engineering), Conferring organization: Tokyo Institute of Technology, Report number:甲第9641号, Conferred date:2014/9/25, Degree Type:Course doctor, Examiner:,,,,
学位種別(和文)	博士論文
Type(English)	Doctoral Thesis

Solution-Processed Zinc Oxide Films Having High Transparency and Conductivity

Thesis Submitted to

Tokyo Institute of Technology

By

JeongSoo Hong

In Partial Fulfillment of the Requirements

For the Degree of

Doctor of Engineering

Supervisor: Prof. Nobuhiro Matsushita

Department of Electronic Chemistry

Tokyo Institute of Technology

Japan

September 2014

Contents

Chapter 1

1.1 Introduction

In recent years, researches for improving the performance and efficiency of optoelectronic devices such as thin film transistors (TFTs), organic light-emitting diodes (OLEDs), solar cells and sensors, have been intensively studied and they are rapidly developed [1-4]. Transparent conductive oxide (TCO) materials have been receiving much scientific attention because of their important role in many devices. TCO materials are used as a transparent electrode in OLED, channel layer in TFT, photoelectrode in solar cell and so on. In the case of transparent electrode, it is a fundamental part and is one of the determinants of efficiency in various devices.

Among the various transparent electrode materials, indium tin oxide (ITO) is the most widely used material due to their unique conductivity and transparency. However, indium is

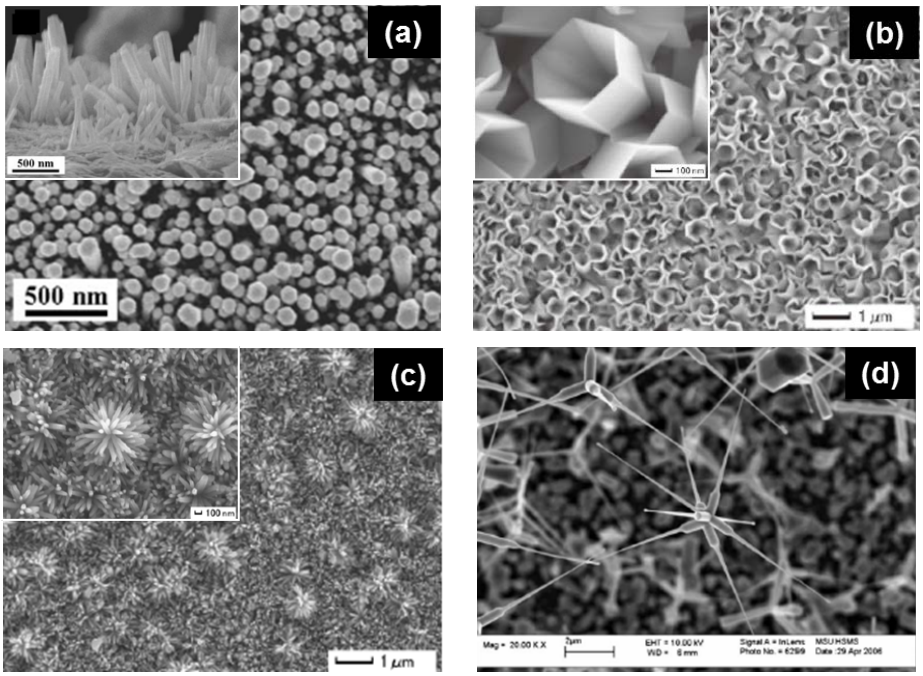

Figure 1-1 SEM images of (a) ZnO nanorod, (b) ZnO nanotube, (c) ZnO nanoflower and (d) ZnO tetrapods.

scarce resource and it lead to increase of raw material cost. Also, other demerits of ITO are unstable in hydrogen plasma, high resistivity in flexible device and absorption of ultraviolet rays.

For these reason, zinc oxide (ZnO), has gained much interest as an alternative material to ITO. It is one of the semiconductor materials having large exciton binding energy (~ 60 meV) with wide gap energy, and these basic properties can lead to blue and ultra-violet optical devices [5]. Additionally, ZnO can be fabricated with various structures such as rods, tubes, flowers and tetrapods, as shown in Figure 1-1, it means that ZnO film can be applied to various application fields [6-8].

1.2 Zinc Oxide (ZnO)

1.2.1 Properties of ZnO

Zinc oxide (ZnO) is an inorganic compound and is widely used for various applications. It is a wide band gap semiconductor of group Ⅱ-Ⅵ, and general properties are listed in Table 1.

Table 1 General properties of ZnO.

Properties	
Molecular formula	ZnO
Molar mass	81.408 g/mol
Density	5.606 g/cm^3
Melting point	1975 °C
Boiling point	1975 °C
Refractive index (n_D)	2.0041
Thermal conductivity	0.46~1.67 W/cm·K
Intrinsic carrier concentration	< 10^6 cm^{-3} (n-type doping > 10^{20}cm^{-3})
Mobility at 300 K for n-type conductivity	200 cm^2/V.s

• Crystal Structure

ZnO is divided to three phase such as cubic rocksalt (B1), zinc blende (B3), and hexagonal wurtzite (B4) structure, as shown in Figure 1-2 [9]. Under ambient conditions, ZnO generally crystalize to hexagonal structure, because other structures requires certain conditions such as cubic substrates (Figure 2-a) and high pressure (Figure 2-b) for formation.

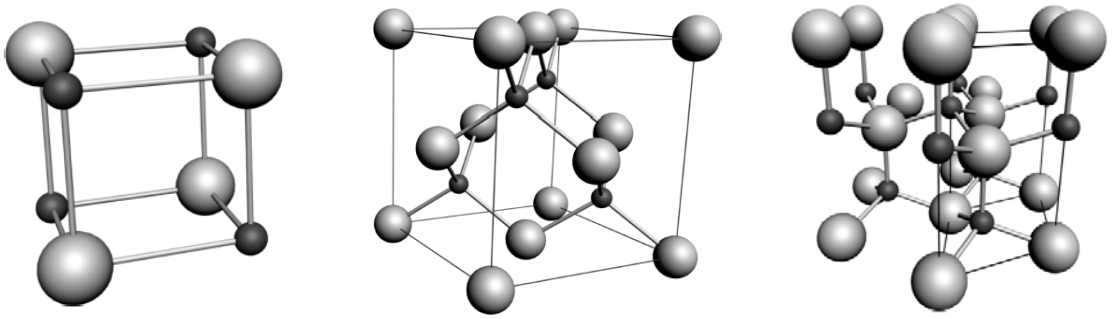

a. Rocksalt (B1) b. Zinc blende (B3) c. hexagonal wurtzite (B4)

Figure 1-2 ZnO crystal structures; O atoms are shown as large grey spheres, Zn atoms as smaller black spheres. [9]

In case of wurtzite hexagonal structure (Figure 1-3), it forms hexagonal unit with two lattice parameters *a* (0.32495 nm) and *c* (0.52069 nm) belong to the space group C^4_{6v} in the Schoenflies notation and p63mc in the Hermann-Mauguin notation. The ratio of *c*/*a* is 1.633 in an ideal wurtzite structure [9-10].

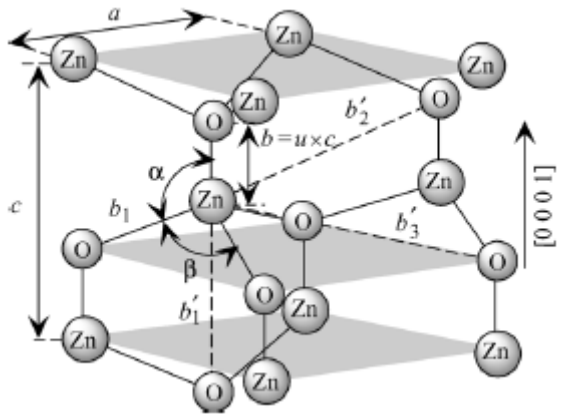

Figure 1-3 Illustration of wurtzite ZnO structure. [9]

The four most common face terminations of wurtzite ZnO are the polar Zn terminated (0001) and O terminated (000-1) faces (*c*-axis oriented), and the non-polar (11-20) (*a*-axis) and (10-10) faces which both contain an equal number of Zn and O atoms [5, 9]. The polar faces are known to posses different chemical and physical properties, and the O-terminated face possess a slightly different electronic structure to the other three faces [5,11]. Additionally, the polar surfaces and the (1010) surface are found to be stable. However the (11-20) face is less stable and generally has a higher level of surface roughness than its counterparts [5, 11].

• Conductivity

The conductivity of ZnO is difficult to define because it is variable under preparation conditions. Generally, ZnO has n-type properties with carrier concentration of ~ 10^{16} cm^{-3}. However, carrier concentration can be more improved by metal ion doping. The n-type doping is easily achieved by substituting Zn with group-III elements such as Al, Ga and In, as a result, carrier concentration is increased to ~10^{20} cm^{-3} [12-15]. In case of electron mobility, it is strongly affected by temperature. Mobility is 200 $cm^2 V^{-1}S^{-1}$ at 300 K (n-type conductivity), though it is increased to ~ 2000 $cm^2 V^{-1}S^{-1}$ at 80 K [16-18].

1.2.2 Various Applications

ZnO has various properties such as conductivity, optical properties, piezoelectric properties and so on. And their various structures are also one of the special features. Because of these properties, it can be apply to various filed such as electronic device including display, sensor, spin resonant tunneling diode (spin RTD), and generator [19-26].

• Transparent Electrode

Transparent electrode is widely used in optoelectronic devices. As a transparent electrode, indium tin oxide (ITO) is the most representative oxide material due to their unique electrical

and optical properties. However, since Indium is a scarce resource, price rise and limited resource is becoming serious problem. Because of these reasons, ZnO is receiving attention as an alternative material to ITO. Conductivity of ZnO is lower than ITO. However, it can be improved by metal ion doping such as Al and Ga [14-15]. Metal ion doped ZnO films can used as a transparent electrode in various electronic fields.

• Photoelectrode

ZnO films deposited by solution process have various structures such as rod array, flower-like, Sphere-like, needle-like, and whisker structure [27-31]. These films are can be used as a photoelectrode in dye-sensitized solar cells (DSSC) [32]. In DSSC application, large specific surface is important to absorb the dye. Nano-structured ZnO film has large specific surface area and it can be improved the efficiency of DSSC.

1.3 Deposition Method of ZnO Film

As shown in Figure 1-4, there are two general types of deposition method for fabricating ZnO film.

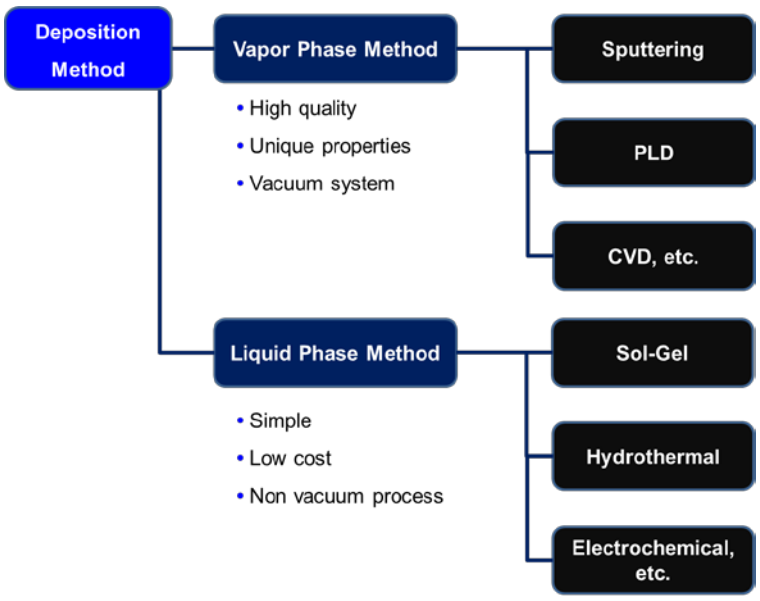

Figure 1-4 Various deposition methods for preparing ZnO film.

1.3.1 Vapor Phase Method

There are several kinds of vapor phase method such as sputtering, ion plating, pulsed laser deposition (PLD), chemical vapor deposition (CVD), and so on [33-38].

Among them, the most widely used method is sputtering because it can fabricate the high quality ZnO film with high crystallinity and dense structure. Types of sputtering are divided by their power source and structure such as DC magnetron sputtering, radio frequency (RF) sputtering, and facing targets sputtering (FTS) system [39-41]. During the deposition process, sputtering use the various process parameter such as working pressure, substrate temperature, input power, reactive gas, substrate, and the kind of target [42-46]. Because of these parameters, sputtering can fabricate ZnO film having diverse characteristic, in contrast, it also means sputtered film is very sensitive to sputtering conditions. Notwithstanding that, sputtering is still representative one for deposition because ZnO film deposited by sputtering has high conductivity and transmittance.

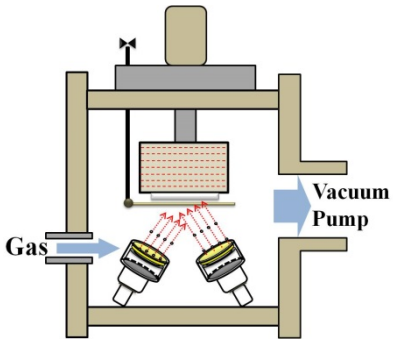

Figure 1-5 Schematic illustration of RF-sputtering. [27]

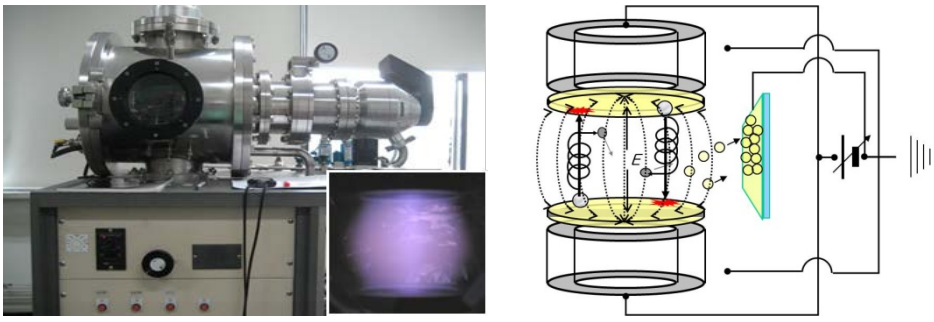

Figure 1-6 Facing targets sputtering (FTS) system. [27]

In case of PLD method, it uses the high-power pulsed laser beam for ZnO film deposition. Process parameter of PLD method is relatively more simple than sputtering. It uses few parameters such as laser energy density and pulse repetition rate, and they are controlled during deposition process. Also, fine control of thickness can be achieved by pulse. Additionally, the target with stoichiometric composition can be used due to extremely high heating rate of target surface by pulsed laser irradiation.

CVD including low-pressure CVD (LPCVD) and plasma-enhanced CVD (PECVD) is material synthesis method, and it can deposit the ZnO film through chemical reaction and surface absorption [48-49]. Various types of chemical reactions are utilized in CVD for the formations of solids are pyrolysis, reduction, oxidation, and hydrolysis. ZnO film deposited by CVD forms various structure such as monocrystalline, polycrystalline, and amorphous. Also, CVD can deposit the films with uniform thickness distribution over large area.

1.3.2 Liquid Phase Method

High quality ZnO films with unique properties can be obtained by vapor phase method. However, these processes have some demerits such as high cost of the equipment and heavy energy consumption due to vacuum system. For these reasons, liquid phase methods including sol-gel method, electrodeposition, hydrothermal synthesis, and chemical bath deposition (CBD) method have been receiving attention for ZnO film deposition [50-57].

Among the liquid phase methods, sol-gel method is one of the most widely used ones due to their simplicity. ZnO films deposited by sol-gel method have variety of shapes, such as porous structures, thin fibers, dense powders and thin films [58-61]. First, precursor is prepared by alkoxides or solution containing metal ions, after that, it is coated several times by immersion or spin-coating for obtaining required thickness. Here, annealing process is necessary for crystallization and removing organic substance in the film. Generally, the range of annealing temperature is 200-800^{o}C [62-63].

Electrodeposition (Electrochemical deposition or electro crystallization) is useful method for fabricating film on conductive substrate. Electrodeposition is consisting of electrolyte, anode, cathode and source of electricity. During deposition process, metal ions are deposited on substrate by passing direct current. Deposition of ZnO films is controlled by the electrical parameters such as, electrode potential and current density. It has various advantages such as possibility for deposition structurally and compositionally modulated alloys and compounds, room temperature process, non-toxic, and simple operation [64].

In the hydrothermal process, it is also one of the methods for preparing metal oxide films. For fabricating films, hydrothermal method requires the heat and pressure. It has several merits such as various forms, low cost for instrumentation, and low energy consumption. On the other hand, hydrothermal method takes a long manufacturing lead time to fabricate the film.

Chemical bath deposition (CBD) is also well known solution process due to their simplicity, and low temperature [56]. This method was used for deposition of semiconductor thin film such as ZnS, ZnSe, and ZnO [65-71].

These various solution-based deposition methods have several advantages. In contrast, they have also some demerits such as high temperature process. Additionally, their conductivity and crystallinity are still lower than those of films deposited by vapor phase method. Therefore, researches for developing novel solution process is highly required and in this study, I investigated novel processed which enable to fabricate ZnO film having excellent transparency and conductivity.

1.4 Spin-Spray Method

Spin-Spray method is one for the aqueous solution process and it has been used for fabricating ferrite film such as magnetite (Fe_3O_4), and hematite (Fe_2O_3) films [72-74]. And their construction is very simple, as shown in Figure 1-7,

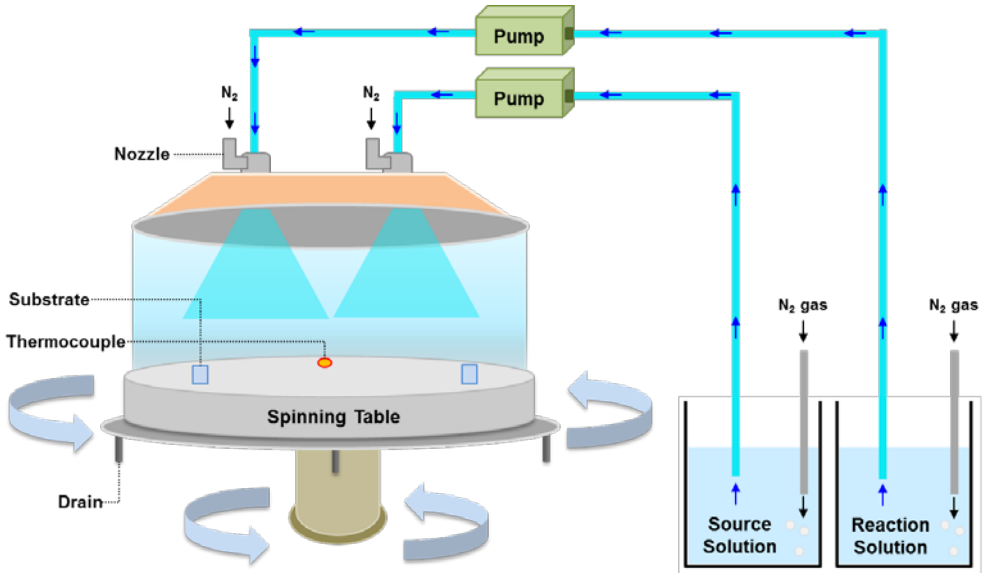

Figure 1-7 Schematic illustration of Spin-spray method.

Elementary chemical reaction of spin-spray method during the deposition process is similar to chemical bath deposition (CBD) because CBD uses the materials in liquid phase for deposition of film. However, Spin-spray method is environmentally friendly and advantageous compared with other solution processes owing to its relatively low initial investment for the apparatus, relatively high deposition rate (>100 nm/min), and low substrate temperature (< 100 ^{o}C). Additionally, general solution-based deposition process requires the seed layer (or a Si substrate) to improve the adhesion between the deposited film and the substrate [75-76]. Furthermore, high temperature substrate and annealing process is necessary for crystallization of film. In contrast, spin-spray method enables to deposit highly crystallized film having high adhesion without using seed layer and high substrate temperature and/or additional annealing process.

Fabrication process of spin-spray method is very simple. Source solution containing metal ions and reaction solution containing pH adjuster and /or surface modifier are sprayed simultaneously on rotating heated substrates. The spin-spray method involves a continuous supply of fresh solutions by spraying and an elimination of unnecessary by-products by centrifugal force, as shown in Figure 1-8.

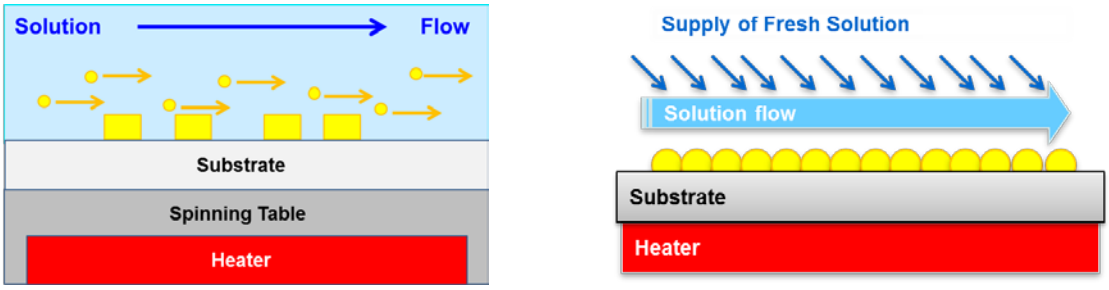

Figure 1-8 Schematic illustrations for chemical reaction on rotating substrate.

Fundamentally, the chemical reaction mechanism is based on the adsorption of metal ions from an aqueous solution and they are crystallized on substrate surface [77]. Hydroxyl groups in reaction solution acts as an adsorption sites and oxidizing reagents is introduced into the source solution. And then, metal ions and/or metal hydroxide species are crystallized and formed metal oxide film under suitable pH conditions and substrate temperature. During the fabrication process of ZnO film, fresh source and reaction solution is continually supplied, it means excessive hydroxyl group exist on initial oxide layer. And adsorption, hydrolysis, and crystallization are repeated and it is reason for increase oh thickness [77].

1.5 Basic Experimental Procedure

All ZnO films used in this study were deposited by spin-spray method. Before deposition, all substrates were ultrasonically cleaned in deionized water and ethanol each to remove impurities on the surface, and all substrates were exposed to discharge plasma for 10 min

(in case of PES substrate exposed to discharge plasma for 3 min) to increase hydrophilicity on their surface, and their basal conditions are summarized as below,

Table 2 Basal conditions used to prepare the samples.

Substrate	Soda lime glass (40 x 30 x 0.17 mm^3) Polyether-sulfone (PES; 40 x 30 x 0.3 mm^3)
Substrate rotation	120 rpm
Substrate Temp.	85 ~ 95^oC
Velocity of sprayed-solution	3.0 L/h
Gas for spray and solution	Nitrogen
Used solution	Millipore deionized water

ZnO films were deposited by spin-spray method with following process,

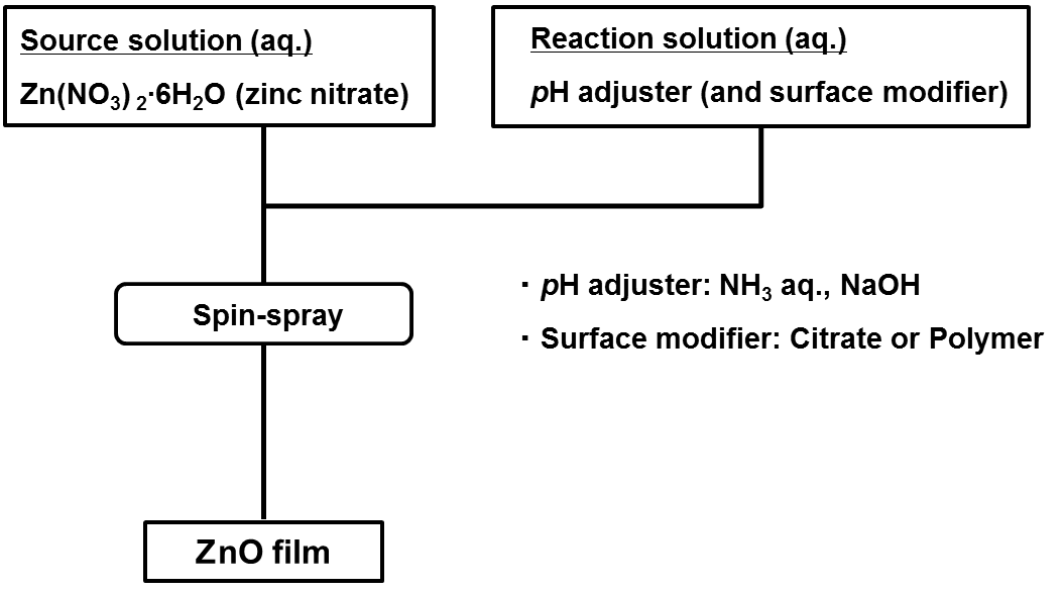

Figure 1-9 Experimental flow chart of ZnO film.

For preparing source solution, $Zn(NO_3)_2 \cdot 6H_2O$ (zinc nitrate hexahydrate, Wako Pure Chemical Industries, 99.0%) was used as a source materials. In case of reaction solution, two kinds of pH adjuster such as aqueous NH_3 solution (ammonia solution, Wako Pure Chemical Industries, 28.0%) or NaOH (sodium hydroxide, Wako Pure Chemical Industries, Ltd., Japan, 99.0%) were used. As a surface modifier, $C_6H_5Na_3O_7$ (trisodium citrate, Wako Pure Chemical Industries, 97.0%) was added in reaction solution.

1.6 Characterization

Solution *p*H with *p*H adjuster was measured by SevenMulti *p*H meter (METTLER TOLEDO, Switzerland). The surface morphology of ZnO films was observed by scanning electron microscopy (SEM; Hitachi S4000), and the film thickness was estimated using cross-sectional SEM images. Crystallographic properties were analyzed by Raman spectroscopy (Ramanor T64000) and X-ray diffraction (XRD; Rigaku Rint2000) with CuKα radiation (λ=1.5418Å). Existence of organic substance in the as-deposited ZnO films were confirmed by Fourier transformed infrared (FT-IR) measurements (JEOL JIR-7000). The electrical and optical properties were measured using a Hall Effect measurement system (ECOPIA HMS-3000) and a Lambda 35 spectrometer (Perkin Elmer Japan), respectively.

1.7 Objective of This Study

In this thesis, there are a several objectives listed as below,

• To fabricate ZnO films with various forms by change of chemical conditions including *p*H adjuster and/or surface modifier

• To obtain the high conductivity of ZnO film via UV irradiation and hydrogen treatment for using transparent electrode

• To fabricate ZnO films on plastic substrate by using solution process for applying to flexible devices

• To propose future study

This thesis is composed of 8 Chapters.

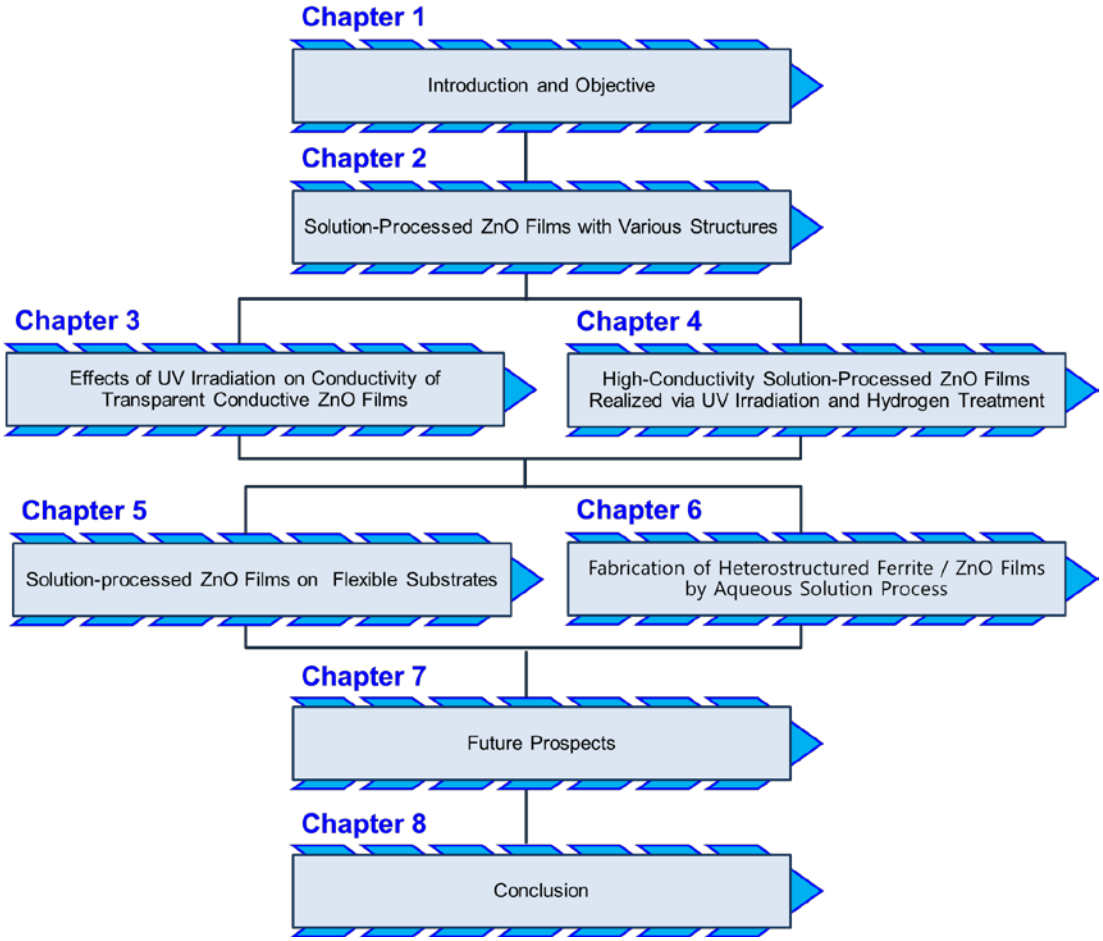

Figure 1-10 Flow chart of thesis

Reference

1. E. Fortunato, P. Barquinha, and R. Martins, Adv. Mater. 24 (2012) 2945.
2. J. S. Hong, K. W. Jang, Y. S. Park, H. W. Choi, and K. H. Kim, Mol. Cryst. Liq. Cryst., 538 (2011) 103.
3. J. Huang, Z. Yin, and Q. Zheng, Energy Environ. Sci. 4 (2011) 3861.
4. S. K. Gupta, A. Joshi, and M. Kaur, J. Chem. Sci. 1 (2010) 57.
5. V. A. Coleman and C. Jagadish, Zinc Oxide Bulk, Thin Films and Nanostructures, 2006 Elsevier Limited.
6. Boris I. Kharisov, Recent Partents on Nanotechnology, 2 (2008) 190.
7. D. Chu, Y. Masuda, T. Ohji and K. Kato, J. Am. Ceram. Soc. 93 (2010)887.
8. Y. Fang, X. Wen, S. Yang, Q. Pang, L. Ding, J. Wang, and W. Ge, J. Sol-Gel Tech. 36 (2005) 227.
9. H. Morkoc, and U. Ozgur, Zinc oxide; Fundamental, Materials and Device Technology, 2009, WILEY-VCH verlag GmbH & Co.KGaA.
10. U. Rossler, (1999). Landolt-Bornstein, New Series, Group III. Vol. 17B, 22, 41B. Springer, Heidelberg.
11. O. Dulub, L. A. Boatner, and U. Diebold, Surf. Sci. 519 (2002) 201.
12. H. Kato, M. Sano, K. Miyamoto, T. Yao, J. Cryst. Growth 538 (2002) 237.
13. T. Minami, T. Miyata, Y. Ohtani, and Y. Mochizuki, Jpn. J. Appl. Phys. 45 (2006) L409
14. J. S. Hong, S. M. Kim, S. J. Park, H. W. Choi, and K. H. Kim, Mol. Cryst. Liq. Cryst. 520 (2010) 19.
15. J. S. Hong, K. W. Jang, Y. S. Park, H. W. Choi, K. H. Kim, Mol. Cryst. Liq. Cryst. 538 (2011) 103.
16. S. J. Pearton, D. P. Norton, K. Ip, Y. W. Heo, T. Steiner, Prog. Mater. Sci. 50 (2005) 293.
17. P. Wagner, R. Helbig, J. Phys. Chem. Solids 35 (1974) 327.

18. Y. R. Ryu, T. S. Lee, H. W. White, Appl. Phys. Lett. 83 (2003) 87.
19. A. Bakin, Proceeding of the IEEE 98 (2010) 1281.
20. B. Y. Oh, M. C. Jeong, T. H. Moon, W. Lee, J. M. Moon, J. Y. Hwang, and D. S. Seo, J. Appl. Phys. 99 (2006) 124505.
21. Y. Qin, X. Wang, and Z. L. Wang, Nature 451 (2008) 809.
22. Z. L. Wang, and J. Song, Science 312 (2006) 242.
23. S. K. Gupta, A. Joshi, and M. Kaur, J. Chem. Sci. 122 (2010) 57.
24. A. Wei, L.Pan, and W. Huang, Mater. Sci. Eng. B 176 (2011) 1409.
25. S. J. PEARTON, D. P. NORTON, Y. W. HEO, L. C. TIEN, M. P. IVILL, Y. LI, B. S. KANG, F. REN, J. KELLY, and A. F. HEBARD, J. Electro. Mater. 35 (2006) 862.
26. C. Ronning, P. X. Gao, Y. Ding, and Z. L. Wang, Appl. Phys. Lett. 84 (2004) 783
27. H. Wagata, N. Ohashi, T. Taniguchi, A. K. Subramani, K. Katsumata, K. Okada, and N. Matsushita, Cryst. Growth Des. 10 (2010) 3502.
28. D. Chu, Y. Masuda, T. Ohji, and K. Kato, J. Am. Ceram. Soc. 93 (2010) 887.
29. A. Umar, and Y. B, Hahn, Nanotechnology 17 (2006) 2174
30. Z. Zhou, W. Peng, S. Ke, and H. Deng, J. Mater. Processing. Tech. 89 (1999) 415
31. Y. Zhang, L. Wang, X. Liu, Y. Yan, C. Chen, and J. Zhu, J. Phys. Chem. B 109 (2005) 13091
32. Q. Zhang, C. S. Dandeneau, X. Zhou, and G. Cao, Adv. Mater. 21 (2009) 4087.
33. W. Gao, and Z. Li, Ceram. Int. 30 (2004) 1155
34. A. M. Rosa, E. P. da Silva, E. Amorim, M. Chaves, A. C. Catto, P. N. Lisboa-Filho, and J. R. R. Bortoleto, J. Phys.: Conf. Ser. 370 (2012) 012020
35. V. Craciun, J. Elders, J. G. E. Gardeniers, and Ian W. Boyd, Appl. Phys. Lett. 65 (1994) 2963
36. J. Zhao, L. Hu, Z. Wang, Z. Wang, H. Zhang, Y. Zhao, and X. Liang, J. Cryst. Growth 280 (2005) 455

37. A. Cheng, Y. Tzeng, Y. Zhou, M. Park, T. Wu, C. Shannon, D. Wang, and W. Lee, Appl. Phys. Lett. 92 (2008) 092113
38. T. M. Barnes, J. Leaf, C. Fry, and C. A. Wolden, J. Cryst. Growth 274 (2005) 412
39. M. Hezam, N. Tabet, and A. Mekki, Thin Solid Films 518 (2010) e161
40. J. B. Lee, H. J. Kim, S. G. Kim, C. S. Hwang, S. H. Hong, Y. H. Shin, and N. H. Lee, Thin Solid Films, 435 (2003) 179
41. J. S. Hong, N. Matsushita, and K. H. Kim, Semicond. Sci. Technol. 29 (2014) 075007
42. Z. Li, and W. Gao, Mater. Lett. 58 (2004) 1363
43. H. Yu, J. Wang, Y. Yan, X. Wang, B. Gao, H. Liu, and Y. Du, Electro. Mech. Eng. Info. Tech. 5 (2011) 2486
44. J. H. Lee, J. Electroceram. 23 (2009) 512
45. S. Eisermann, J. Sann, A. Polity, and B.K. Meyer, Thin Solid Films 517 (2009) 5805
46. A. J. Hashim, A. J. Ghazai, M. S. Jaafar, N. Mansor, and Z. Zain, Int. J. Electrochem. Sci. 7 (2012) 11876
47. J. S. Hong, Y. S. Park, and K. H. Kim, J. Semicon. Dis. Tech. 9 (2010) 23
48. M.D. Barankin, E. Gonzalez II, A.M. Ladwig, and R.F. Hicks, Sol. Ener. Mater. Sol. Cells 91 (2007) 924
49. S. Fay, J. Steinhauser, S. Nicolay, and C. Ballit, Thin Solid Films 518 (2010) 2961
50. L. Znaidi, Mater. Sci. Eng. B 174 (2010) 18
51. S. Ilican, Y. Caglar, and M. Caglar, J. Optoelectro. Adv. Mater. 10 (2008) 2578
52. K. Sun, W. Wei, Y. Ding, Y. Jing, Z. L. Wang, and D. Wang, Chem. Commun. 47 (2011) 7776
53. T. Sahoo, J. W. Jeon, V. Kannan, C. R. Lee, Y. T. Yu, Y. W. Song, and I. H. Lee, Thin Solid Films 516 (2008) 8244

54. J. S. Wellings, N. B. Chaure, S. N. Heavens, and I. M. Dharmadasa, Thin Solid Films 516 (2008) 3893
55. T. Mahalingama, V. S. Johna, M. Rajaa, Y. K. Sub, and P. J. Sebastianc, Sol. Ener. Mater. Sol. Cells 88(2005) 227
56. H. Khallaf, G. Chai, O. Lupan, H. Heinrich, S. H. Park, A. Schulte, and L. Chow, J. Phys. D: Appl. Phys. 42 (2009) 135304
57. X. D. Gao, X. M. Li, and W. D. Yu, Mater. Resear. Bulletin 40 (2005) 1104
58. V. Musat, B. Teixeira, E. Fortunato, R.C.C. Monteiro, and P. Vilarinho, Surf. Coat. Tech. 180-181 (2004) 659
59. J. Li, S. Srinivasan, G. N. He, J. Y. Kang, S. T. Wu, and F.A. Ponce, J. Cryst. Growth 310 (2008) 599
60. J. Lee, A. J. Easteal, U. Pal, and D. Bhattacharyya, Current. Appl. Phys. 9 (2009) 792
61. M. Farhadi-Khouzani, Z. Fereshteh, M. R. Loghman-Estarki, and R. S. Razavi, J. Sol-Gel Sci. Tech. 64 (2012) 193
62. Technology of Transparent Conducting Thin Films, Ohrmsha, Ltd. 2007
63. M. Ohyama, H. Kozuka, and T. Yoko, Thin Solid Films, 306 (1997) 78
64. K. L. Chopra, 'Thin Film Phenomena', McGraw Hill, New York (1969)
65. A. Pudov, J. Sites, and T. Nakada, Jpn. J. Appl. Phys. 41 (2002) L672
66. J. Cheng, D. Fan, H. Wang, B. Liu, Y. Zhang, and H. Yan, Semicond. Sci. Technol. 18 (2003) 676
67. A. Chaparro, C. Maffiotte, M. Gutierrez, J. Herrero, J. Klaer, K. Siemer, and D. Braunig, Thin Solid Films 387 (2001) 104
68. C. Lokhande, P. Patil, A. Ennaoui, and H. Tributsch, Appl. Surf. Sci. 123 (1998) 294
69. T. Saeed, and P. OBrien, Thin Solid Films 271 (1995) 35
70. P. OBrien, T. Saeed, and J. Knowles, J. Mater. Chem. 6 (1996) 1135

71. M. Ortega-Lopez, A. Avila-Garcıa, M. Albor-Aguilera, and V. Resendiz, Mater. Res. Bull. 38 (2003) 1241
72. M. Abe, and Y. Tamaura, J. Appl. Phys., 5 (1984) 2614
73. T. Itoh, M. Abe, and Y. Tamaura, Jpn. J. Appl. Phys. Part I Regular Paper Short Notes & Review Papers, 27 (1988) 839
74. E. E. Carpenter, V. Cestone, G. Landry, V. G. Harris, and K. M. Kemner, Chem. Mater. 15 (2003) 1235
75. Y. Fang, X. Wen, and S. Yang: J. Sol-Gel. Sci. Technol. 36 (2005) 227.
76. H. I. Abdulgafour, Z. Hassan, N. Al-Hardan, and F. K. Yam: Physica B 405 (2010) 2570.
77. H. Wagata, Thesis: Solution-Processed Zinc Oxide Films and Their Photo-Induced Functional Properties, Tokyo Institute of Technology

Chapter 2

Solution-Processed ZnO Films with Various Structures

In this chapter, ZnO films having various forms such as rod array, flower like, and dense structure were obtained by change of chemical conditions such as *p*H adjuster or surface modifier in spin-spray method, and their crystallographic properties and formation mechanism were investigated.

2.1 Introduction

Zinc Oxide is functional material owing to their diverse characteristic such as conductivity, piezoelectric, and optical properties [1-3]. Above all, one of the attractive properties of ZnO is their variety of forms. ZnO film deposited by solution process is strongly affected by chemical conditions such as chemical substance, *p*H conditions and temperature, it lead to enable to fabricate the ZnO film having various forms [4-10].

Low-dimensional structure ZnO film has been receiving much attention because their shape and dimensionality strongly affects to the performance of various devices. Especially, low-dimensional structure ZnO films are expected to apply to sensor and dye-sensitized solar cell (DSSC). In case of DSSC, vertically aligned low-dimensional structure ZnO film is expected to use as a photo-electrode because porous structure with wide specific area is advantageous for the absorption of dye molecule and photon. Therefore, surface morphology is important factor for improving efficiency.

There are various kinds of low-dimensional ZnO structure such as wires, needles, bridges, tubes, disks and belts [11-16]. These ZnO structures have been intensively studied with

several solution-based processes such as spray pyrolysis, hydrothermal method and sol-gel method. These methods are much simpler than dry process however they require seed layer for good adhesion, high substrate temperature and/or post annealing process for crystallization. On the other hand, spin-spray method used in this study is also one of the solution processes and it enables to obtain ZnO film having low-dimensional structure by change of chemical substance without seed layer. In our previous study, rod array and continuously structured ZnO films deposited by spin-spray method were reported [17-18]. ZnO film deposited by using NH_3 solution as a *p*H adjuster has rod array structure with preferred orientation along the c-axis. And changed surface morphology by absorbing citrate ions to film was also confirmed. Rod structured ZnO film was changed to that haddense structure.

Additionally, solution *p*H is also one of the factors for changing films structure because growth mechanism is influenced by solution *p*H. The *p*H at the region of film growth is one of the most important conditions because it is the determinative factor that influences the formation mechanism and resultant structure of the ZnO film [19]. The degree of supersaturation, which is related to the driving force of nucleation and crystal growth, can be also controlled by the *p*H at the film growth region.

In this chapter, rod array, dense, and flower-like ZnO films were simply obtained by changing of solution conditions such as *p*H adjuster and surface modifier. And then, changed surface morphology and crystallographic properties were investigated.

2.2 Experimental Procedure

2.2.1 Deposition Process of ZnO Films Having Various Structures

The soda-lime glass substrate was ultrasonically cleaned in de-ionized water and ethanol for 10 min each to remove impurities on the surface, followed by glow discharge plasma treatment in air for 10 min to enhance the hydrophilicity of the substrate.

For the deposition, two kinds of solutions were used. The source solution was prepared by dissolving 10 mM of $Zn(NO_3)_2 \cdot 6H_2O$ (zinc nitrate hexahydrate, Wako Pure Chemical Industries, Ltd., Japan, 99.0%) in 1.0 L of de-ionized water. Reaction solution was prepared by using NaOH (sodium hydroxide, Wako Pure Chemical Industries, Ltd., Japan, 99.0%) or NH_3 solution (Ammonia solution, Wako Pure Chemical Industries, Ltd., Japan, 28.0%) in 1.0 L of de-ionized water, as a pH adjuster. And $C_6H_5Na_3O_7$ (trisodium citrate, Wako Pure Chemical Industries, Ltd., Japan, 97.0 %) was added in reaction solution as a surface modifier. ZnO films were deposited by spraying these solutions onto glass substrates fixed on a heated rotating disk (temperature = 95^oC).

2.2.2 Characterization

Variations of solution pH with *p*H adjuster were measured by SevenMulti pH meter (METTLER TOLEDO, Switzerland). The crystallographic properties were evaluated by using X-ray diffraction (XRD, Rint2000, Rigaku Corp., Japan) in the scanning angle (2θ) from 20 to 80°. The surface morphology of as-deposited ZnO films was confirmed by scanning electron microscopy (SEM, S4000, Hitachi, Ltd., Japan). Optical properties were evaluated by Lambda 35 spectrometer (Perkin Elmer Japan Co., Ltd.).

2.3 Results and Discussion

2.3.1 Rod Array and Continuous Structure ZnO Films

ZnO films were deposited using ammonia solution as a *p*H adjuster and trisodium citrate as a surface modifier. As a result, I observed two different types of film structure in the SEM images, as shown in Figure 2-1. The films deposited without adding citrate ions in the

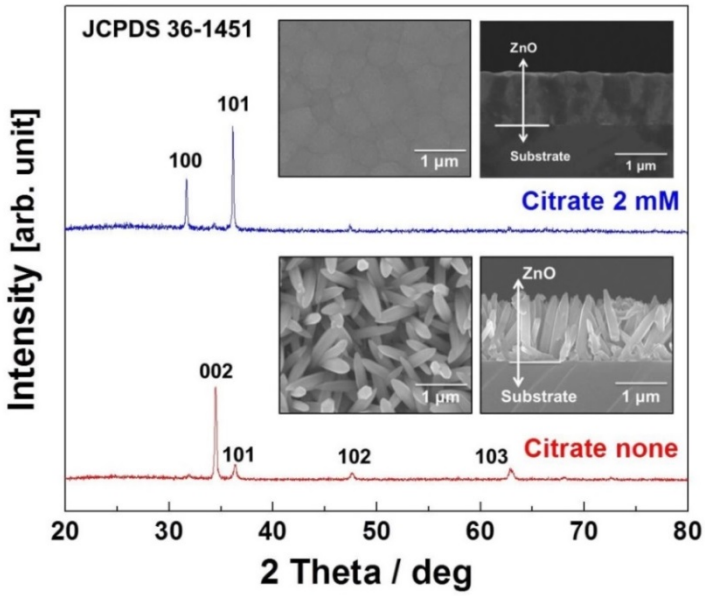

Figure 2-1 XRD and SEM images of ZnO film.

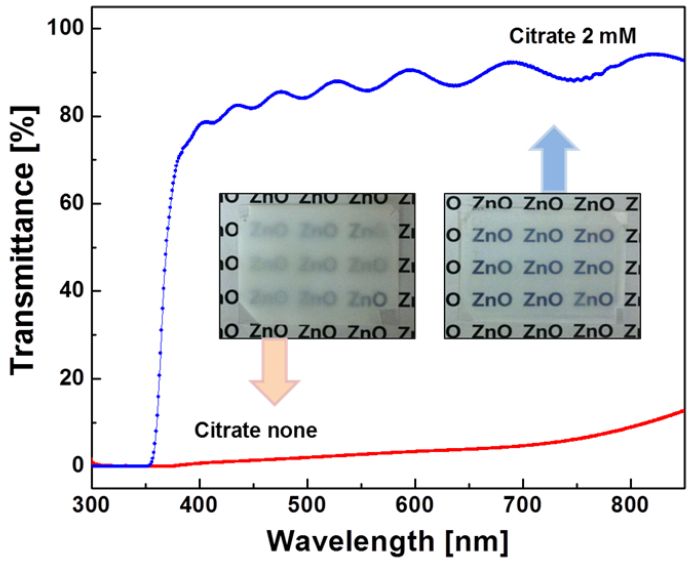

Figure 2-2 Transmittance of as-deposited ZnO films. (Inset is as-prepared samples)

solution had a rod array structure oriented perpendicular to the substrate surface. On the other hand, the ZnO films deposited using citrate in the solution had a smooth surface and a continuous structure. As shown in XRD patterns, the rod-structured ZnO film indicates the preferred orientation along the c-axis. However, citrate ions were absorbed on the (001) plane to suppress the growth along the c-axis, forming a ZnO film with a continuous structure [18].These structural changes also affect to their optical properties, as shown in Figure 2-2.

As-deposited ZnO films indicated clearly different result. ZnO film having rod array structure indicated low transmittance, in contrast, the as-deposited ZnO film having dense structure showed transmittance higher than 80% in visible region. It is thought that the light scattering of ZnO film surface was suppressed by dense and continuous film surface.

2.3.2 Change of structure by solution pH

The *p*H of the reaction solution was controlled by changing the amount of ammonia solution. Figure 2-3 indicates the variation of *p*H in reaction solutions containing various concentrations of ammonia solution. The *p*H in the source solution was approximately 7.0

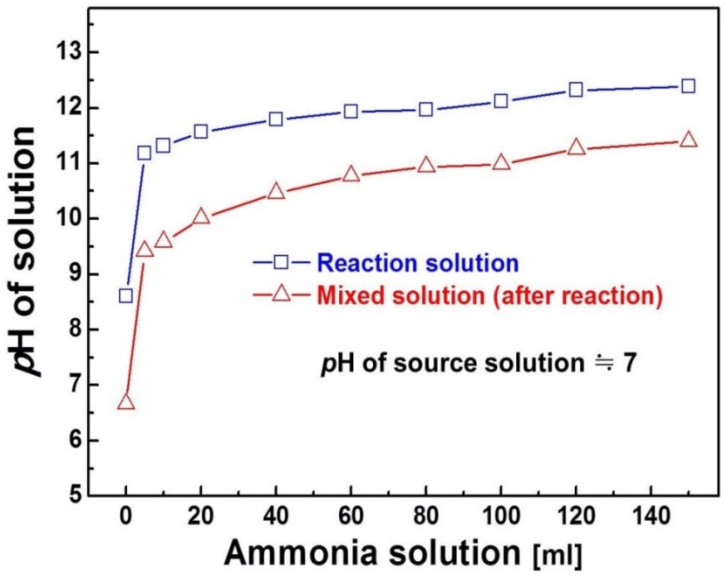

Figure 2-3 Variation of solution pH by adding an ammonia solution.

and that in the reaction solution was increased from 8.6 to 12.3 with an increase of the ammonia concentration at room temperature. The *p*H of the mixed solution increased from 6.7 to 11.3 with the increase of the reaction solution *p*H. The actual *p*H on the film growth surface was difficult to measure; therefore the *p*H of the mixed solution at room temperature was used as the major parameter to discuss the change in the structural, optical, and electrical properties of the resultant films.

Fundamentally, ZnO formation in the solution is supposed to progress according to the following reactions [17, 19]

$$NH_3 + H_2O \rightarrow NH_4+ + OH^-$$

$$Zn^{2+} + NH_4^+ \rightarrow Zn\ (NH_3)_4^{\ 2}$$

$$Zn\ (NH_3)_4^{2+} + 2OH^- \rightarrow ZnO + 4NH_3 + H_2O$$

Here, ammonia ions play an important role for ZnO crystal formation. Ammonia molecules coordinate with zinc ions to form zinc amine complexes such as $Zn(NH_3)_n^{2+}$. These zinc amine complexes react with OH^- and form ZnO crystals. Thus ZnO cannot be crystallized without the presence of ammonia during the film growth process.

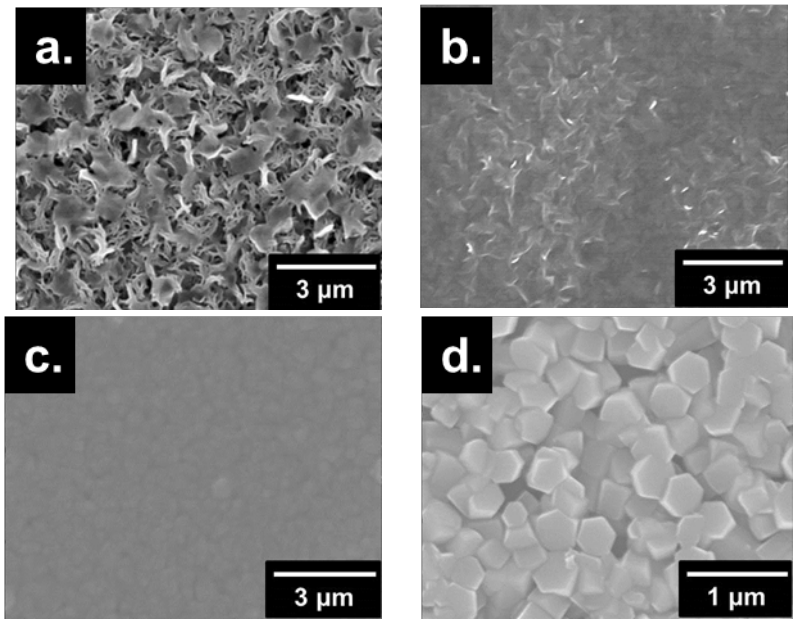

Figure 2-4 SEM images of as-deposited ZnO films at different *p*H conditions (mixed solution) ; a. *p*H9.4, b. *p*H10.0, c. *p*H10.7, d. *p*H11.3.

Figure 2-4 shows SEM images of ZnO films deposited under various *p*H conditions prior to UV treatment. No film was formed at a mixed solution *p*H of 6.7 (without ammonia solution). This result supports that ammonia ions are necessary to form the ZnO film (Eqs. 1-3). The ZnO morphology was gradually changed with an increase of the mixed solution *p*H, and a two-dimensional continuous ZnO film with a smooth surface was obtained at a mixed solution *p*H of 10.7. In case of a mixed solution *p*H of 11.3, the as-deposited ZnO film surface was discontinuous and rough surface with 300~400 nm hexagonal shaped grain. ZnO film deposited by the spin-spray method generally has a rod array structure that can be tuned to form a transparent continuous film by the addition of citrate ions to the solution [17]. However, despite the addition of citrate ions, the ZnO film deposited at a mixed solution *p*H of 11.3 had a rough surface.

To confirm the change in the surface morphology, the crystallographic properties of the as-deposited ZnO films were analyzed using XRD. Figure 2-5 shows that no reflection peaks were detected for the films deposited at a mixed solution *p*H of 6.7. In contrast, at mixed solution *p*H higher than 9.4, all detected reflection peaks were verified as a wurtzite ZnO,

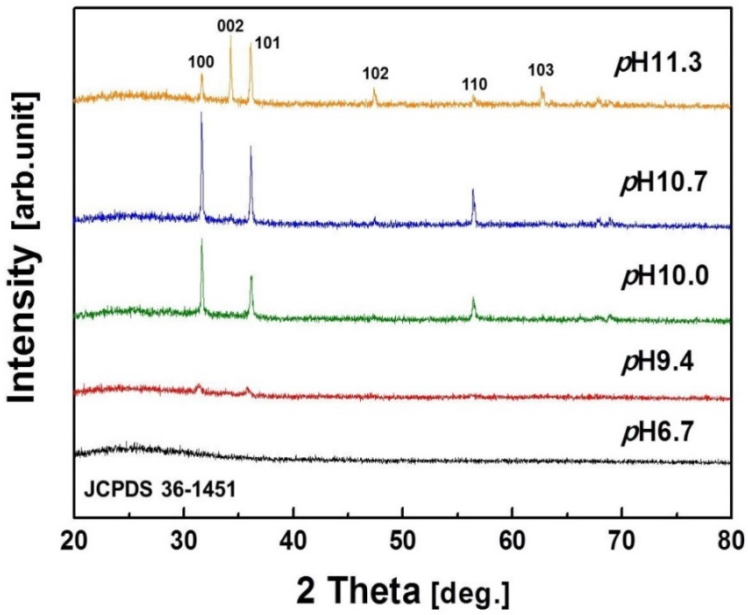

Figure 2-5 XRD patterns of as-deposited ZnO films.

and no impurity peaks were observed. The peak intensity differed for films deposited at different mixed solution *p*H. The intensities of the dominant peaks, such as (100) and (101), increased with the *p*H up to 10.7. However a different reflection peak of (002) was observed at higher pH and it was dominant for the film deposited at a *p*H of 11.3. The film morphology was also different, as evident from the SEM image in Figure 2-3-d.

Here, the texture coefficient (TC) was calculated by a following formula to confirm the details [20-23].

$$TC(hkl) = \frac{I_{(hkl)}/I_{r(hkl)}}{(1/n)(\sum I_{(hkl)}/I_{r(hkl)})}$$

where $I_{(hkl)}$ is the XRD peak intensity obtained from the ZnO films and $Ir_{(hkl)}$ is the standard intensity for the diffraction plane. A *TC(hkl)* of 1 indicates the growth of randomly oriented crystallites and the highest calculated *TC(hkl)* indicates preferential orientation in the *(hkl)* direction.

Figure 2-6 show that the preferred orientation was varied with the *p*H. The calculated TC for the (002) peak was very low from *p*H 10.0 to 10.7, while it increased sharply at *p*H 11.3.

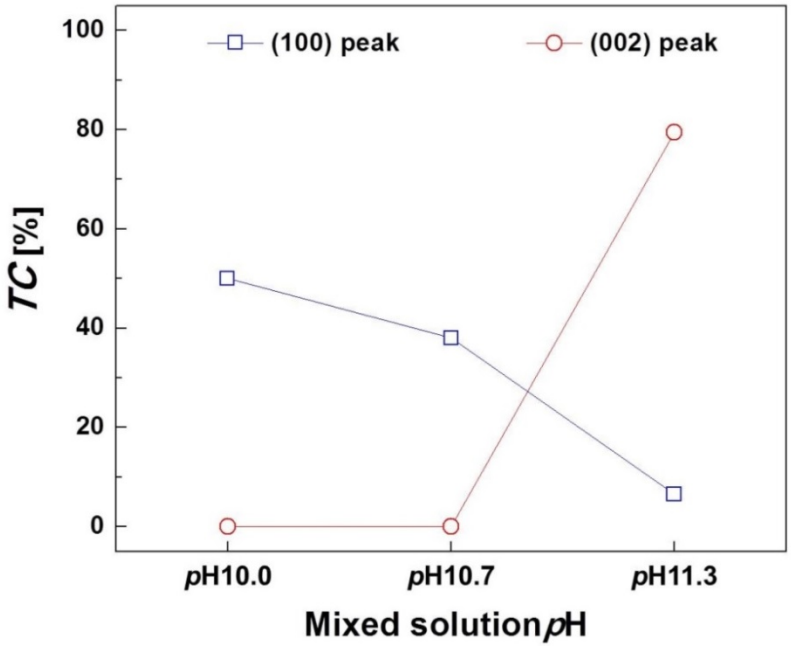

Figure 2-6 Calculated texture coefficients.

In contrast, the calculated TC (100) was gradually decreased with an increase of *p*H. These changes in crystallite orientation may affect the surface morphology to yield surface from continuous and smooth to discontinuous and rough. The reason for the morphological change is considered to be the insufficient of citrate ions onto the ZnO (00n) planes during the deposition process at high mixed solution *p*H.

Figure 2-7 shows the optical properties of the ZnO film deposited at *p*H 10.0 and 10.7. The ZnO Films had high transmittance above 90% in the visible range (wavelength = 400-700 nm). The transmittance was decreased to 80% for the ZnO film deposited at *p*H11.3. These results are also related to the change in the surface morphology with variation in the solution *p*H. The decrease in transmittance is caused by light scattering due to the surface roughness [24-26]. The optical band gap values calculated by Tauc/Davis Mott model were 3.44 and 3.47 eV for ZnO films deposited at mixed solution *p*H of 10.0 and 10.7, respectively [27-28]. However, the optical band gap energy for the ZnO film deposited at a mixed solution *p*H of 11.3 decreased to 3.42 eV, from which a decrease in carrier concentration was estimated according to the Burstein-Moss effect [30].

2.3.3 Flower-like ZnO Films

Flower-like ZnO films could simply obtained by change in *p*H adjuster from NH_3 solution to NaOH. As shown in Figure 2-8, surface morphologies of as-deposited ZnO films were gradually changed with increasing NaOH concentration. First, ZnO rod array structure was obtained at low NaOH concentration of 4 mM. It has width of 60 ~ 130 nm and length of around 1.2 μm. After that, surface morphology was changed once more by increasing NaOH concentration. As-deposited ZnO film at 12 mM indicated branch-like structure (Figure 2-8-b). Large amount of small-sized nanorods were formed on pre-existing rod surface. And then, as-deposited ZnO film at concentration of 40 mM, exhibited flower-like surface morphology, as shown in Figure 2-8-c.

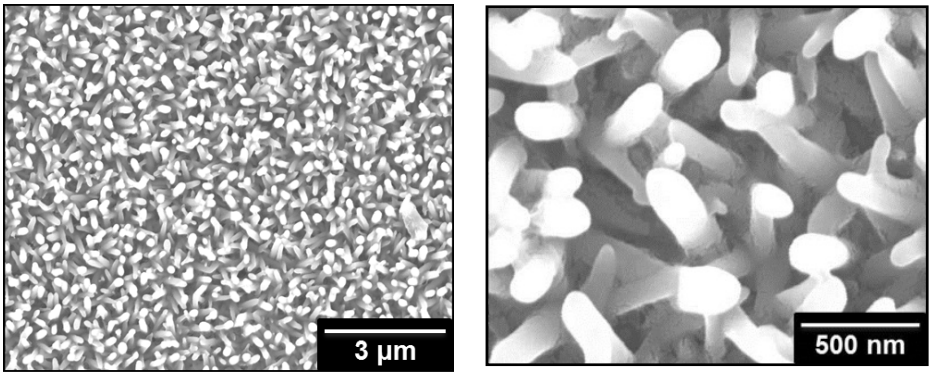

a. NaOH 4 mM

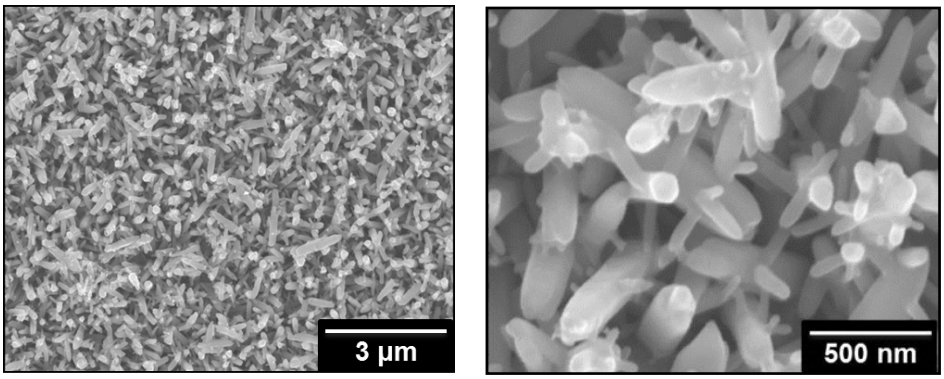

b. NaOH 12 mM

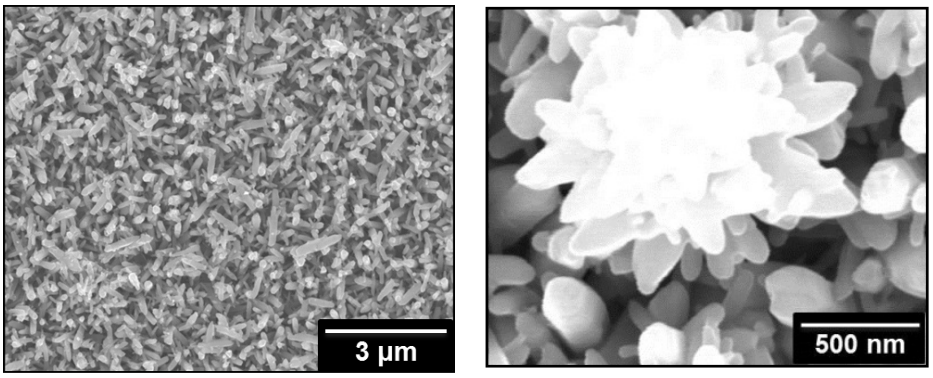

c. NaOH 40 mM

Figure 2-8 change of surface morphologies by NaOH concentrations.

Crystallographic properties of as-deposited ZnO films were investigated by X-ray diffraction. As shown in Figure 2-9, impurity peak such as hydroxide was not found. Observed all diffraction peaks were confirmed as a hexagonal structured ZnO, it is in good agreement with other literatures [31-32]. Dominant peak corresponding to (002) is observed at 34.4^{o} and intensity of (002) peak conspicuously increased with increasing NaOH concentrations.

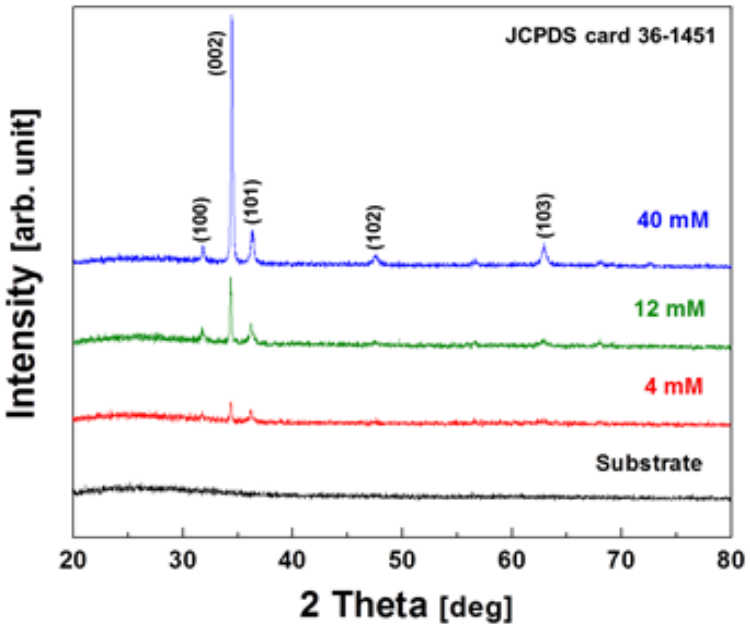

Figure 2-9 change of peak intensities by NaOH concentrations.

Figure 2-10 shows Raman spectra of as-deposited ZnO film. According to Group theory, the crystal structure of wurtzite ZnO belong to C^{4}_{6v} space group having two formula units per primitive cell with all the atoms occupying the *C*3v sites [32-33]. In case of E_2 mode, it has two nonpolar modes such as E_2 (low) and E_2 (high). However, only E_2 (high) peak was confirmed at 432 cm^{-1}, other peak or peak shift were not observed. Intensity of E_2 (high) slightly increased with increasing NaOH concentration, it means that as-deposited ZnO film has wurtzite hexagonal structure and improved crystalline quality.

Through the result of an experiment, it is thought that flower-like ZnO morphology is in close contacts with OH^- ion, because surface morphology changed with variation of NaOH

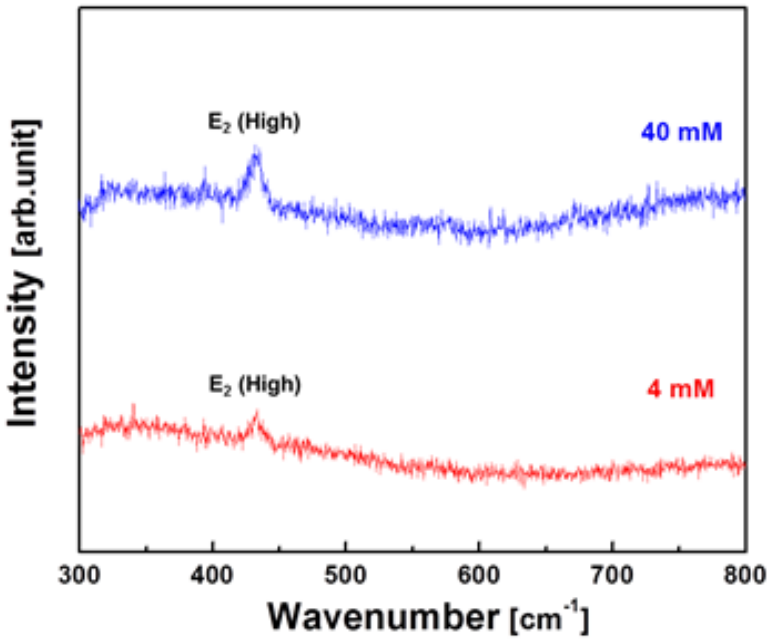

Figure 2-10 Raman spectra of as-deposited ZnO films.

concentration at fixed Zn concentration in source solution. Expected ZnO growth reaction by using NaOH as a pH adjuster is as following process

$$Zn^{2+} + 2OH^- \rightarrow Zn\,(OH)_2(aq) \rightarrow ZnO(s) + H_2O$$

$$Zn\,(OH)_2(aq) + 2H_2O \rightarrow Zn(OH)_4^{2-} + 2H^+ \rightarrow ZnO(s) + 3H_2O$$

In initial reaction stages, the reaction between Zn^+ and OH^- form the rod array structure on substrate, as illustrated in Figure 2-11. After that, successive supply of fresh solutions and increasing NaOH concentration might be formed sites for growth of rod structure on the pre-existing rod surface. Other literature reported the formation of sites by multinucleate aggregates, thermal condition and reaction time. However, in case of spin-sprayed film, it is thought that increased OH^- ion by increasing NaOH concentration and successive supply of

solution affect to formation of sites on the pre-existing rod surface, and ZnO grew as a single crystal on the sites.

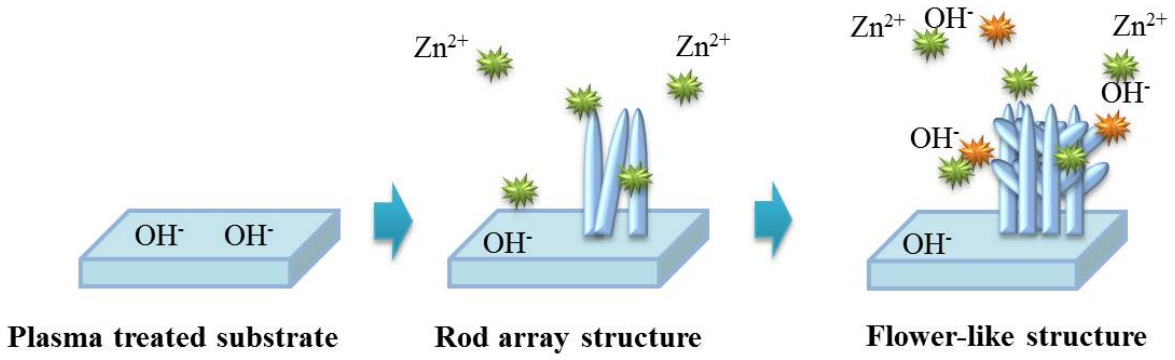

Figure 2-11 Growth mechanisms of flower-like ZnO films.

2.4 Summary

ZnO films having various structures such as rod array, dense, and flower like structure were simply obtained by changing solution conditions such as *p*H adjuster and surface modifier. Without surface modifier, ZnO film had rod array structure and film structure was changed to dense structure by adding citrate ions. Changed surface morphology of dense ZnO film by solution *p*H was also observed. ZnO film having flower-like structure was obtained by change of *p*H modifier from ammonia solution to sodium hydroxide. These various forms of ZnO films is expected to apply to various applications such as DSSC as a photoanode, and optoelectronic devices as a transparent electrode.

Reference

1. M. Caglar, S. Ilican, Y. Caglar, and F. Yakuphanoglu, Appl. Surf. Sci. 255 (2009) 4491
2. L. Xu, X. Li, Y. Chen, and F. Xu, Appl. Surf. Sci. 257 (2011) 4031
3. I. K. Bdikin, J. Gracio, R. Ayouchi, R. Schwarz, and A. L. Kholkin, Nanotech. 21 (2010) 235703
4. A. Degen, and M. Kosec, J. European. Ceram. Soc. 20 (2000) 667
5. G. Amin, M. H. Asif, A. Zainelabdin, S. Zaman, O. Nur, and M. Willander, J. Nanomater. 2011 (2011) 269692
6. Z. L. Wang, J. Phys.: Condens. Matter 16 (2004) R829
7. F. S. S. Chien, C. R. Wang, Y. L. Chan, H. L. Lin, M. H. Chen, and R. J. Wu, Sensors and Actuators B, 144 (2010) 120
8. M. Breedon, M. B. Rahmani, S. Keshmiri, W. Wlodarski, K. Kalantar-zadeh, Mater. Lett. 64 (2010) 291
9. H. I. Abdulgafour, Z. Hassan, N. Al-Hardan, and F. K. Yam, Physica B, 405 (2010) 2570
10. C. Y. Jiang, X. W. Sun,_ G. Q. Lo,_ and D. L. Kwong, Appl. Phys. Lett, 90 (2007) 263501
11. N. K. Park, G. B. Han, J. D. Lee, S. O. Ryu, T. J. Lee, W. C. Chang, and C. H. Chang, Current Appl. Phys. 6S1 (2006) e176
12. T. You, J. Yan, Z. Zhang, J. Li, J. Tian, J. Yun, W. Zhao, Mater. Lett. 66 (2012) 246
13. J. S. Lee, M. Saif Islam, S. T. Kim, Sensors and Actuators B, 126 (2007) 73
14. J. Zhou, Z. Wang, L. Wang, M. Wu, S. Ouyang, and E. Gu, Superlattices and Microstructures, 39 (2006) 314
15. R. C. Pawar, J. S. Shaikh, A. A. Babar, P. M. Dhere, and P. S. Patil, Solar Ener. 85 (2011) 1119

16. Y. Ding, and Z. L. Wang, Micron, 40 (2009) 335
17. H. Wagata, N. Ohashi, T. Taniguchi, A. K. Subramani, K. Katsumata, K. Okada, and N. Matsushita, Cryst. Growth Des. 10 (2010) 3502
18. H. Wagata, N. Ohashi, T. Taniguchi, K. Katsumata, K. Okada, and N. Matsushita, Cryst. Growth Des. 10 (2010) 4968
19. G. Amin, M. H. Asif, A. Zainelabdin, S. Zaman, O. Nur, and M. Willander, J. Nanomater. 1 (2011) 269692
20. S. Agouram, J. Zunigaperez, and V. Munoz-sanjose, Appl. Phys. A 88 (2007) 83
21. S. Ilican, M. Caglar, and Y. Ccaglar, Mater. Sci –Poland 25 (2007) 709
22. T. P. Rao, and M. C. Santhoshkumar, Appl. Surf. Sci. 255 (2009) 7212
23. M. Caglar, Y. Caglar, and S. I. Ilican, J. Optoelectro. Adv. Mater. 8 (2006) 1410
24. R. Tena-Zaera, J. Elias, and C. Levy-Clement, Appl. Phys. Lett. 93 (2008) 233119
25. Y. Zheng, X. Tao, L. Wang, H. Xu, Q. Hou, W. Zhou, and J. Chen, J. Chem. Mater. 22 (2010) 928
26. J. Krc, M. Zeman, O. Kluth, F. Smole, and M. Topic, Thin Solid Films 426 (2003) 296
27. J. Tauc, 1974 Amorphous and Liquid Semiconductors Plenum
28. E. A. David, and N. F. Mott, Philos. Mag. 22 (1970) 903
29. B. E. Sernelius, K. F. Berggren, Z. C. Jin, I. Hamberg, and C. G. Granqvist, Phys. Rev. B 37 (1998) 10244
30. D. Raoufi, and T. Raoufi, Appl. Surf. Sci. 255 (2009) 5812
31. X. D. Gao, X. M. Li, and W. D. Yu, Mater. Resear. Bulletin 40 (2005) 1104
32. G. Li, A. Sundararajan, A. Mouti, Y. J. Chang, A. R. Lupini, S. J. Pennycook, D. R. Strachan, and B. S. Guiton, Nanoscale 5 (2013) 2259
33. P. Suresh Kumar, A. Dhayal Raj, D. Mangalaraj, and D. Nataraj, Appl. Surf. Sci. 255 (2008) 2382

Chapter 3

Effects of UV Irradiation on Conductivity of Transparent ZnO Films

The as-deposited ZnO films by spin-spray method adding citrate in the reaction solution had a good transparency but high resistivity a several hundred Ω·cm, because they were not doped and contained the organic substance such as carboxyl groups and/or H_2O in the films. However, their resistivity drastically decreased to ~10^{-2} Ω·cm by UV irradiation due to the increase of career concentration due to the doping of C and H which was generated by photocatalytic reaction of ZnO. In this chapter, the effects of UV irradiation on the conductivity of as-sprayed transparent ZnO films were investigated. Here, UV irradiation conditions such as UV intensity and its wave length are important factor for decomposing organic substance in the films. As-sprayed ZnO films were subjected to UV irradiation using different UV lamp, i.e. UV A and UV C.

3.1 Introduction

The as-deposited ZnO films fabricated by spin-spray method adding tri-sodium citrate in reaction solution had high transparency and dense structure. However they are not applicable as using transparent electrode due to their high resistivity in several hundred Ω·cm order. Reason for such high resistivity was due to the existence of H_2O and organic substance in the as-sprayed film. First, spin-spray method is aqueous solution process,

therefore the existence of H_2O in the film can be easily supposed. Additionally, one of the organic substances, citrate ions consist of carboxyl groups were necessary to fabricate ZnO films having dense structure and high transparency. They are absorbed to (0001) plane on the ZnO for forming dense structure, while it can be cause to high resistivity [1].

To remove the H_2O and organic substance, a common process is a thermal treatment [2-5]. However, a high annealing temperature above 300^oC deteriorates their structural and optical properties. Additionally, it is not suitable to flexible devices due to generation of strain for the substrate. Therefore, another method which enables to remove H_2O and/or organic substance to improve the conductivity without causing thermal damage to the films is highly required.

In this chapter, the effect of UV irradiation on conductivity of transparent ZnO films was investigated. UV irradiation is one of the simple and effective methods for improving conductivity. ZnO is well-known photocatalytic material, and it decomposed organic substance in the film under UV illumination [6-7]. Here, UV intensity and wavelength are important factors because these conditions affect to the speed and degree of the decomposition of organic substance.

As-deposited ZnO films were subjected UV irradiation with various conditions, and change in their properties were analyzed.

3.2 Experimental Procedure

3.2.1 Deposition Process of ZnO Films

The source solution contained 10 mM $Zn(NO_3)_2 \cdot 6H_2O$ (zinc nitrate hexahydrate, Wako Pure Chemical Industries, 99.0%) in 2.0 L of deionized water. The reaction solution contained aqueous NH_3 solution (ammonia solution, Wako Pure Chemical Industries, 28.0%) and 4 mM $C_6H_5Na_3O_7$ (trisodium citrate, Wako Pure Chemical Industries, 97.0%) in 2.0 L of

deionized water. Here, the NH_3 solution was used as a *p*H adjuster and $C_6H_5Na_3O_7$ was used as a surfactant. These solutions were sprayed simultaneously on rotating substrates heated at 95 ^oC for 10 min.

3.2.2 UV Irradiation

The kinds of UV lamps are listing in Table 1 and their spectra energy distributions were shown in Figure 3-1.

Table 1 UV lamps.

	Wavelength	**Etc.**	
UV A	300~400 nm (main peak: 352, 368 nm)	BLB lamp	
UV C	100~280 nm (main peak: 253 nm)	-	

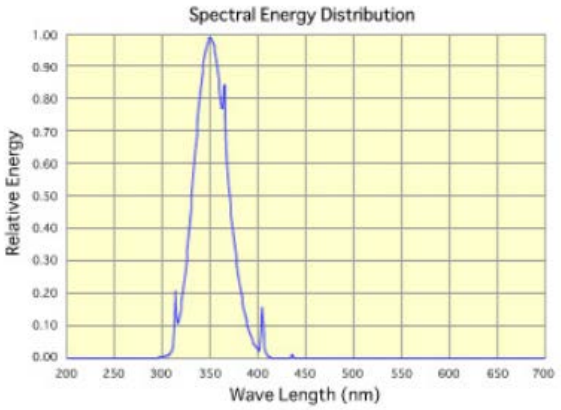

a. UV A

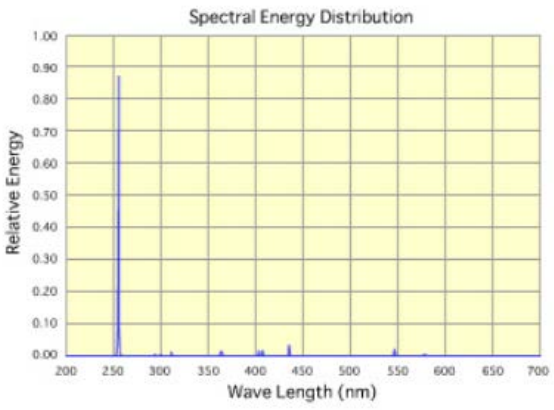

b. UV B

Figure 3-1 Spectra energy distribution of UV lamps used in this study.

As-deposited ZnO films were subjected to UV irradiation by using these UV lamps for 24 hour, and their change in conductivity was investigated.

3.2.3 Characterization

The surface morphology and cross sectional images of ZnO films were observed by scanning electron microscopy (SEM; Hitachi S4000) performed at 15 kV. Crystallographic properties were analyzed by X-ray diffraction (XRD; Rigaku Rint2000) with CuKα radiation (λ=1.5418Å). The samples for the Fourier transformed infrared (FT-IR) measurements were prepared by peeling off the deposited films from the glass substrate by scribing with a diamond knife. The scribed ZnO samples were mixed with KBr (potassium bromide, Wako Pure Chemical Industries, 99.0-100.2%) and pelletized. The electrical and optical properties were measured using a Hall Effect measurement system (ECOPIA HMS-3000) and a Lambda 35 spectrometer (Perkin Elmer Japan), respectively.

3.3 Results and Discussion

3.3.1 UV Irradiated ZnO films

In chapter 2, two different types of film structure were observed in the SEM images (Chapter 2, Figure 2-1). The films deposited without using citrate ions in the solution had a rod array structure oriented perpendicular to the substrate surface. On the other hand, the ZnO films deposited using citrate ions in the solution had a smooth surface and a continuous structure.

Although as-sprayed ZnO films had a dense structure formed by adding citrate ions in the solution, the films were not suitable for use as a transparent electrode owing to their low conductivity. As-deposited ZnO films have a low conductivity, though it can be reduced by doping (in case of dry process). Another reason for the high resistivity was attributed to the unwanted incorporations of organic substances in the films. As-confirmed COO^- vibration in FT-IR spectra meant that the as-deposited films contained the organic substance. To improve the conductivity, As-deposited ZnO films were subjected to photoinduced ion

substitution with UV irradiation (Black-Light-Blue lamp). Organic substance in the film would be decomposed by photocatalytic reaction of ZnO under UV irradiation [7].

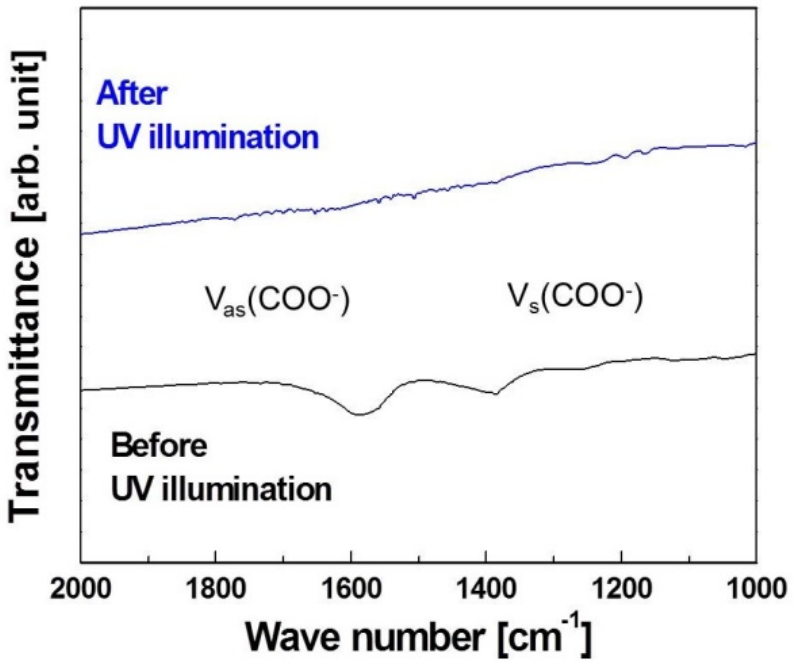

Figure 3-2 FT-IR spectra of ZnO films before and after UV illumination.

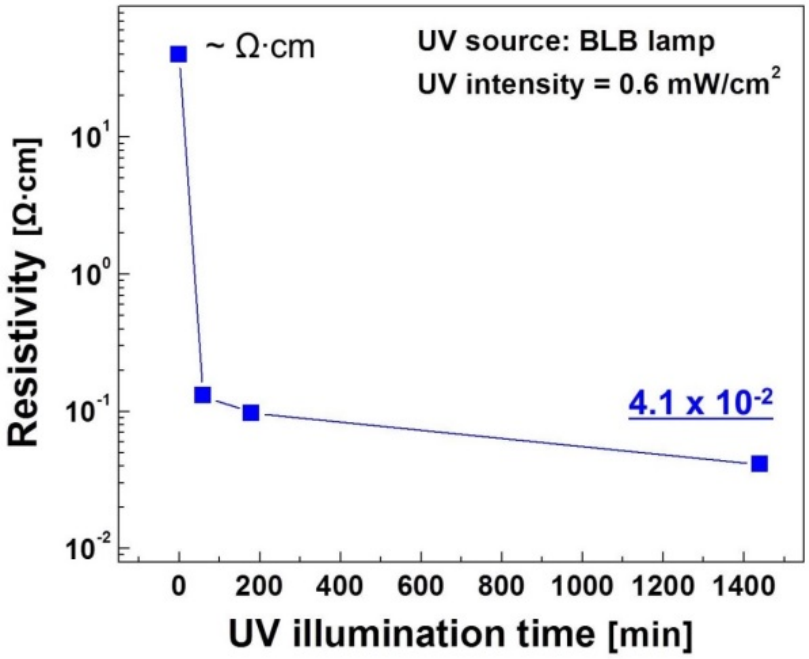

Figure 3-3 Change in resistivity following UV illumination.

As shown in Figure 3-2, disappearance of COO^- vibration peak meant the decomposition of organic substance such as citric ions. The resistivity was decreased by UV irradiation as shown in Figure 3-3. Although the ZnO films had a high resistivity before UV irradiation, it decreased down to 4.1 x 10^{-2} Ω·cm. It is though that the decrease in resistivity was attributed to the increase of carrier concentrations.

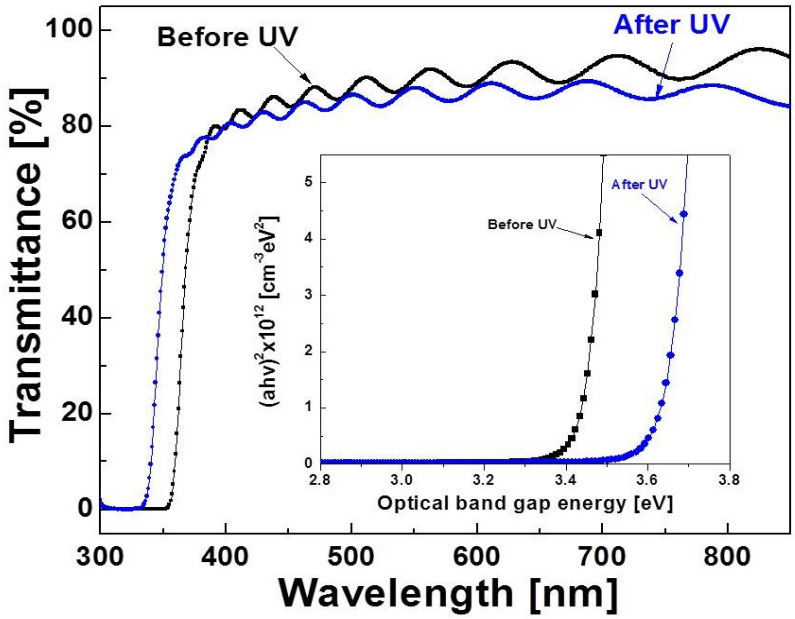

Figure 3-4 Optical properties of ZnO films before and after UV irradiation.

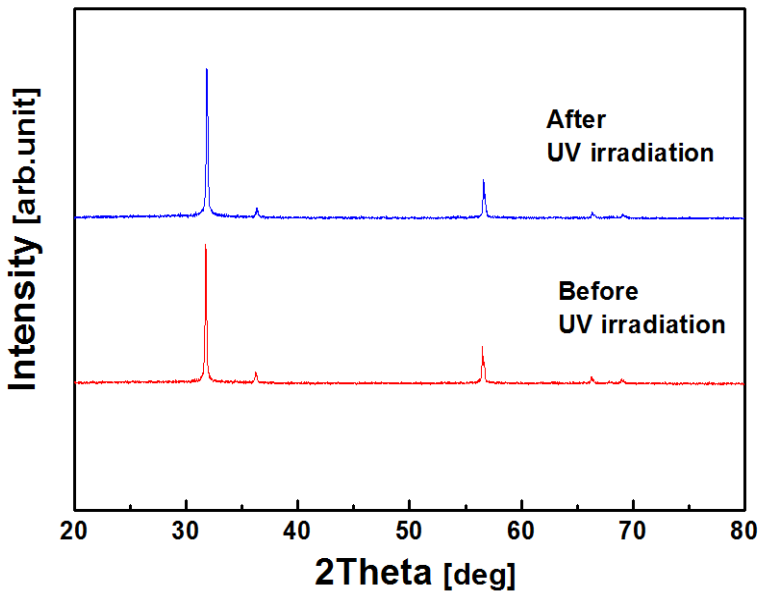

Figure 3-5 XRD patterns of as-deposited and UV irradiated ZnO films.

ZnO is one of the well-known photocatalytic materials, and it conducts the photocatalytic reaction under UV irradiation. Organic substances, such as carboxyl groups in the films, were decomposed by photocatalytic reaction of ZnO and C, and/or H doping into ZnO generated many carriers in the film, as a result [2, 7]. These increased carrier concentrations can be confirmed by change of optical band gap energy.

Figure 3-4 shows the change of optical properties. As-deposited ZnO film without UV irradiation has high transmittance approximately 90 %. In contrast, transmittance was slightly decreased after UV irradiation, while it has still high transparency above 80%. In case of optical band gap energy, as-deposited ZnO film without UV irradiation has 3.4 eV, while it was increased to 3.6 eV, after UV irradiation. The increase in optical band gap energy corresponds to the increase in carrier concentration, and it is well known as the Burstein-Moss effect [8-9].

Figure 3-5 shows the XRD patterns of as- deposited and UV irradiated ZnO films. As shown in Figure 3-5, changes in crystallographic properties such as crystallinity, peak shift, and intensity were not observed, before and after UV irradiation.

From the results, ZnO films having high transmittance and low resistivity after UV irradiation were confirmed and there was no variation of crystallographic properties. Based on these results, from now on, effects of UV irradiation conditions on conductivity of ZnO films were investigated.

3.3.2 UV Intensity

UV intensity is one of the UV irradiation conditions and it can be controlled by distance from UV lamp to substrate ($D_{L\text{-}S}$). As shown in Figure 3-6, variation of surface resistance by UV intensity was investigated.

Before UV irradiation, surface resistance of ZnO films was very high (~ MΩ), while it was decreased as UV irradiation time goes. UV irradiated ZnO films for 24 h, have 103, and 61 Ω,

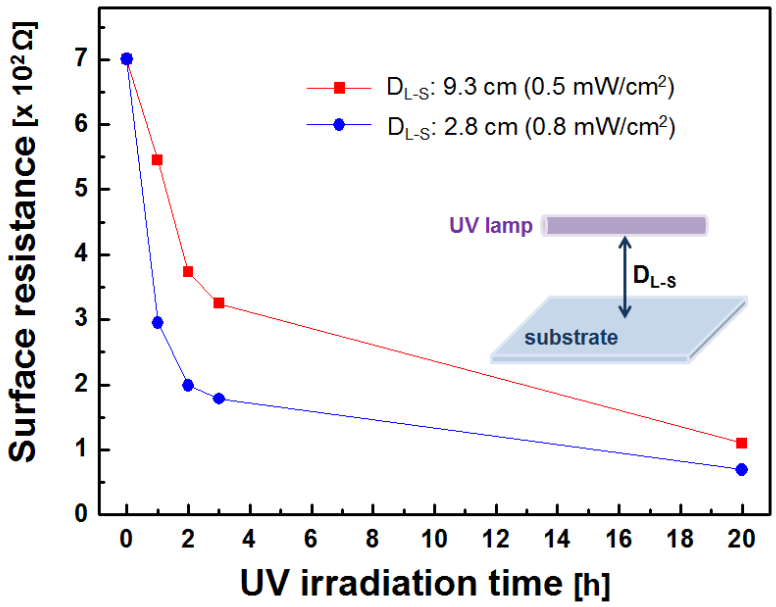

Figure 3-6 Variation of surface resistance using different UV intensities.

at D_{L-S} of 9.3, and 2.8 cm, respectively. Here, noticeable thing is decreasing speed in resistivity. As shown in Figure 3-6, the decreasing speed in resistivity at D_{L-S} 2.8 is faster than that of film at D_{L-S} 9.3 during UV irradiation from 1 to 3 h. However, they indicated similar values of surface resistance, after 20h. From these results, it is considered that UV intensity is influence to speed of ZnO photocatalytic reaction, and it became a factor for deciding the decreasing speed in the resistivity.

Table 2 UV wavelength.

	Abbreviation	Wavelength	Energy pre photon
Ultraviolet	UV	400 ~ 100 nm	3.10 ~ 12.4 eV
Ultraviolet A	UV A	400 ~ 315 nm	3.10 ~ 3.94 eV
Ultraviolet B	UV B	315 ~ 280 nm	3.94 ~ 4.43 eV
Ultraviolet C	UV C	280 ~ 100 nm	4.43 ~ 12.4 eV
Near Ultraviolet	NUV	400 ~ 300 nm	3.10 ~ 4.13 eV
Middle Ultraviolet	MUV	300 ~ 200 nm	4.13 ~ 6.20 eV
Far Ultraviolet	FUV	200 ~ 122 nm	6.20 ~ 10.16 eV
Extreme Ultraviolet	EUV	121 ~ 10 nm	10.25 ~ 124 eV

3.3.3 UV Wavelength

There are lots kinds of UV light and they can be categorized in Table 2 [10-11],

Here, as-deposited ZnO films were subjected UV irradiation at different wavelength by using UV A lamp and UV C lamp.

As shown in Figure 3-6, as-deposited ZnO film indicated dense and smooth surface. And there were no changes of surface morphology and cross sectional structure by UV irradiation.

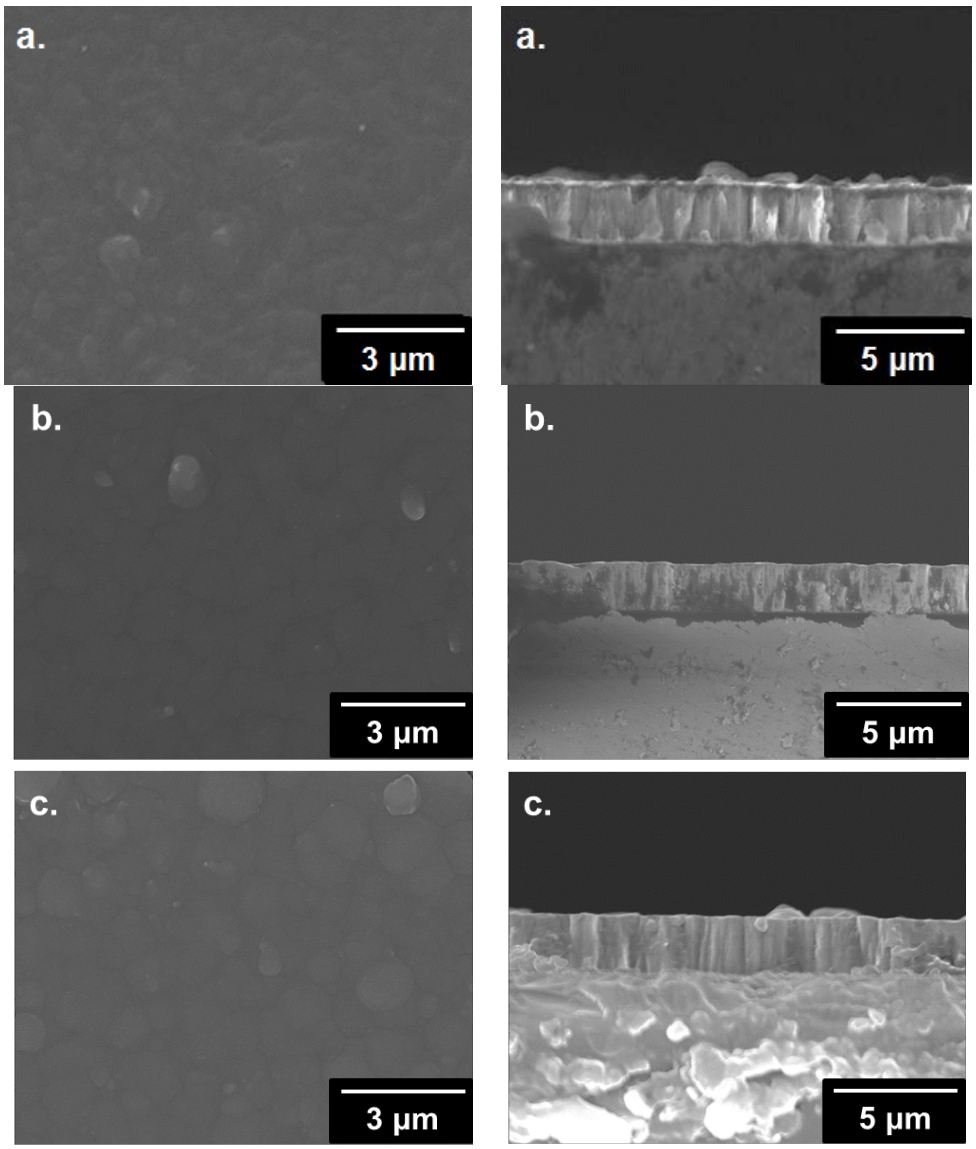

Figure 3-6 Surface and cross sectional images of as-deposited and UV*-irradiated ZnO films; a. as-deposited ZnO film, b. UV-irradiated ZnO film with UV A, and c. UV irradiated ZnO film with UV C.

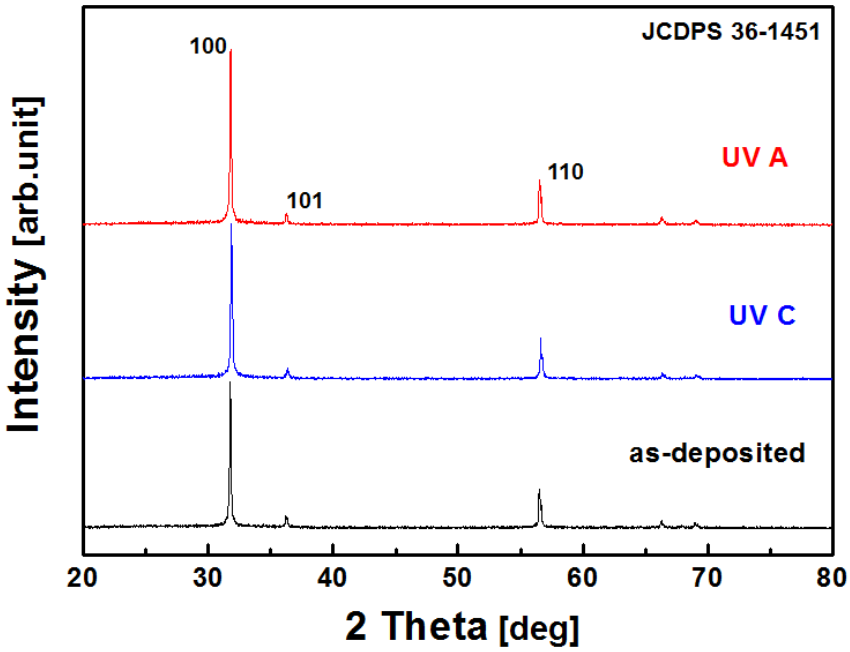

Figure 3-7 XRD patterns of as-deposited and UV-irradiated ZnO films.

Figure 3-7 shows the XRD patterns of as-deposited and UV-irradiated ZnO films. From the XRD patterns, three dominant peaks corresponding to (100), (101), and (110) were observed.

at 31.8, 35.7, and 56.1^{o}, respectively. Crystallite size of as-deposited ZnO film calculated from Scherrer's equation was 45.7 nm, and UV irradiated ZnO film also indicated similar values (UV A: 44.3 nm, UV B: 45.4 nm) [12-13]. Additionally, the full width at half maximum (FWHM) of all ZnO films was approximately 0.18^{o}, it means UV irradiation does not affect to crystallographic properties of ZnO films.

Figure 3-8 show the change in the resistivity of UV irradiated ZnO films at difference wavelength. As-deposited ZnO film has high resistivity, while it decreased by UV irradiation. In case of ZnO film irradiated by UV A lamp, the lowest resistivity was 2.2 x 10^{-2} Ω·cm with mobility of 0.8 $cm^2V^{-1}s^{-1}$. However, ZnO film irradiated by UV C lamp indicated higher value, the resistivity was 4.3 x 10^{-1} Ω·cm with mobility of 0.5 $cm^2V^{-1}s^{-1}$. The reason for the

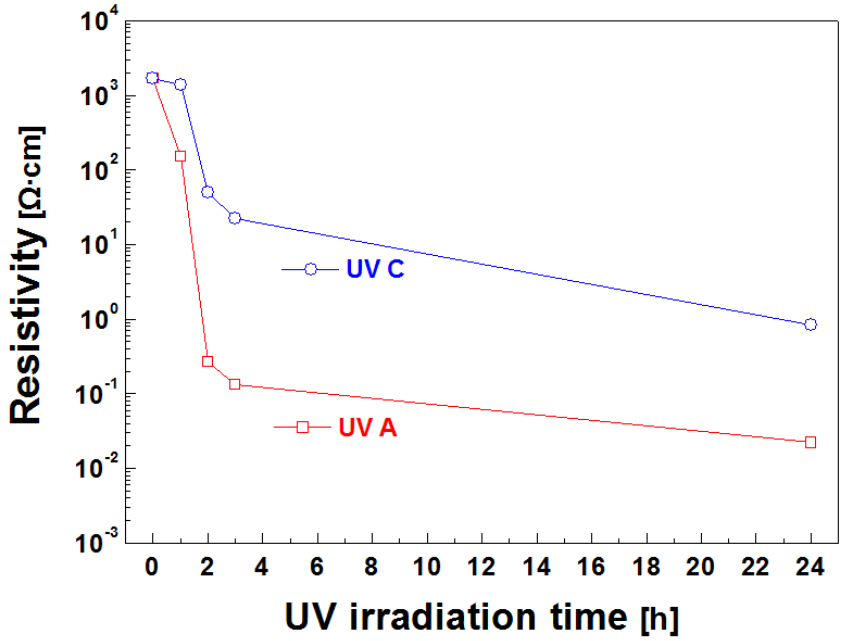

Figure 3-8 Change in resistivity for ZnO films irradiated by UV A and UV C.

variations in the resistivity was attributed to the difference in the carrier concentration. Carrier concentration of ZnO film irradiated by UV A lamp was 2.1 x 10^{20} cm^{-3} and, it was higher than that of irradiated film by UV C (4.7 x 10^{19} cm^{-3}). Basically, ZnO film deposited by spin-spray method attains the conductivity by UV irradiation. As mentioned before, free electrons were generated by decomposition of organic substance, under UV irradiation, and it becomes the main reason for low resistivity. Here, deposition condition and UV irradiation time were same, while one difference is UV wavelength. Therefore, it was supposed that UV wavelength might affect to decomposition of organic substance, and it can be a cause of low carrier concentration.

These variations of carrier concentration can be confirmed by optical properties, as shown in Figure 3-9. First, all ZnO films had high transmittance above 80% regardless of UV irradiation. On the other hands, blue shift in spectra was observed in wavelength from 320 to 360 nm; it means the increase of optical band gap energy. As shown in Figure 3-9-b, optical

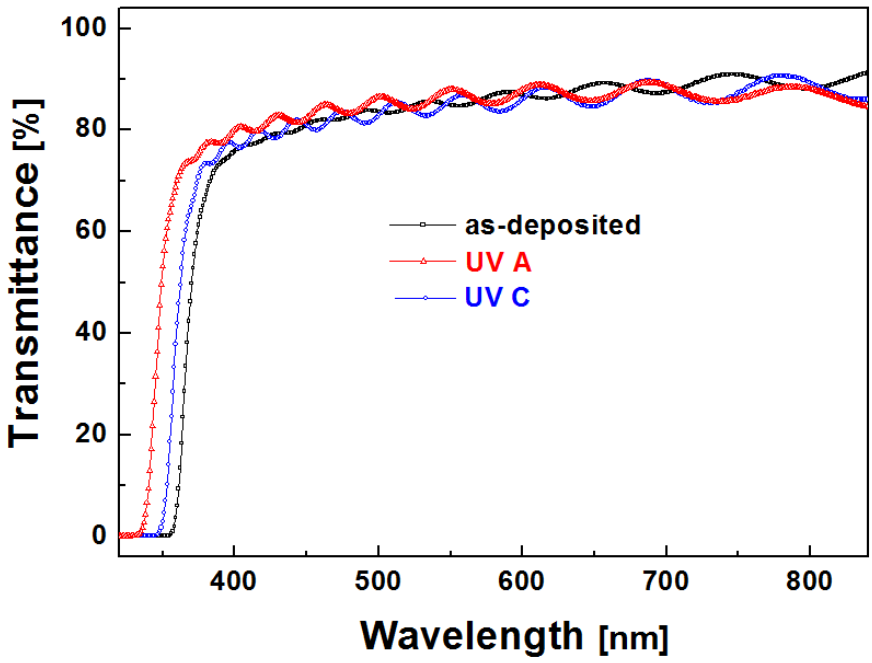

a. Transmittance.

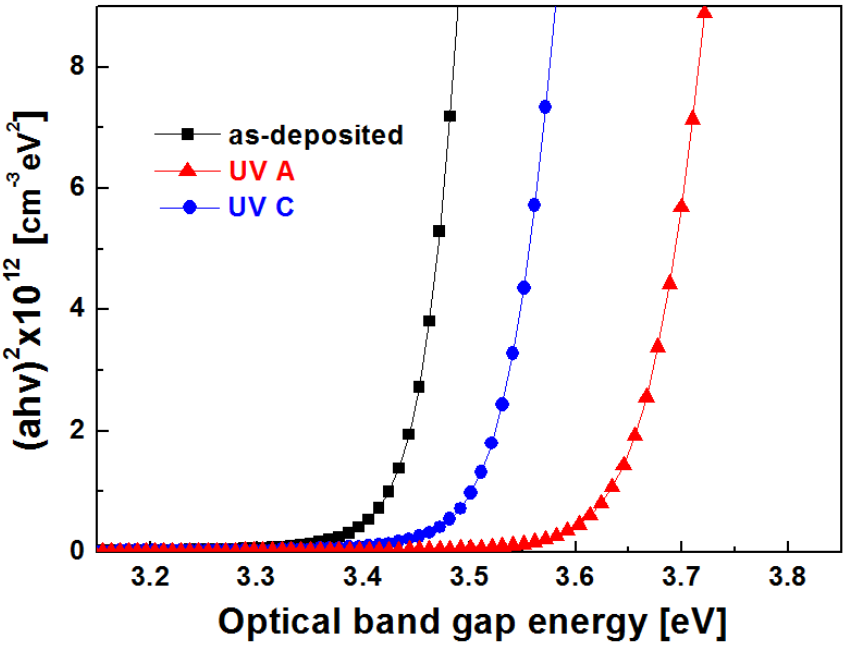

b. Optical band gap energy.

Figure 3-9 Optical properties of as-deposited and UV irradiated ZnO films.

band gap energy of as-deposited ZnO film was 3.42 eV and the optical band gap energy of ZnO films irradiated by UV A and UV C were 3.63 and 3.51 eV, respectively.

These increased band gap energy means increase in carrier concentrations, and it is well known as the Burstein-Moss effect [8-9].

It is thought that reason for low carrier concentration for UV C irradiation might be related to the different degree of decomposition of organic substance at difference UV wavelength. To confirm the more details, as-deposited and UV irradiated ZnO films were analyzed by Fourier transformed infrared (FT-IR).

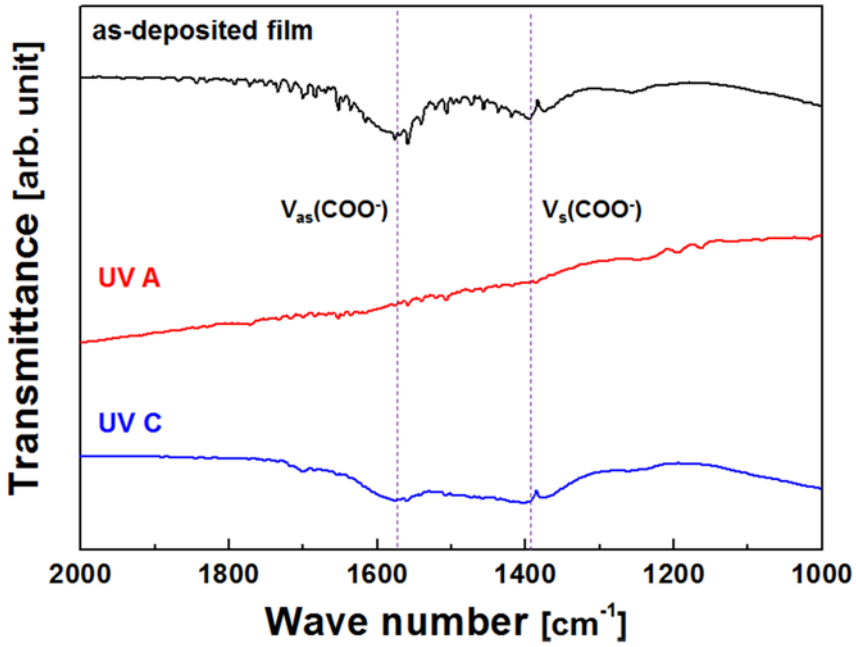

Figure 3-10 FT-IR spectra of as-deposited and UV irradiated ZnO films.

As shown in Figure 3-10, a COO^- vibration which means organic substance such as citric ions was observed before UV irradiation. However, COO^- vibration of UV irradiated ZnO film by UV A lamp was completely disappeared, and it means increase of carrier concentration caused by decomposition of organic substance. In contrast, COO^- vibration of ZnO film irradiated by UV C lamp was still observed, and it means organic substance such as citric ions remained in the ZnO film. These results can be the reason for lower carrier concentration than that of film irradiated by UV A lamp. From the results, it is thought that UV

lamp having spectra in a wide range is more effective to decompose the organic substance in the film and to increase the career concentration.

3.3.4 UV Patterning

ZnO film is applicable to various devices as a transparent electrode, and UV patterning is required for fabricating electric circuit [14-16]. The transparent ZnO film deposited by spin-spray method adding citrate ions in the reaction solution can obtain the conductivity by UV

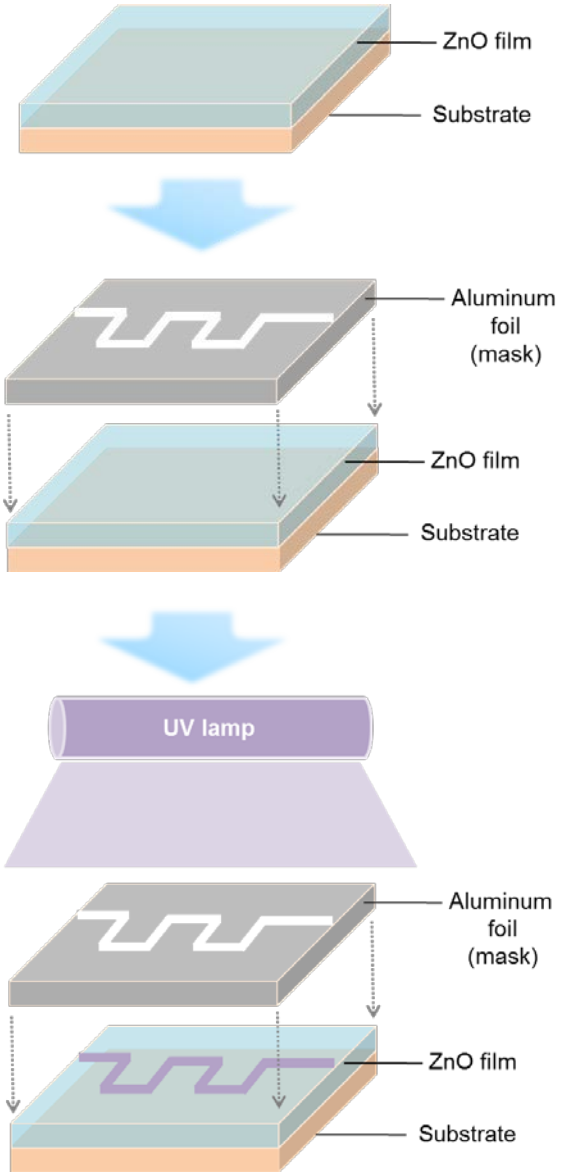

Figure 10 UV patterning process.

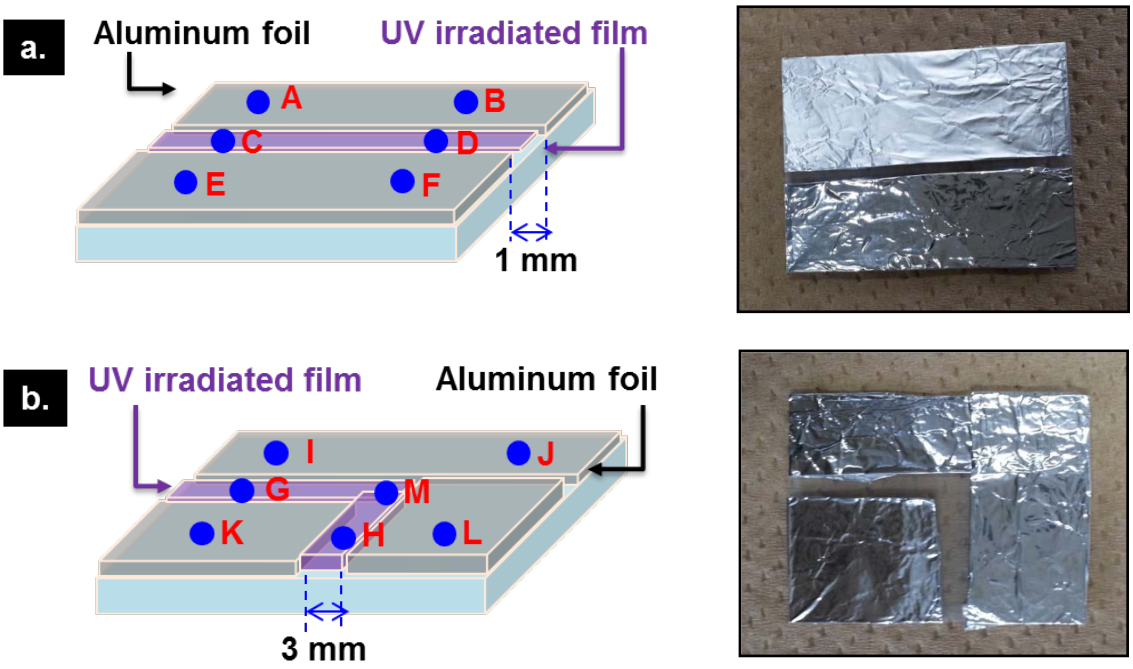

Figure 3-10 UV patterning process.

irradiation. Here, UV irradiation can be one of the simple methods to fabricate UV patterning by drawing electric circuit in ZnO film. For UV patterning, aluminum foil was used as a mask during UV irradiation, as shown in Figure 3-10. As-deposited ZnO film was covered with aluminum foil, and then, ZnO film was subjected UV irradiation for 24 h.

Figure 3-11 shows the UV patterned samples. Here, width of UV patterned film is too narrow to measure the resistivity by Hall Effect measurement system. Therefore surface resistance was measured by volt-ohm-milliammeter (VOM) to confirm the UV patterning (Blue circles means measurement point), and measured surface resistance are summarized in Table 3.

As shown in Table 3, UV irradiated section indicated lower surface resistance than the other place. Film covered with mask (aluminum foil) indicated dozens of kΩ resistance, while section of UV irradiated film had the surface resistance of 0.5 ~ 1.7 kΩ (bold in Table 3). Additionally, even electric circuit has curve, UV irradiated section had still low surface resistance of 0.8 kΩ.

From these results, it is thought that UV irradiation can be one of the simple methods for fabricating electric circuit in transparent ZnO films fabricated by spin-spray method.

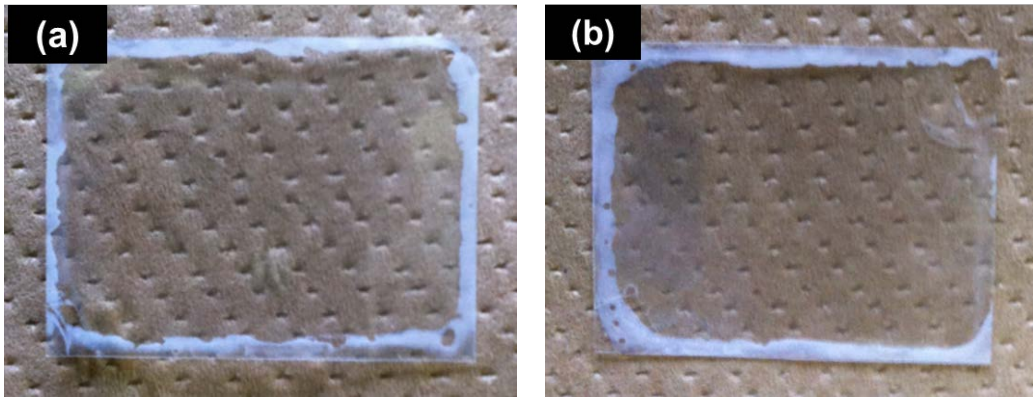

Figure 3-11 UV patterned samples.

Table 3 Measured surface resistance.

a.	Measurement point	A-B	A-D	A-F	C-B	**C-D**	C-F	E-B	E-D	E-F
	Resistance [kΩ]	81.7	59.4	49.4	244.3	**1.7**	18.9	68.1	14.4	28.9
b.	Measurement point	**G-M**	**M-H**	**G-H**	G-K	G-L	M-I	M-L	H-I	H-L
	Resistance [kΩ]	**0.6**	**0.5**	**0.8**	16.9	40.5	11.6	3.8	6.5	3.5

3.4 Summary

In this chapter, effect of UV irradiation on conductivity of transparent ZnO film deposited by spin-spray method was discussed. As-deposited ZnO film without UV irradiation had high resistivity, while resistivity of ZnO film was gradually decreased to ~10^{-2} Ω·cm with high carrier concentration of ~10^{20} cm^{-3}, after UV irradiation. Under UV irradiation, organic substance in the ZnO films is decomposed by photocatalytic reaction of ZnO, C, and /or H doping into ZnO. These reactions cause the generating many carriers, as a result, resistivity was decreased. In case of UV intensity, decreasing speed of resistivity increased by

increasing intensity. Additionally, it was also confirmed that UV condition having wide wavelength was more effective to decompose the organic substance in the film, and it resulted lower resistivity.

Reference

1. H. Wagata, N. Ohashi, T. Taniguchi, K. Katsumata, K. Okada, and N. Matsushita, Cryst. Growth Des. 10 (2010) 4968
2. J. S. Hong, H. Wagata, K. Katsumata, K. Okada, and N. Matsushita, Jpn. J. Appl. Phys. 52 (2013) 110108.
3. J. Zhang, E. Guo, L. Wang, H. Yue, G. Cao, and L. Song, Trans. Nonferrous Met. Soc. China, 24 (2014) 736
4. K. Agnieszka, and J. Teofil, Materials 7 (2014) 2833.
5. M. Ohyama, H. Kozuka, T. Yoko, Thin Solid Films, 306 (1997) 78.
6. H. Wagata, K. Katsumata, N. Ohashi, M. Sakai, A. Nakajima, A. Fujishima, K. Okada, and N. Matsushita, Photochem. Photobio. 87 (2011) 1009.
7. H. Wagata, N. Ohashi, K. Katsumata, H. Segawa, Y. Wada, H. Yoshikawa, S. Ueda, K. Okada, and N. Matsushita, J. Mater. Chem. 22 (2012) 20706.
8. B. E. Semelius, K. F. Berggren, Z. C. Jin, I. Hamberg, and C.G. Granqvist, Phys. Rev. B 37 (1988) 10244.
9. Y. S. Jung, J.Y. Seo, D.W. Lee, and D.Y. Jeon, Thin Solid Films 445 (2003) 63.
10. ISO 21348 Definitions of Solar Irradiance Spectral Categories.
11. B. L. Diffey, Methods 28 (2002) 4.
12. G. B. Williamson, and Smallman, Phios. Mag. 1 (1956) 34
13. B. Cllity, 1978 Elements of X-ray Diffraction (Reading: Addison-Wesley) 102
14. J. Wang, C. Larsen, T. Wagberg, and L. Edman, Adv. Fumc. Mater. 21 (2011) 3723.
15. D. Sameoto, and C. Menon, J. Micromech. Microeng. 20 (2010) doi:10.1088/0960-1317/20/11/115037
16. C. M. Doherty, G. Grenci, R. Ricco, J. I. Mardel, J. Reboul, S. Furukawa, S. Kitagawa, A. J. Hill, and P. Falcaro, Adv. Mater. 25 (2013) 4701

Chapter 4

High-Conductivity Solution-Processed ZnO Films Realized via UV Irradiation and Hydrogen Treatment

The dependence of thermal treatment temperature before UV illumination on their crystallographic and electrical properties was investigated in this study. ZnO films were deposited by the spin-spray method and thermally treated at different temperatures from 100 to 300 ^{o}C. All films had a high transmittance of 80% in the visible range and exhibited conductivity after UV illumination for 24 h. The resistivity after the UV illumination of the sample without thermal treatment was 4.1 x 10^{-2} Ω·cm, and it decreased to 1.6 x 10^{-2} Ω·cm in the sample thermally treated at 100 ^{o}C. The sample with the lowest resistivity exhibited a relatively high mobility of 3.3 cm^2 V^{-1} s^{-1} and a very high carrier concentration of 1.1 x 10^{20} cm^{-3} as the solution-processed ZnO film. In case of hydrogen treated and UV irradiated ZnO film, it was markedly lowered by hydrogen treatment and UV irradiation. A ZnO film with a low resistivity of 1.8 × 10^{-3} Ω·cm, high mobility of 11.2 $cm^2V^{-1}s^{-1}$ and high carrier concentration of 1.5 × 10^{20} cm^{-3} was attained by both hydrogen reduction and UV irradiation. Hydrogen treatment increased mobility by decreasing the number of negatively charged oxygen species present in the films. Meanwhile, UV irradiation caused ZnO to photocatalytically degrade organic materials in the film to increase carrier concentration.

4.1 Introduction

Zinc oxide (ZnO), a wide-band-gap oxide semiconductor, has been receiving much attention as a transparent electrode for optoelectronic devices such as flexible displays, solar cells, sensors, thin film transistors and organic light-emitting diodes [1-6]. ZnO is a

superior alternative to indium tin oxide because of the low cost of raw materials and its high transparency in the visible region.

ZnO films for use as transparent electrodes are usually deposited by dry processes like sputtering, pulsed laser deposition and ion plating to fabricate films with high crystallinity [7-8]. However, these processes are complicated and energy-intensive because they require vacuum systems. Additionally, because their deposition rate is low and the usage efficiency of expensive target is also low, the cost of ZnO film production is high. For these reasons, an environmentally friendly solution-based process to fabricate ZnO film is required, and many studies on ZnO films deposited by solution-processes have been reported [9-12]. However, the conductivity of solution-processed ZnO films remains lower than that of films deposited by dry processes and ITO films. Thus, researchers are attempting to improve the conductivity of solution-processed ZnO films [13-14].

Theoretically, the conductivity (σ) of a transparent conductive oxide (TCO) film can be expressed as follows, [15]

$$\sigma = 1/\rho = ne\mu \qquad (1)$$

where ρ is resistivity, e is carrier charge, n is carrier concentration and μ is mobility. As shown in Equation (1), both high mobility and carrier concentration are essential to attain high conductivity [16-17].

A widely used method to improve conductivity is increasing carrier concentration by metal ion doping, often with group III dopants such as In, Al, and Ga [18-21]. These dopants substitute Zn ions and generate free electrons, causing the carrier concentration of ZnO to increase. However, in the case of solution-processed metal ion-doped ZnO films, hydroxide and/or layered double hydroxides are formed in the solution or on the film surface, which lead to decreased conductivity [22]. Therefore, an effective, simple method to increase the

carrier concentration of solution-processed ZnO films without changing their properties or forming hydroxide and/or layered double hydroxides needs to be developed.

Another method to improve the conductivity of ZnO is to increase its mobility by thermal treatment using a suitable temperature, time and atmosphere [23-26]. Crystallographic properties such as crystallinity and crystallite size strongly affect mobility and thus conductivity [27]. However, conventional thermal treatment processes generally use high temperature and/or long treatment time, resulting in negative side effects such as films peeling-off from the substrate because of defect formation, stress, and oxygen deficiency in the films [28]. Oxygen deficiency can degrade electrical conductivity because of photon scattering [19, 29]. Therefore, thermal treatment at low temperature for a short period is required to increase mobility without adversely affecting crystallographic properties.

In this chapter, effects of thermal treatment temperature before UV irradiation on crystallographic and electrical properties of transparent conductive ZnO films were investigated. ZnO film deposited by spin-spray method contains the H_2O and organic substance, because spin-spray method uses the solution and various organic materials for deposition of ZnO film. Here, H_2O and organic substance are may affect to properties of ZnO film. To confirm the influence, as-deposited ZnO films by spin-spray method were thermally treated before UV irradiation.

Additionally, transparent ZnO films are fabricated by a spin-spray process using aqueous solutions followed by thermal treatment under different atmospheres and/or UV irradiation. The ZnO films treated by both hydrogen reduction and UV irradiation exhibited high conductivity because of their high mobility and high carrier concentration.

In our ZnO films, high mobility is achieved by thermal treatment in hydrogen atmosphere at 100 °C for 1 h. One of the main reasons for low mobility is adsorption of negatively charged oxygen species at grain boundaries, which increase the potential barrier and act, as trapping centers [30-31]. The trapping centers suppress electron transfer and/or diffusion,

causing mobility to decrease. Thermal treatment in hydrogen atmosphere can simply decrease the potential barrier at grain boundaries by introduction of hydrogen ions. High carrier concentration is realized in the ZnO films by UV irradiation, which causes the ZnO film to undergo photocatalytic reaction, producing shallow donors through decomposition of organic substances in the film [15].

4.2 Experimental Procedure

4.2.1 Deposition Process of ZnO Films

All films were deposited on glass substrates. The substrates were first ultrasonically cleaned in deionized water and ethanol for 10 min to remove impurities on the substrate surface. Then, the glass substrates were exposed to discharge plasma for 10 min to increase the hydrophilicity of their surfaces. To deposit the ZnO films, the source and reaction solutions were continuously sprayed for 10 min onto the substrates fixed on a rotating table. The source solution consisted of zinc nitrate hexahydrate (Wako Pure Chemical Industries, 99.0%) dissolved in Millipore deionized water (2.0 L) to give a concentration of 10 mM. The reaction solution was trisodium citrate (Wako Pure Chemical Industries, 97.0 %) in de-ionized water (2.0 L). Ammonia (Wako Pure Chemical Industries, 28.0 %) was used to adjust the *p*H of the reaction solution.

4.2.2Thermal Treatment and UV Irradiation

As-deposited ZnO films were thermally treated in the oven with change of treatment temperature from 100 to 300^{o} for 1h. And Tube furnace was used for thermal treatment in hydrogen atmosphere (hydrogen 3 % and Argon 97 %). Before the treatment, tube furnace was evacuated by using a rotary pump to pressure of 2 Pa to remove the residual gas in the chamber. Treatment temperature fixed at 100^{o}C (increasing temperature = 5^{o}C/min) and hydrogen gas flow rate was 200 ml/min. As-deposited ZnO film was thermally treated for 60

min including increasing temperature time (15 min). UV illumination was subjected by using the Back-Light-Blue lamp (intensity = 0.8 mW/cm^2, Toshiba Lighting & Technology Co., Japan) for 24 hours.

4.2.3 Characterization

The surface morphology of ZnO films was observed by scanning electron microscopy (SEM; Hitachi S4000) performed at 15 kV, and the film thickness was estimated using cross-sectional SEM images. Crystallographic properties were analyzed by X-ray diffraction (XRD; Rigaku Rint2000) with CuKα radiation (λ=1.5418Å) in the scanning angle (2θ) range from 20 to 80°. The samples for the Fourier transformed infrared (FT-IR) measurements were prepared by peeling off the deposited films from the glass substrate by scribing with a diamond knife. The scribed ZnO samples were mixed with KBr (potassium bromide, Wako Pure Chemical Industries, 99.0-100.2%) and pelletized for FT-IR measurements. As-prepared samples for FT-IR measurements were analyzed using an FT-IR spectrometer (JEOL JIR-7000) in the transmission mode at room temperature. The electrical and optical properties were measured using a Hall Effect measurement system (ECOPIA HMS-3000) and a Lambda 35 spectrometer (Perkin Elmer Japan), respectively. Changes in chemical states were investigated by XPS (ESCA-3200, Shimadzu Corp.).

4.3 Results and Discussion

4.3.1 Effect of Thermal Treatment Temperature

It is thought that as-deposited ZnO films by spin-spray method contained H_2O and an organic substance that affected their properties. Accordingly, effects of thermal treatment on the properties of solution-processed ZnO films before UV irradiation were investigated.

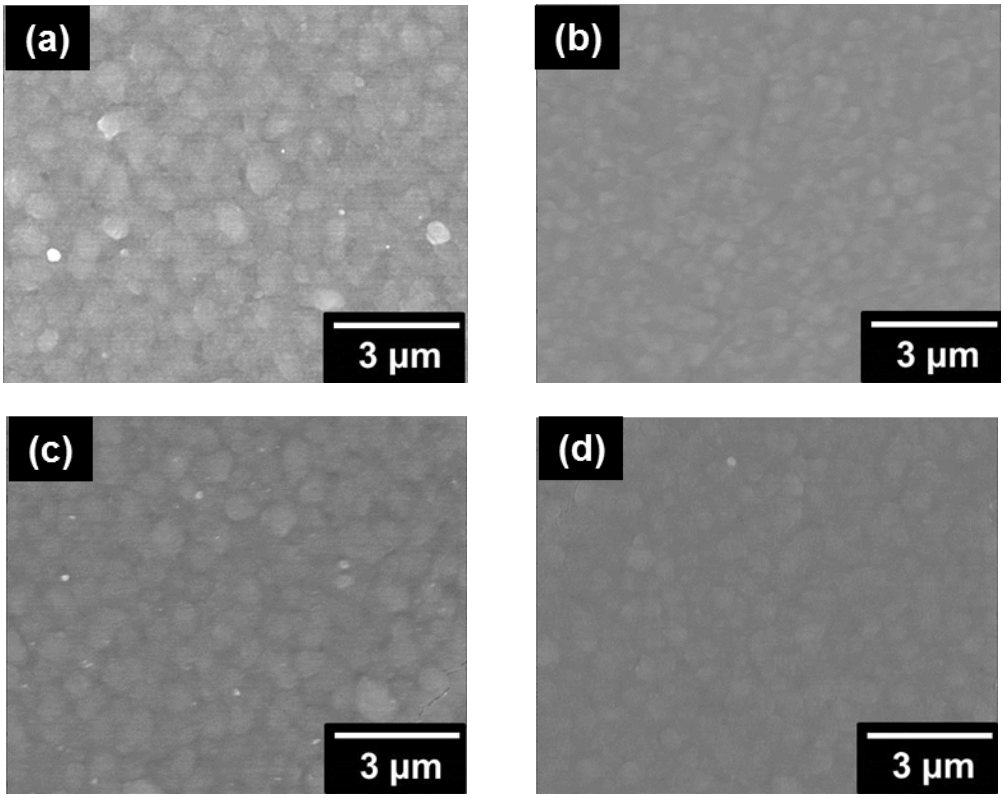

Figure 4-1 SEM images of (a) untreated ZnO film and ZnO film thermally treated before UV illumination at (b) 100, (c) 200, and (d) 300^{o}C

ZnO films were thermally treated at different temperatures from 100 to 300 ^{o}C for 1 h before UV illumination.

As a result, significant change in surface morphology before and after thermal treatment was not observed, as shown in Figure 4-1. To confirm the changes in structural properties in more detail, I analyzed the X-ray diffraction patterns.

Figure 4-2 shows XRD patterns of thermally treated ZnO films at different temperatures. All diffraction peaks originated from the hexagonally structured ZnO, and another impurity phase, such as zinc hydroxide, was not observed. From the XRD patterns, three dominant peaks corresponding to (100), (101), and (110) were observed at 31.5, 35.9, and 56.4^{o}, respectively, and these results are very close to the results of the standard ZnO crystal [JCPDS 36-1451: (100), (101) and (110) at 31.7, 36.2, and 56.6^{o}] and those reported in the literature [32-34]. And the change in full width at half maximum (FWHM) by thermal

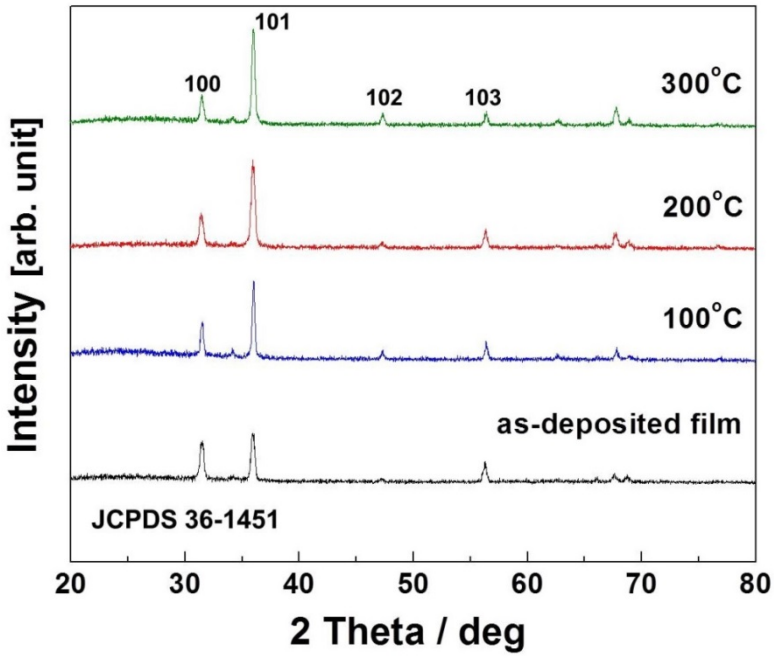

Figure 4-2 XRD patterns of thermally treated ZnO films before UV illumination.

treatment was confirmed. The lowest FWHM of the (101) peak was 0.26^{o} at the temperature of 100 ^{o}C; this value was lower than that of the ZnO film without thermal treatment (0.35^{o}). The FWHM values deteriorated to 0.31 and 0.37^{o} at temperatures of 200 and 300 ^{o}C, respectively. The decrease in FWHM value indicated the increase in crystallite size, and the crystallite size calculated from Scherrer's equation increased from 23.7 (without heat treatment) to 31.4 nm (heated at 100 ^{o}C). Increase in diffraction peak intensity with increasing treatment temperature was also observed. These results indicate that the crystallinities of as-deposited ZnO films were improved by thermal treatment.

Figure 4-3 shows changes in electrical properties following thermal treatment. After thermal treatment, ZnO films were subjected to UV illumination using the BLB lamp. As a result, improvement of electrical properties was I observed, and the lowest resistivity of 1.6 x 10^{-2} Ω·cm was attained for the sample heat-treated at 100^{o}C; this value was lower than that of the ZnO film without thermal treatment before UV illumination. The highest mobility (3.3 cm^2 V^{-1} s^{-1}) and carrier concentration (1.1 x 10^{20} cm^{-3}) were also attained for the sample

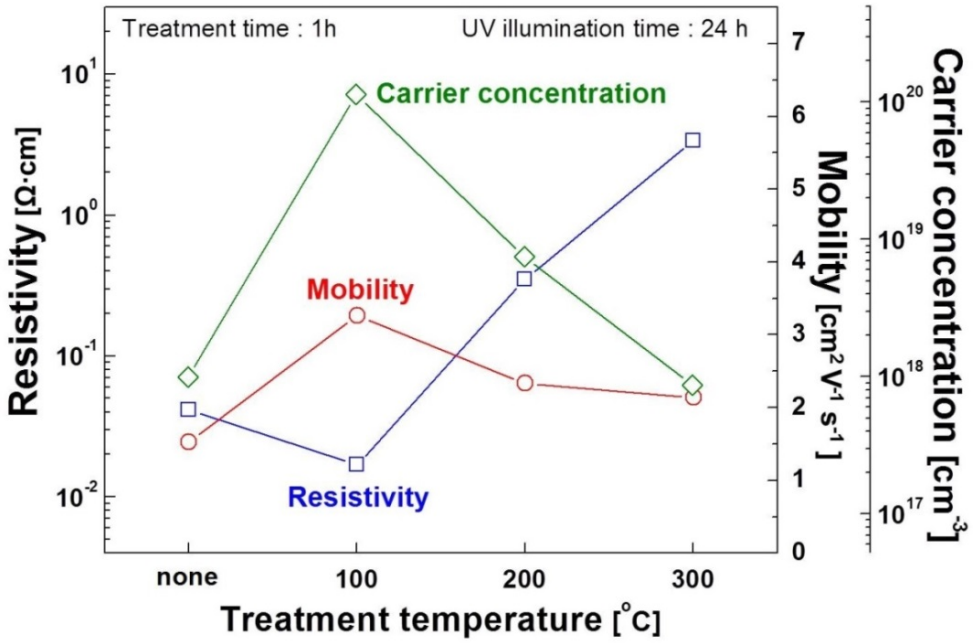

Figure 4-3 Effects of treatment temperature on electrical properties..

heat-treated at 100 ^{o}C. Improvement in crystallinity, as shown in XRD patterns in Figure 4-2, caused the increase in mobility, and the increase in the number of oxygen vacancies was caused by thermal treatment and resulted in the increase in carrier concentration. However, electrical properties, such as resistivity, carrier concentration, and mobility, were degraded for the sample heat-treated above 200 ^{o}C. The mobility slightly decreased from 3.3 to 2.1 cm^2 V^{-1} s^{-1} with increasing thermal treatment temperature from 100 to 300 ^{o}C. This result seems to originate from the change in crystallinity. The FWHM of the thermally treated ZnO film increased from 0.26 to 0.37^{o} with increasing thermal treatment temperature from 100 to 300 ^{o}C. The degradation of crystallinity might cause the decrease in mobility. The decrease in the carrier concentration of the ZnO films thermally treated at above 200 ^{o}C is the other reason for their degraded conductivity.

Under UV illumination, organic substances, such as carboxyl groups, were decomposed by photocatalytic reaction of ZnO and C, and/or H doping into ZnO formed many carriers; as a result, conductivity was improved [15]. Here, the H_2O and organic substance in the film are considered performance degradation factors, but they also played an important role in carrier

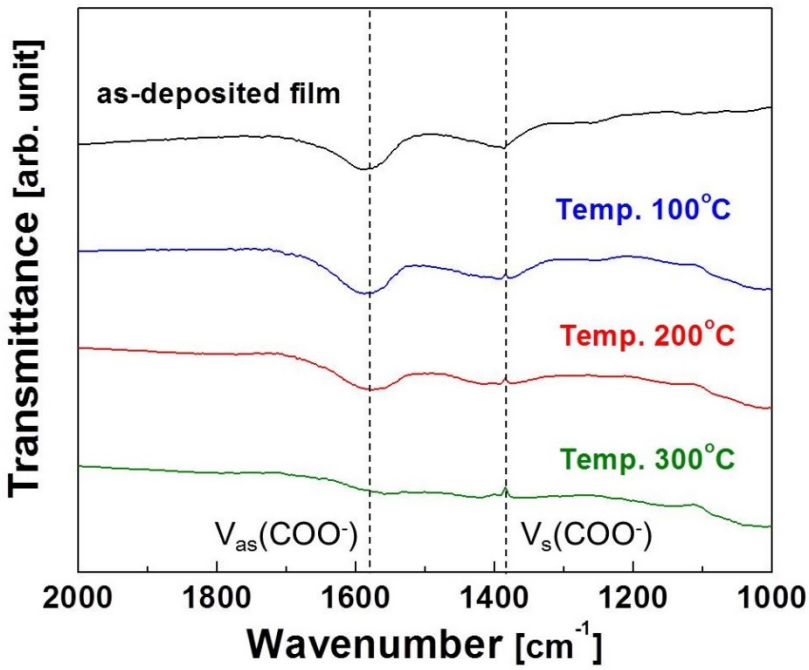

Figure 4-4 FT-IR spectra of thermally treated ZnO films (before UV illumination).

generation under UV illumination. To confirm these results in more detail, the as-deposited and thermally treated ZnO films were analyzed using FT-IR spectra.

It is confirmed that thermal treatment decreased the amount of organic substance in the films, as shown in Figure 4-4. Before UV illumination, ZnO films thermally treated at 100 ^{o}C indicated nearly the same intensity as the as-deposited film. However, peak intensities of carboxyl groups, such as V_{as} (COO^{-}) and V_{s} (COO^{-}), gradually decreased with increasing thermal treatment temperature. This might decrease carrier concentration because the decomposition of the organic substance was the main factor for generating carriers in the films after UV illumination. Therefore, a large amount of H_2O and a certain amount of organic substance were removed from the sample thermally treated at a temperature higher than 200 ^{o}C. This seemed to cause less doping in the film and decrease the carrier concentration after UV illumination.

Figure 4-5 shows the optical properties of ZnO films. All of the as-deposited ZnO films showed transmittances above 80% in the visible range (400-700 nm). However, the absorption edge slightly shifted with increasing thermal treatment temperature. As a result,

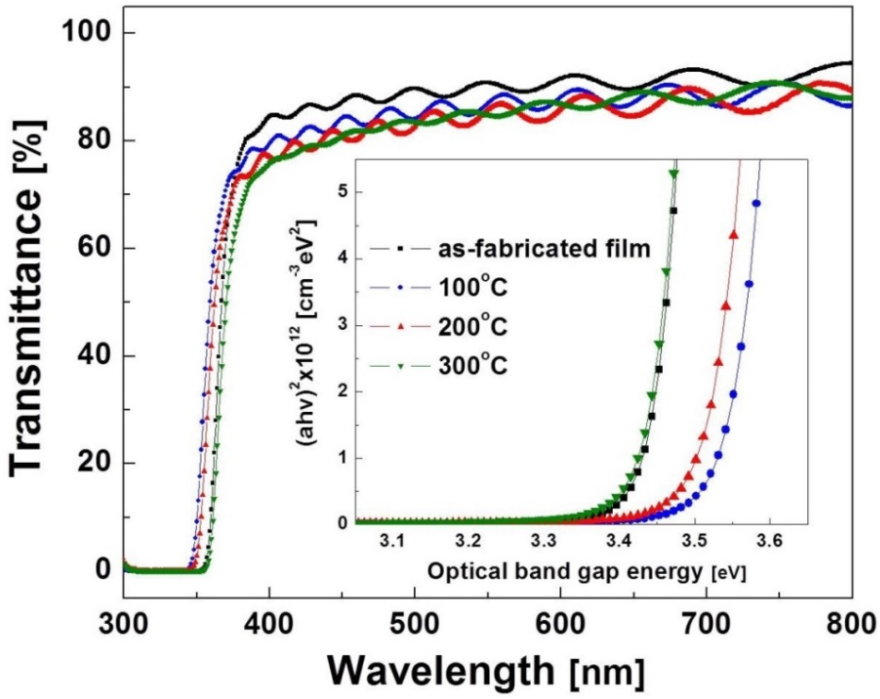

Figure 4-5 Optical properties of thermally treated ZnO films (after UV illumination).

decrease in optical band gap energy was observed. In the case of the sample thermally treated at 100 ^{o}C, the optical band gap energy was 3.53 eV, which is higher than that of the film without thermal treatment (3.43 eV). However, the optical band gap energy gradually decreased, and the ZnO film heated at 300 ^{o}C showed the optical band gap energy of 3.42 eV. The decreased optical band gap energy meant the decrease in carrier concentration (by the Burstein-Moss effect) [29, 35].

4.3.2 Hydrogen Treatment and UV Irradiation

ZnO films were prepared by a solution-based method and they were treated under different conditions, as shown in Table 1, to examine the effect of treatment conditions on the crystallographic properties and conductivity of the films. Figure 4-6 shows surface and cross-sectional scanning electron microscopy images of the ZnO films prepared in this study.

All films exhibited dense, smooth surfaces without cracks and pinholes even after

Table 1 conditions used to prepare samples.

Sample	Thermal treatment	UV irradiation
S1	-	-
S2	100 °C in air	-
S3	-	BLB lamp
S4	100 °C in air	BLB lamp
S5	100 °C in hydrogen	-
S6	100 °C in hydrogen	BLB lamp

hydrogen reduction and UV irradiation treatments. Crystallographic properties of the films were analyzed the by X-ray diffraction (XRD); the results are presented in Figure 4-7. All diffraction peaks were consistent with hexagonally structured ZnO, and no other peaks were detected. In the case of as-deposited ZnO film (S1), the dominant peak corresponding to the (100) plane was observed at 31.7°. The crystallite size calculated from this peak using

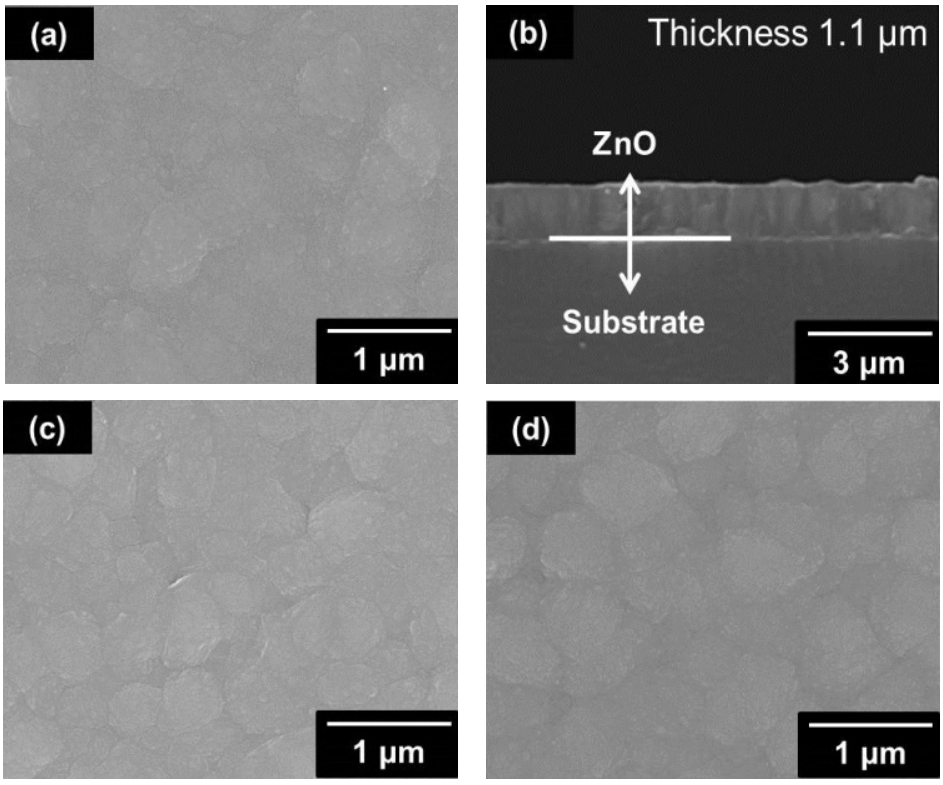

Figure 4-6 SEM images of as-prepared samples. a) Surface morphology of S1, b) cross sectional structure of S1, c) surface morphology of S4, d) surface morphology of S6.

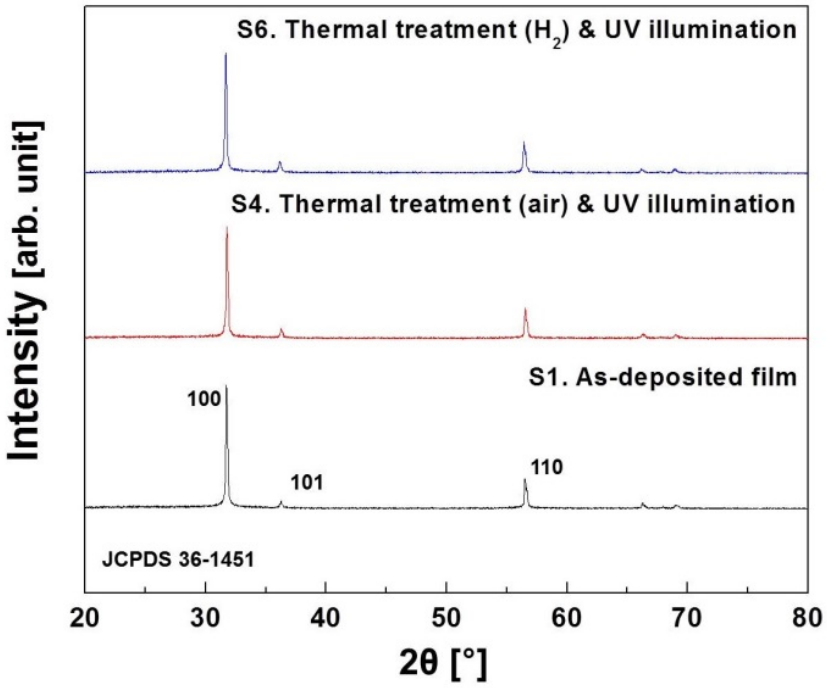

Figure 4-7 XRD patterns of as-prepared samples

Scherrer equation is 43.5 nm [36-37]. Marked changes in peak intensity and crystallite size were not observed after thermal treatment and UV irradiation. The full width at half-maximum values of the diffraction peak decreased slightly from 0.19° for S1 to 0.18° for S4 and S6.

Figure 4-8 shows the transmittance and optical band gap energy of the ZnO films. All of the ZnO films exhibited high transmittance of above 80% in the visible range (400–700 nm). Absorption edges shifted depending on the type of film treatment. The absorption edges for the ZnO films not exposed to UV radiation, S1, S2 and S5, appeared at wavelengths from 350 to 360 nm. In contrast, the absorption edges of UV-irradiated ZnO films (S3, S4 and S6) were observed at 330 to 340 nm. These results suggest that UV irradiation caused the increase of optical band gap energy of ZnO films.

To confirm this, the optical band gap energy of each sample was calculated by the Tauc and Davis–Mott models [38-39]. S1, S2 and S5 had almost the same optical band gap energy even though they were thermally treated under different atmospheres. The optical band gap energy of S3, S4 and S6 was shifted to 3.58 eV because of the Burstein-Moss

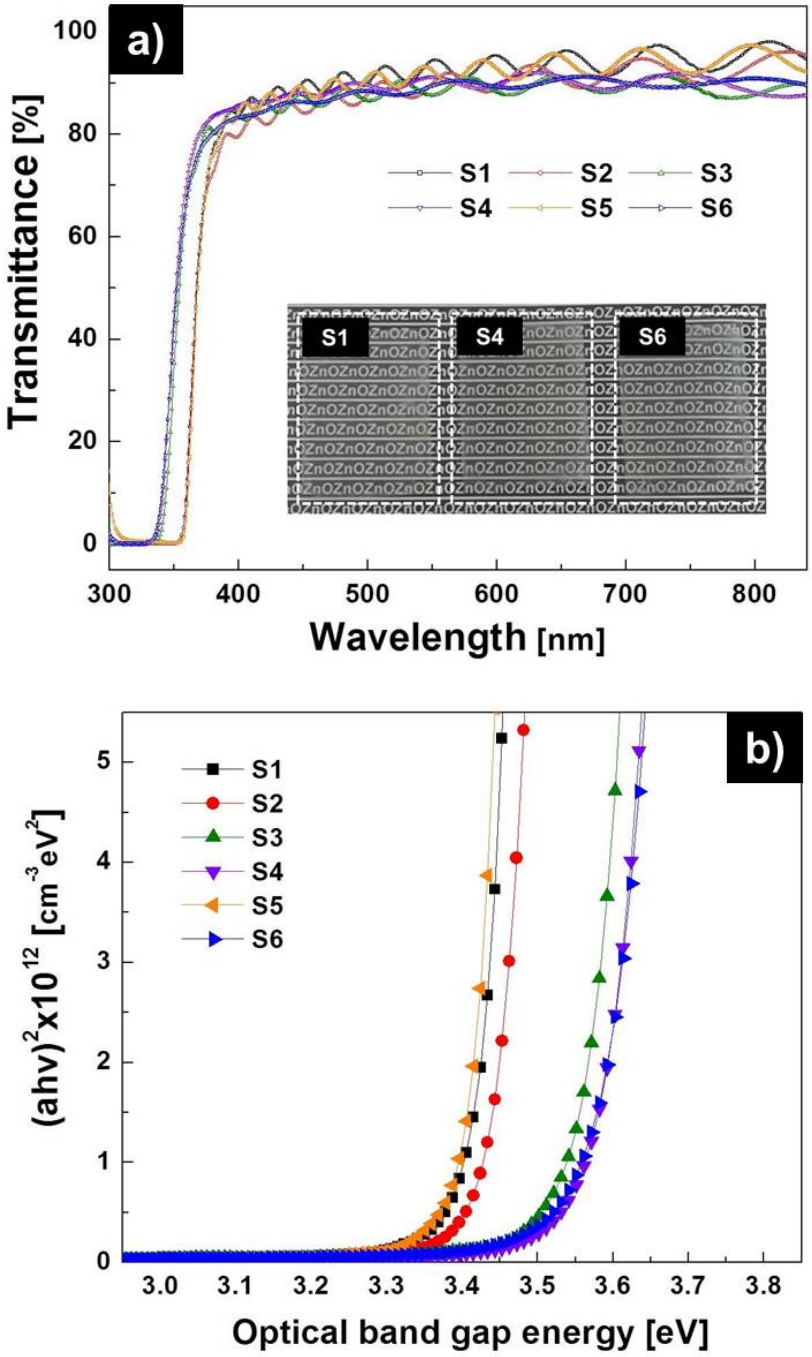

Figure 4-8 Optical properties of as-prepared samples. a) Transmittance, and b) optical band gap energy. Inset in a) are photographs of samples S1, S4 and S6.

effect [35]. This suggests that UV irradiation is effective to increase the carrier concentration in ZnO films [15].

The resistivity of the ZnO films treated under different conditions is displayed in Figure 4-9.

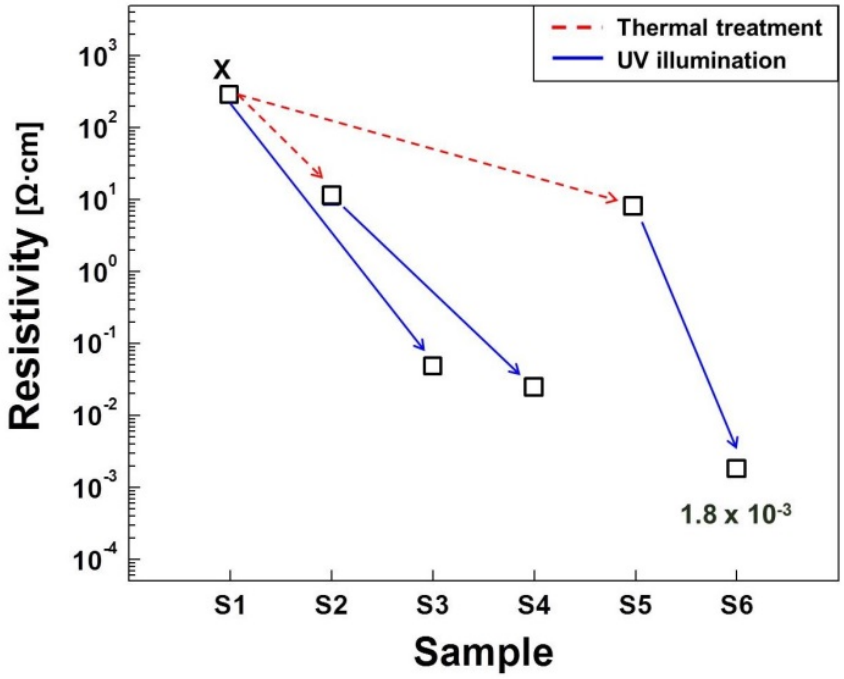

Figure 4-9 Dependence of resistivity on thermal treatment and UV irradiation

Here, dotted and solid arrows indicate the decrease in resistivity induced by hydrogen reduction and UV irradiation, respectively. The resistivity of the as-deposited film (S1) was as high as several hundred Ω·cm. The resistivity of the films was dramatically decreased by thermal treatment and UV irradiation. As shown in Figure 4-9, the lowest resistivity of 1.8×10^{-3} Ω·cm (mobility = 11.2 $cm^2V^{-1}s^{-1}$, carrier concentration = 1.5×10^{20} cm^{-3}) was attained for the hydrogen-treated and UV-irradiated ZnO film (S6). This improvement in conductivity can be explained by increase of both carrier concentration and mobility in this film induced by the treatment processes.

Comparing S1 and S3, there was marked decrease in resistivity from several hundreds to 4.9×10^{-2} Ω·cm because of the high carrier concentration of 5.1×10^{19} cm^{-3} (mobility = 0.8 $cm^2V^{-1}s^{-1}$) of S3. A similar tendency was also observed for the comparison of S2 and S4. While S2 (thermally treated ZnO film without UV irradiation) exhibited a resistivity of 10.4 Ω·cm with a low carrier concentration of < 10^{18} cm^{-3} (mobility = 0.4 $cm^2V^{-1}s^{-1}$), the resistivity of S4 was 2.4×10^{-2} Ω·cm with a moderately high carrier concentration of 9.7×10^{19} cm^{-3}

(mobility = 1.2 $cm^2V^{-1}s^{-1}$). These results mean carrier concentration was dramatically increased after UV irradiation, which it led to decreased resistivity. This phenomenon may be related to the decomposition of citrate in ZnO crystallites. Citrate contains organic functional groups such as carboxyl moieties that remain in the ZnO film after deposition. The presence of citrate ions in solution is required to attain transparent ZnO films. During the deposition process, the carboxyl groups of citrate ions are adsorbed on Zn ions in the (001) plane, suppressing anisotropic growth along the c-axis, and resulting in ZnO films with a dense structure and smooth surface [41]. While high transparency was attained by adding citrate ions to the solution, the resistivity of the film was still high (hundreds Ω·cm). However, high conductivity could be achieved simply by UV irradiation. ZnO is a well-known photocatalytic materials that can decompose organic species captured in its films by photocatalytic reaction under UV irradiation [15, 42]. In previous result, decrease in the intensity of signals from carboxyl groups such as V_{as} (COO^-) and V_s (COO^-) in the Fourier transform infrared spectra of ZnO film after UV irradiation was observed [15, 43]. This decrease in peak intensity suggests the decomposition of carboxyl groups, which leads to photo-induced doping of C and/or H into the ZnO film. Such doping can effectively generate electrons, resulting in an increase of carrier concentration.

Another reason for the improved conductivity of the ZnO films following thermal treatment with hydrogen and UV irradiation was an increase in mobility. The conductivity of ZnO films is affected by surface defects, negatively charged oxygen species and/or organic impurities [44-46]. Negatively charged oxygen species form depletion regions at grain boundaries and act as trapping sites [45], which has negative effects on both electron mobility and conductivity. Thermal treatment with hydrogen is a simple and effective method to improve mobility because hydrogen readily removes negatively charged oxygen species.

Comparing S4 (treated in air) and S6 (treated in hydrogen) reveals that hydrogen reduction effectively improved mobility; the mobility of S6 (11.2 $cm^2V^{-1}s^{-1}$) was about ten

times higher than that of S4 (1.2 $cm^2V^{-1}s^{-1}$). This high mobility also contributed to the low resistivity of S6 of 1.8×10^{-3} Ω·cm. During hydrogen reduction, negatively charged oxygen species are desorbed from grain boundaries so that the potential barrier is lowered [46]. Additionally, hydrogen passivates the grain boundary surface to remove organic materials and negatively charged oxygen species [47]. To confirm that hydrogen reduction increases mobility, S1 (as-deposited ZnO), S4 (thermally treated in air followed by UV irradiation) and S6 (thermally treated in hydrogen followed by UV irradiation) were analyzed by X-ray photoelectron spectroscopy.

The O1s spectra for S1, S4 and S6 are presented in Figure 4-10. Two peaks at 530.2 and 532.5 eV were observed by fitting with a Lorentzian distribution. The peak at 530.2 eV is assigned O^{2-} ions surrounded by Zn atoms in the wurtzite-structured ZnO, while that at 532.5 eV is attributed to loosely bound oxygen species such as CO_3, O_2, H_2O and carboxyl groups on the ZnO surface and/or grain boundaries [15, 48-49].

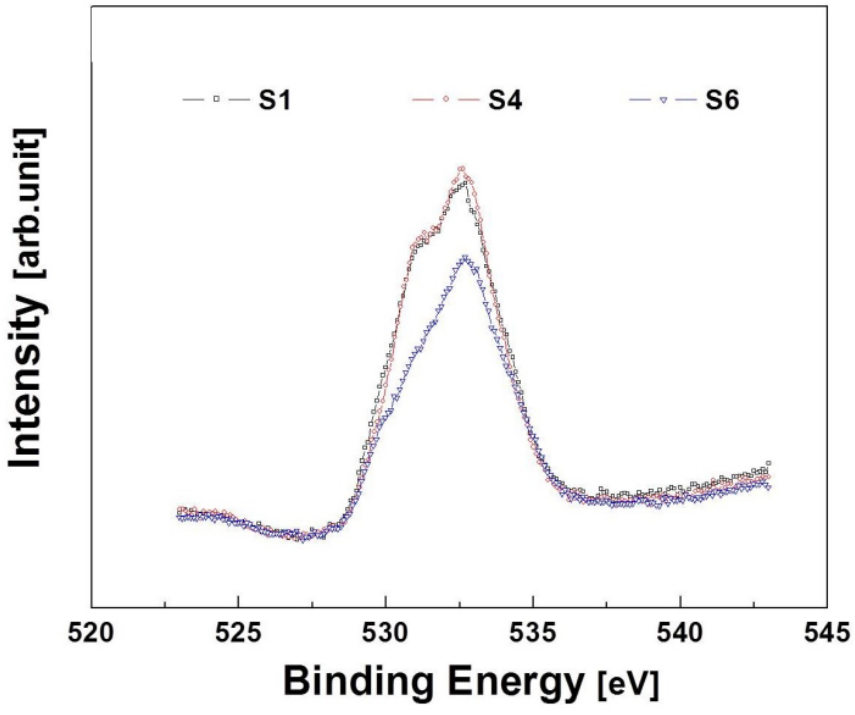

Figure 4-10 Dependence of XPS O1s peaks on preparation conditions.

Here, loosely bound oxygen species generated by negatively charged oxygen might deteriorate film mobility by hindering electron transfer and trapping free electrons. The O1s signals of S1 and S4 were similar. In contrast, the peak at 532.5 eV for S6 was of lower intensity that those of S1 and S4. This corresponds to reduction in the amount of negatively charged oxygen species on the ZnO surface and/or grain boundaries in S6 compared with those in S1 and S4. As mentioned above, this would lead to a decrease in potential barrier, causing the mobility of the hydrogen-treated ZnO film to increase. Additionally, a marked decrease in the intensity of the peak at 530.2 eV was also observed for S6 compared with those of S1 and S4. This means the number of O^{2-} ions surrounded by Zn atoms in the wurtzite-structured ZnO was decreased in S6, so the number of oxygen vacancies was increased, which also improved the mobility.

4.4 Summary

In this study, transparent ZnO films were fabricated by an aqueous solution process using citrate ions. And the effects of thermal treatment temperature before UV illumination on film properties were investigated. The improved crystallographic properties were confirmed through the increase in peak intensity and the decrease in the FWHM of the (101) peak from 0.35 to 0.26^{o} at the thermal treatment temperature of 100 ^{o}C. Decreases in the peak intensities of V_{as} (COO^{-}) and V_{s} (COO^{-}) with increasing temperature were also confirmed using FT-IR spectra. Such decreases corresponded to the reduced amount of organic substance in the films and affected the generation of carriers. The resistivity of 4.1 x 10^{-2} Ω·cm for the sample without heat treatment decreased down to the lowest value of 1.6 x 10^{-2} Ω·cm for the sample thermally treated at 100 ^{o}C. This sample, which has the lowest FWHM and many organic substances, exhibited a high mobility of 3.3 cm^{2} V^{-1} s^{-1} and a very high carrier concentration of 1.1 x 10^{20} cm^{-3}.

And high conductivity was attained by UV irradiation and hydrogen reduction treatment of the films. All films exhibited high transmittance of over 80%, and their optical band gap energy was increased by UV irradiation. The lowest resistivity of 1.8×10^{-3} Ω·cm with a mobility of 11.2 $cm^2V^{-1}s^{-1}$ and carrier concentration of 1.5×10^{20} cm^{-3} was achieved by hydrogen reduction and UV irradiation. Under UV illumination, organic materials present in the ZnO films were decomposed by photocatalytic reaction, which increased the carrier concentration of the films. In the case of mobility, it is thought that negatively charged oxygen species that acted as trap sites at grain boundaries in the ZnO films were removed by hydrogen treatment, resulting in higher mobility.

Reference

1. J. S. Meena, M. C. Chu, Y. C. Chang, H. C. You, R. Singh, P. T. Liu, H. D. Shieh, F. C. Chang, and F. H. Ko, J. Mater. Chem. C 1 (2013) 6613.
2. C. S. Li, Y. N. Li, Y. L. Wu, B. S. Ong, and R. O. Loutfy, J. Mater. Chem. 19 (2009) 1626.
3. J. Hupkes. J. I. Owen, S. E. Pust, and E. Bunte, Chem. Phys. Chem. 13 (2012) 66.
4. J. S. Hong, S. M. Kim, S. J. Park, H. W. Choi, and K. H. Kim, Mol. Cryst. Liq. Cryst. 520 (2010) 19.
5. S. M. Chou, L. G. Teoh, W. H. Lai, Y. H. Su, and M. H. Hon, Sensors 6 (2006) 1420.
6. X. Wen, W. Wu, Y. Ding, and Z. L. Wang, Adv. Mater. 25 (2013) 3371.
7. W. Gao, and Z. Li, Ceram. Int. 30 (2004) 1155.
8. V. Cracium, J. Elders, J. G. E. Gardeniers, and I. W. Boyd, Appl. Phys. Lett. 65 (1994) 2963.
9. X. D. Gao, X. M. Li, W. D. Yu, Mater. Res. Bulletin 40 (2005) 1104.
10. S. Mondal, K. P. Kanta, and P. Mitra, J. Phys. Sci. 12 (2008) 221.
11. H. Bahadur, A. K. Srivastava, R. K. Sharma, S. Chandra, Nanoscale Res. Lett. 2 (2007) 469.
12. R. Ayouchi, F. Martin, D. Leinen, and J. R. Ramos-Barrado, J. Cryst. Growth 247 (2003) 497.
13. Y. Tseng, and J. Wang, Thin Solid Films 534 (2013) 186.
14. K. Schellens, B. Capon, C. De Dobblelaere, C. Detavernier, A. Hardy, and M. K. Van Bael, Thin Solid Films 524 (2012) 81.
15. H. Wagata, N. Ohashi, K. Katsumata, H. Segawa, Y. Wada, H. Yoshikawa, S. Ueda, K. Okada, and N. Matsushita, J. Mater. Chem. 22 (2012) 20706.
16. S. Bang, S. Lee, J. Park, S. Park, W. Jeong, and H. Jeon, J. Phys. D: Appl. Phys. 42 (2009) 235102.

17. R. J. Mendelsberg, S. H. N. Lim, Y. K. Zhu, J. Wallig, D. J. Milliron, and A. Anders, J. Phys. D: Appl. Phys. 44 (2011) 232003.
18. R. C. Hoffmann, M. Kaloumenos, S. Heinschke, E. Erdem, P. Jakes, R. A. Eichel, and J. J. Schneider, J. Mater. Chem. C 1 (2013) 2577.
19. J. S. Hong, N. Matsushita and K. H. Kim, Thin Solid Films 531 (2013) 238.
20. T. T. T. Vo, Y. H. Ho, P. H. Lin, and Y. Tai, Cryst. Eng. Comm. 15 (2013) 6695.
21. A. Z. Barasheed, S. R. Sarath Kumar, and H. N. Alshareef, J. Mater. Chem. C 1 (2013) 4122.
22. E. Hosono, S. Fujihara, and T. Kimura, J. Mater. Chem. 14 (2004) 881.
23. Z. Lin, J. Chang, C. Jiang, J. Zhang, J. Wu, and C. Zhu, RSC Adv. 4 (2014) 6646.
24. D. Raoufi, and T. Raoufi, Appl. Surf. Sci. 255 (2009) 5812.
25. K. Laurent, D. P. Yu, S. Tusseau-Nenez, and Y. Leprince-Wang, J. Phys. D: Appl. Phys. 41 (2008) 195410.
26. F. Ruske, M. Roczen, K. Lee, M. Wimmer, S. Gall, J. Hupkes, D. Hrunski, and B. Rech, J. Appl. Phys. 107 (2010) 013708.
27. X. Yan, Z. Li, R. Chen, and W. Gao, Cryst. Growth Des. 8 (2008,) 2406.
28. B. P. Shantheyanda, V. O. Todi, and K. B. Sundaram, J. Vac. Sci. Technol. A 29 (2011) 051514.
29. Y. S. Jung, J.Y. Seo, D.W. Lee, and D.Y. Jeon, Thin Solid Films 445 (2003) 63.
30. Y. J. Kim, and H. J. Kim, Mater. Lett. 41 (1999) 159.
31. V. Kumar, R. G. Singh, L. P. Purohit, and R. M. Mehra, J. Mater. Sci. Technol. 27 (2011) 481.
32. K. Yu, Z. Jin, X. Liu, J. Zhao, and J. Feng, Appl. Surf. Sci. 253 (2007) 4072
33. M. Babar Shahzad, H. Lu, P. Wanga, and Y. Qi, Cryst. Eng. Commun. 14 (2012) 7123
34. Y. Masuda and K. Kato, Thin Solid Films 516 (2008) 2474

35. B. E. Semelius, K. F. Berggren, Z. C. Jin, I. Hamberg, and C.G. Granqvist, Phys. Rev. B 37 (1988) 10244
36. G. B. Williamson, and R. E. Smallman, Phios. Mag. 1 (1956) 34.
37. B. D. Cullity, Elements of X-ray Diffraction, Addison-Wesley, Reading, MA 1978, p. 102.
38. J. Tauc, Amorphous and Liquid Semiconductors Plenum, Plenum Press, 1974, P. 159.
39. E. A. David, and N. F. Mott, Philos. Mag. 22 (1970) 903.
40. B. E. Sernelius, K. F. Berggren, Z. C. Jin, I. Hamberg, and C. G. Granqvist, Phys. Rev. B 37 (1998) 10244.
41. H. Wagata, N. Ohashi, T. Taniguchi, K. Katsumata, K. Okada, and N. Matsushita, Cryst. Growth Des. 10 (2010) 4968.
42. H. Wagata, K. Katsumata, N. Ohashi, M. Sakai, A. Nakajima, A. Fujishima, K. Okada, and N. Matsushita, Photochem. Photobio. 87 (2011) 1009.
43. J. S. Hong, H. Wagata, K. Katsumata, K. Okada, and N. Matsushita, Jpn. J. Appl. Phys. 52 (2013) 110108.
44. A. Kushwaha, and M. Aslam, J. Phys. D: Appl. Phys. 46 (2013) 485104.
45. Z. G. Wang, X. T. Zu, and S. L. M. Wang, Physica E 35 (2006) 199.
46. H. J. Jin, Y. H. Jeong, and C. B. Park, Trans. Electr. Electr. Mater. 9 (2008) 67.
47. N. H. Nickel, N. M. Johnson, and W. B. Jackson, Appl. Phys. Lett. 62 (1993) 3285.
48. H. J. Bong, W. H. Lee, D. Y. Lee, B. J. Kim, J. H. Cho, and K. W. Cho, Appl. Phys. Lett. 96 (2010) 192115.
49. T. Ohsawa, Y. Adachi, I. Sakaguchi, K. Matsumoto, H. Haneda, S. Ueda, H. Yoshikawa, K. Kobayashi, and N. Ohashi, Chem. Mater. 21 (2009) 144.

Chapter 5

Solution-processed ZnO Films on Flexible Substrates

Rod structure and transparent conductive ZnO films were directly deposited on polyethersulfone (PES) substrate by aqueous solution process at low substrate temperature of 85^{o}C. All films crystallized in wurtzite hexagonal structure without seed layer and another impurity phases were not detected. As-deposited ZnO film without citrate ions in reaction solution had rod array structure. In contrast, ZnO film with citrate ions indicated dense structure with smooth surface. These changed structures affect to their transparency, as a result, transmittance of as-deposited ZnO films were improved from 11.9 to 85.3 % with their change of structure from rod to continuous structure. ZnO film having dense surface had low resistivity of 9.1 x 10^{-3} Ω·cm, high carrier concentration of 2.1 x 10^{20} cm^{-3} and mobility of 1.5 cm^{2} $V^{-1}s^{-1}$, after UV irradiation.

5.1 Introduction

Recently, researches for the flexible electronic devices have been intensively studied and one of the most promising fields due to light, portability, and their development possibility. Because of these merits, it can be applied to various applications such as electronic papers, digital signage and flexible organic light emitting devices (OLEDs) [1-4]. Among the several researches for flexible electronics, deposition of TCO film on plastic substrate to use as electrode is very important because, transparent electrode is fundamental part to operate the all of the devices.

There are many kinds of dry processes like sputtering, pulsed laser deposition, and ion plating to deposit ZnO film on plastic substrate, representative one is sputtering. However,

they are energy-intensive and complicated, for these reasons, solution-processed deposition methods have been proposed due to their simplicity, easy to handle and low in cost. In another words, solution process is the most optimum method to fabricate the cost-effective electronic devices. However, these solution processes such as sol-gel method, chemical bath deposition (CBD) and spray pyrolysis requires long period of reaction and seed layer for good adhesion to substrate [5-8]. Especially, high substrate temperature and/or post annealing process are necessary for crystallization. These things lead to warping of substrate and it causes the peeling-off of the thin film. For these reason, conventional solution processes are difficult to deposit the ZnO film on plastic substrate. Therefore, another method which can be stably deposit the film on plastic substrate without peeling off is necessary. In contrast, the spin-spray method is low temperature process, it can deposit high quality crystallized ZnO film without high substrate temperature and post-annealing process [9-10].

Plastic substrates such as polyether-sulfone (PES), polyethylene-terephthalate (PET), polycarbonate (PC), polyimide (PI), polymethyl-methacrylate (PMMA) and polyethylene-naphthalate (PEN), have been intensively studied for flexible electronic device [11-17]. Among them, in this study, ZnO films were deposited on PES substrates by the spin-spray method and their properties were investigated.

5.2 Experimental Procedure

5.2.1 Deposition of ZnO Films on PES substrates

Before the deposition, plastic substrate such as PES (40 x 30 x 0.3 mm) was ultrasonically cleaned to remove the impurity on the substrate surface. The substrates were cleaned in deionized water and ethanol for 5 min and dried for 10 min in conventional oven at 60^{o}C to remove the residual moisture adsorbed onto the surface. And then, PES substrate

was subjected to plasma treatment for 3 min using discharge plasma to increase hydrophilicity on their surface. As a result, contact angle which criterion of hydrophilicity decreased to 5.9^{o}, as shown in Figure 5-1.

Two kinds of solution were used for deposition of ZnO film. The source solution was prepared by dissolving 10 mmol of $Zn(NO_3)_2 \cdot 6H_2O$ in 2.0 L of Millipore deionized water. The reaction solution was prepared by dissolving 120 mL of NH_3 solution (as a pH adjuster) in 1.88 L of Millipore deionized water. $C_6H_5Na_3O_7$ was added to the reaction solution 0 and 2 mmol. Here, the NH_3 solution was used as a *p*H adjuster and $C_6H_5Na_3O_7$ was used as a surfactant to fabricate the continuous structure. These source and reaction solution were simultaneously and continuously spayed onto the rotated substrates for 10 min at 85^{o}C. After deposition process, as-deposited ZnO film which has dense surface was subjected UV irradiation by black-light-blue (intensity = 0.8 mW/cm^2) to obtain the conductivity.

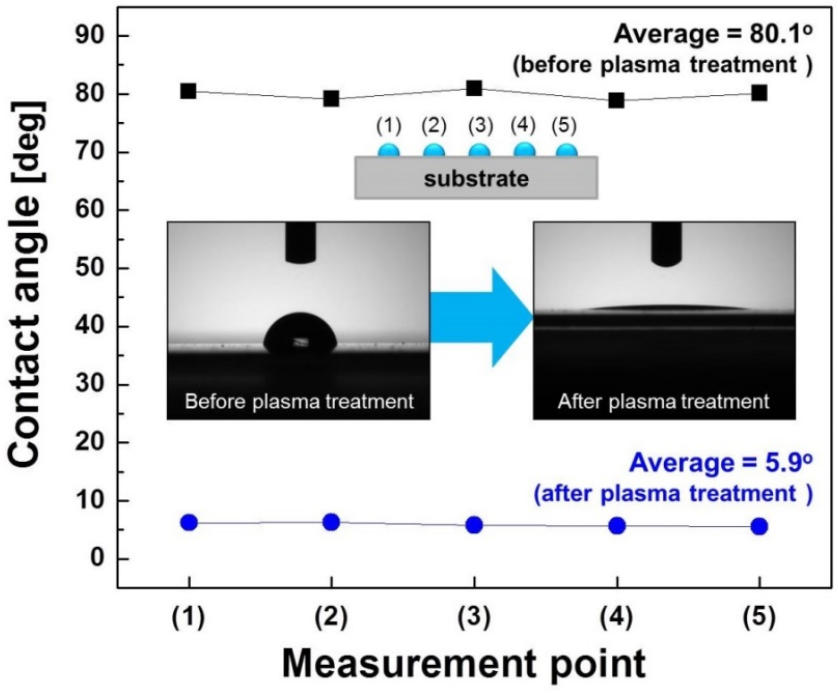

Figure 5-1 Variation of contact angles by discharge plasma.

5.2.2 Characterization

Contact angles and transmittance were measured by (Kyowa Interface Science co., Ltd DMs-400) and Lambda 35 spectrometer (Perkin Elmer Japan), respectively. The surface morphology of ZnO films was observed by scanning electron microscopy (SEM; Hitachi S4000) performed at 15 kV. Structural properties were analyzed by X-ray diffraction (XRD; Rigaku Rint2000) with CuKα radiation (λ=1.5418Å). And the electrical properties were measured by using a Hall Effect measurement system (Nanometrics HL5500).

5.3 Results and Discussion

5.3.1 Rod array structure ZnO film on plastic substrate

Rod array structure ZnO film on PES substrate was successfully deposited by spin-spay method at low substrate temperature of 85^{o}C without seed layer. To evaluate the more details of film properties, surface morphology and crystallographic properties of as-deposited

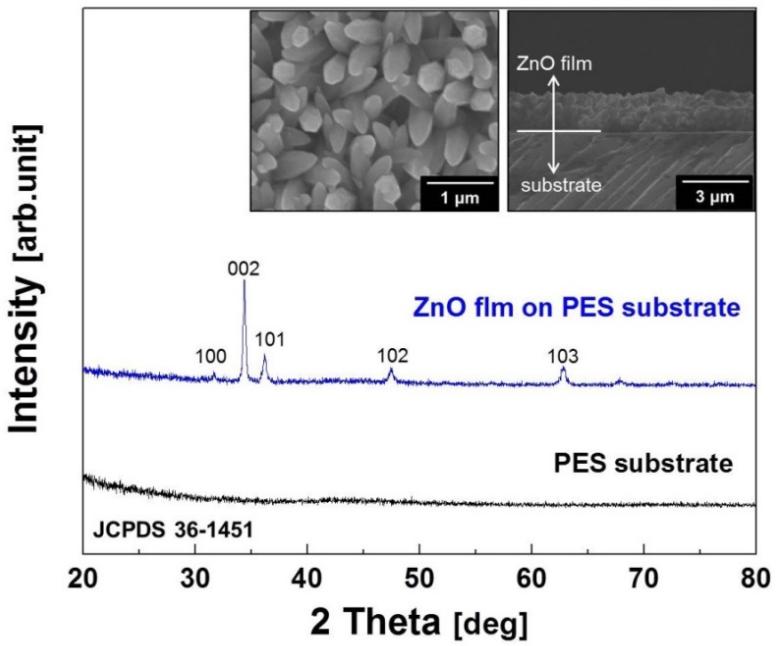

Figure 5-2 XRD pattern and SEM image of rod array ZnO film on PES substrate.

ZnO film was confirmed by SEM and XRD. As shown in Figure 5-2, as-deposited ZnO film on PES substrates by spin-spray method exhibited rod array structure. These images means that as-deposited rod array ZnO films has the preferred orientation along the c-axis, and it can be confirmed by XRD. All diffractions peaks of ZnO films on PES substrate was identified as a hexagonal wurtzite ZnO crystal structure, another impurity phase was not observed. Dominant peak of (002) was observed at 34.4^{o} and it is close to the standard ZnO crystal corresponding to JCPDS 36-1451. The full width at half maximum (FWHM) was confirmed to evaluate the crystallinity, as a result, the FWHM values of (002) peak was 0.25^{o}. This FWHM value is lower than that of reported ZnO film which using a seed layer such as ITO and Si (100) substrates [18]. The crystallite size was also calculated by using Scherrer's equation [19-20]. Calculated crystallite size of ZnO film deposited on PES substrate was 33.3 nm. In case of transmittance, as-deposited ZnO films on PES substrate is very low. As shown in Figure 5-3, ZnO film deposited on PES substrate showed 11.9% transmittance in visible range due to scattering caused by rod array structure. From the results, high crystallinity rod array structure ZnO films deposited on could be confirmed.

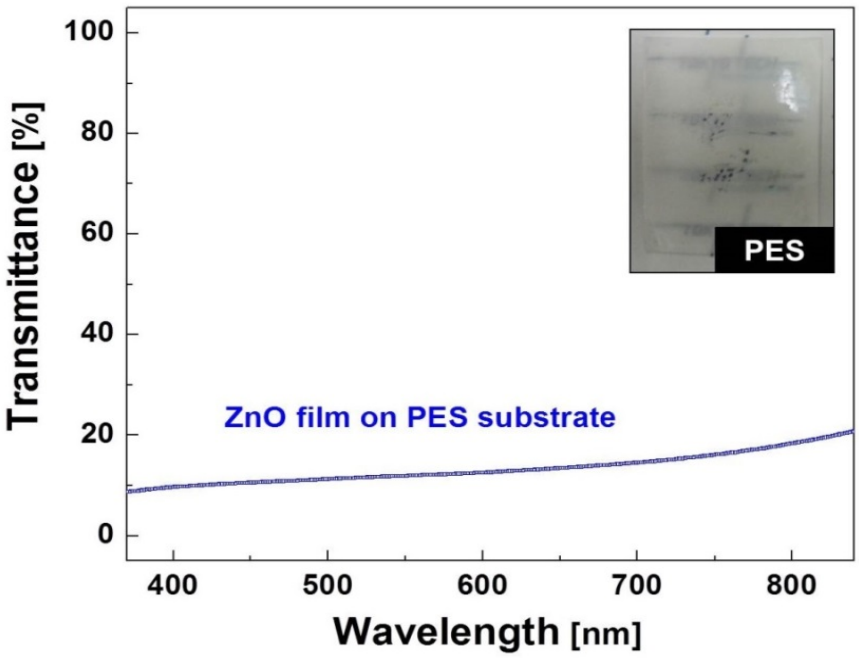

Figure 5-3 Transmittance of rod array ZnO film on PES substrate.

5.3.2 Transparent conductive ZnO films on plastic substrate

Transparent and continuous ZnO films can be fabricating by using a citrate [21]. As shown the inset in Figure 5-4, ZnO film deposited on PES substrate by spin-spray method indicated different morphology clearly. The structure of as-deposited ZnO films changed from rod array to continuous structure by adding citrate in reaction solution. Also, continuously structured ZnO film had a smooth and dense surface. As shown in XRD patterns, the preferred orientation also changed from the (002) to the (101). This changed preferred orientation originated from the existence of citrate ions in solution. Citrate ions selectively adsorb to ZnO (001) plane, it induces the change of the crystal growth. Because of this phenomenon, intensity of the (002) peak and the thickness was decreased due to the suppression of c-axis growth. Additionally, surface morphology also changed to continuous structure [10, 21]. Theses changed morphology result in improving optical properties

As shown in Figure 5-5, as-deposited ZnO film indicated high transparency (above 80%) in visible range and optical band gap energy value calculated by Tauc model and the Davis and Mott model was 3.46 eV [22-23].

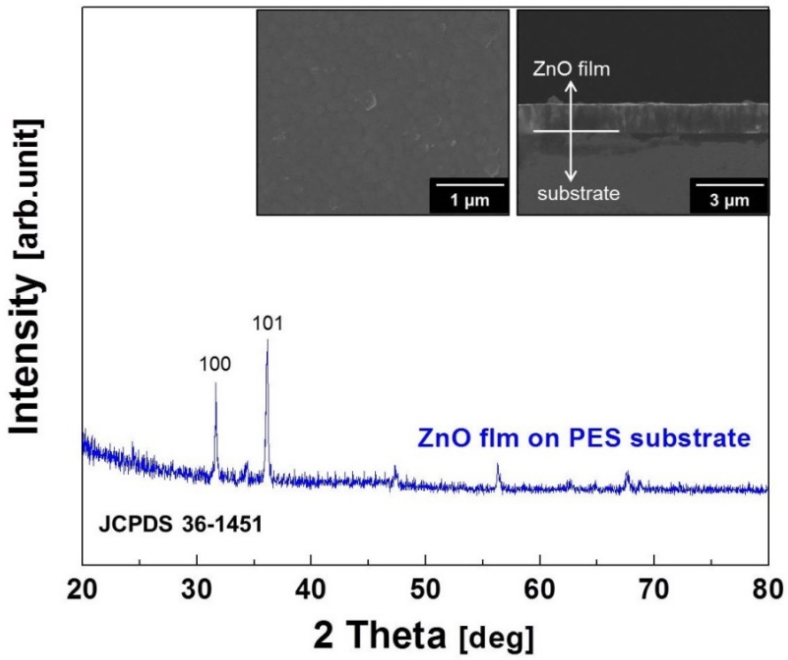

Figure 5-4 XRD pattern and SEM image of rod array ZnO film on PES substrate.

As a transparent electrode, there are many requirements such as high conductivity, smooth surface, high transparency and so on. Among them, the most important factor is conductivity. In case of spin-sprayed ZnO film on PES substrate, it has continuous structure

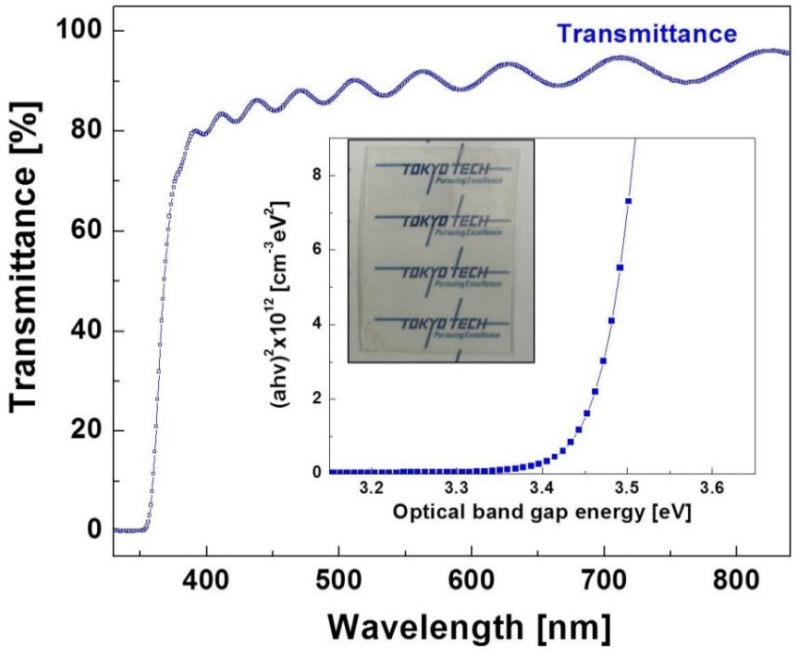

Figure 5-5 Transmittance and optical band gap energy of ZnO film on PES substrate

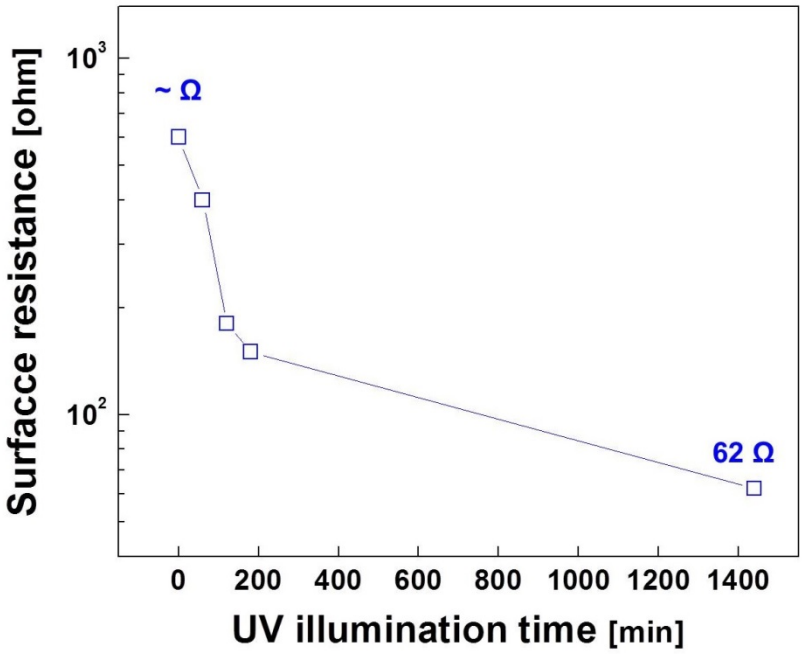

Figure 5-6 XRD pattern and SEM image of rod array ZnO film on PES substrate.

and high transmittance by adding citrate in solution, however, the film exhibited low conductivity due to the organic substance in the film. To obtain the conductivity, as-deposited ZnO film on PES substrate was subjected to UV illumination by using the back-light-blue lamp (intensity = 0.8 mW/cm^2) for 24 hours. I expected that organic substance in the ZnO film would be decomposed by photocatalytic reaction and as a result, conductivity will be obtained by photoinduced ion substitution such as C, and/or H [10, 24].

To confirm the variation of conductivity by UV illumination, surface resistance of UV illuminated ZnO film was measured by tester. As shown in Figure 5-6, as-deposited ZnO film has high surface resistance of several hundred Ω before UV illumination. However, it was drastically decreased to 62 Ω, during UV illumination. In case of resistivity measured by Hall Effect measurement system, UV illuminated ZnO film exhibited 9.1 x 10^{-3} Ω·cm with carrier concentration of 2.1 x 10^{20} cm^{-3} and mobility of 1.5 cm^2 V^{-1}s^{-1}. These improved conductivities are attributed to the increase in carrier concentration, which originated from the decomposition of organic substance such as carboxyl groups under UV illumination [14, 28].

5.3.3 Bending Test

Mechanical flexural strength of TCO film deposited on flexible substrate is important factor for the life time of devices. To improve the mechanical flexural strength, widely used method is multilayer. Generally, multilayer film is consisted of triple layer, such as TCO-Metal-TCO. However, fabrication of multilayer is not simple because establishing the optimum condition of each layer is difficult and complicated. Therefore, it is thought that the best way for flexible devices, is using single layer which has strong flexural strength [25].

Mechanical properties of as-deposited ZnO film on PES substrate was evaluated by using bending test equipment, as shown the in Figure 5-7. Here, ZnO films were deposited on different size of PES substrate (25 x 50 mm^2) for bending test. The bending tests were carried out using cyclic bending equipment at duration of 5000cycles.

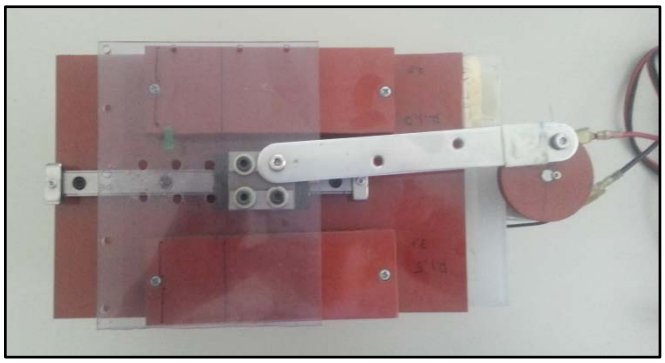

a. View from above

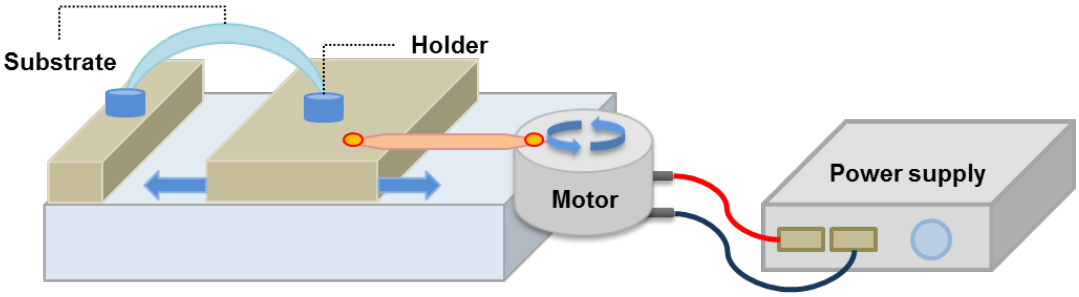

b. Schematic illustration

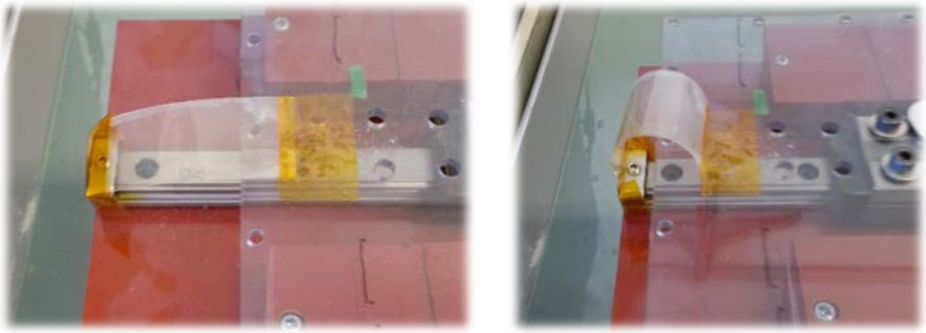

c. Bending test

Figure 5-7 Bending test equipment.

As shown in Figure 5-8, during bending testing, resistivity of as-deposited films was rapidly increased from 9.6 x 10^{-3} Ω·cm to 618 kΩ·cm. In case of 5000 cycles, resistivity could not measure. As a reason for increased resistivity is generation of crack on the film surface (Figure 5-9). In cease of bending tested ZnO film with 500 cycles, crack was not observed on film surface having still low resistivity of 6.7 x 10^{-1} Ω·cm.

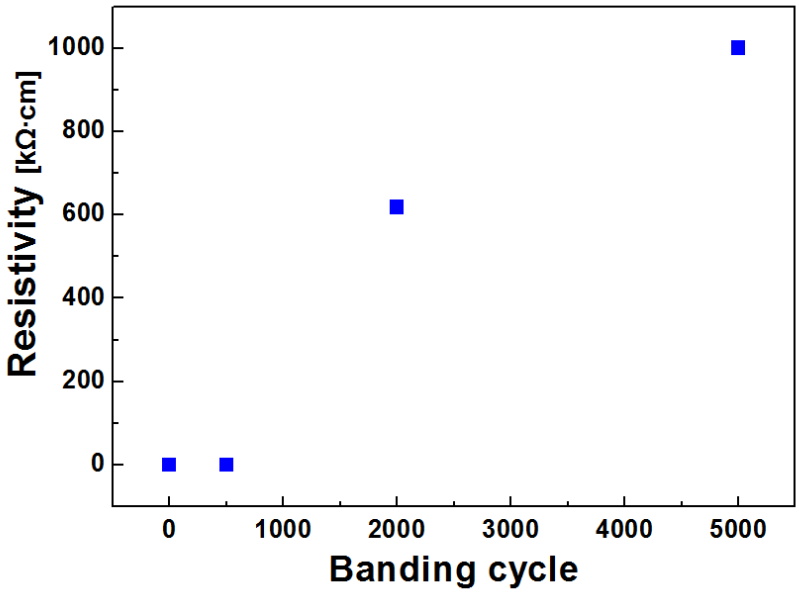

Figure 5-8 Variation of resistivity after bending test

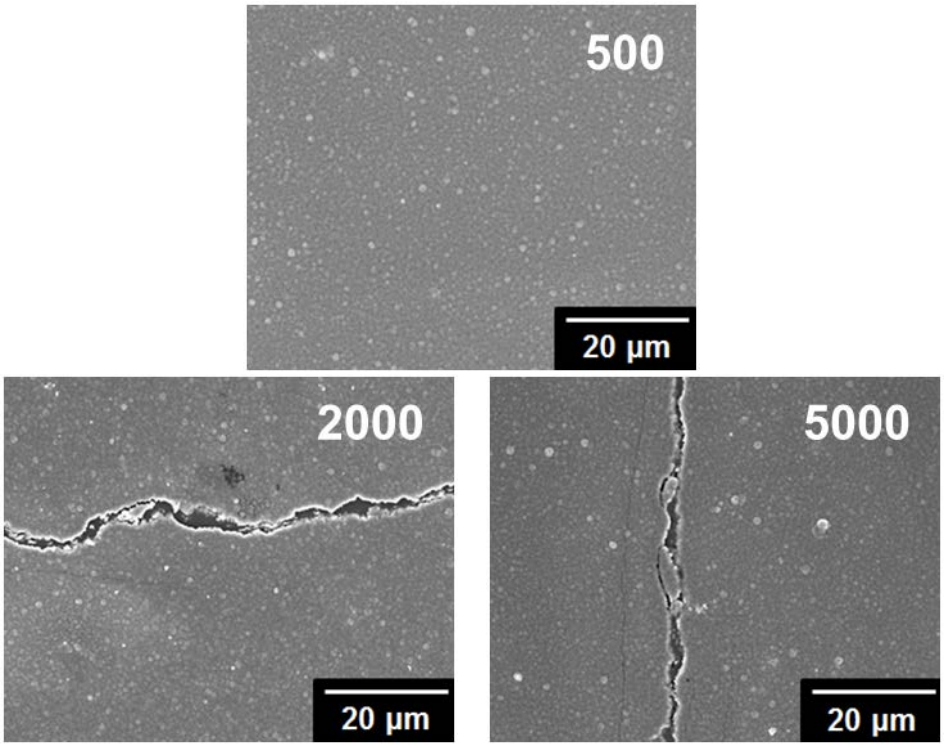

Figure 5-9 Surface morphology of ZnO films after bending test

In contrast, bending tested ZnO films with 2000, and 5000 cycles, they indicated cracks on film surface and had very high resistivity. During bending testing, strain of films is increased, it causes the generation of crack on surface. And it may affect to degradation of resistivity.

5.4 Summary

In this study, rod array structure and transparent conductive ZnO films were successfully deposited on PES substrate by aqueous solution process named Spin-Spray method at low substrate temperature of 85^{o}C, without using seed layer.

Rod array structured ZnO film indicated the preferred orientation along the c-axis and dominant XRD peak of (002) was observed. And continuously structured ZnO film was obtained by adding a citrate in the reaction solution. It has smooth surface morphology and high transmittance above 80%. The conductivity was attained for the film subjected to UV irradiation. UV-irradiated ZnO film has low resistivity of 9.1 x 10^{-3} Ω·cm, high carrier concentration of 2.1 x 10^{20} cm^{-3} and mobility of 1.5 cm^{2} $V^{-1}s^{-1}$.

Reference

1. H. C. You, J. Electrochem. Sci. 8 (2013) 9773.
2. J. J. Ho, and C. Y. Chen, J. Electrochem. Society 152 (2005) G57.
3. D. W. Choi, S. J. Kim, H. J. Lee, K. B. Chung, and J. S. Park, Current Appl. Phys. 12 (2012) S19.
4. D. J. Rogers, F. Hosseini Teherani, V. E. Sandra, and M. Razeghi, Proc. of SPIE 7605 (2010) 76050K-1.
5. N. S. Ridhuan, K. A. Razak, Z. Lockman, and A. A. Aziz, PLOS ONE 7 (2012) e50405.
6. X. Yan, Z. Li, R. Chen, and W. Gao, Cryst. Growth Des. 8 (2008) 2406.
7. Q. Yu, W. Fu, C. Yu, H. Yang, R. Wei, Y. Sui, S. Liu, Z. Liu, M. Li, G. Wang, C. Shao, Y. Liu, and G. Zou, J. Phys. D. Appl. Phys. 40 (2007) 5592.
8. M. Krunks, T. Dedova, E. Karber, V. Mikli, I. Oja Acik, M. Grossberg, and A. Mere, Physica B 404 (2009) 4422.
9. H. Wagata, N. Ohashi, T. Taniguchi, A. K. Subramani, K. Katsumata, K. Okada, and N. Matsushita, Cryst. Growth Des. 10 (2010) 3502.
10. J. S. Hong, H. Wagata, K. Katsumata, K. Okada, and N. Matsushita, Jpn. J. Appl. Phys. 52 (2013) 110108.
11. P. H. Lei, C. M. Hsu, and Y. S. Fan, Org. Electron. 14 (2013) 236.
12. T. Gui, G. Dong, F. Gao, Y. Xiao, Q. Chen, and X. Diao, Appl. Surf. Sci. 282 (2013) 467.
13. Q. Shi, K. Zhou, M. Dai, S. Lin, H. Hou, C. Wei, and F. Hu, Vacuum 94 (2013) 81
14. M. Matsumura, and R. P. Camata, Thin Solid Films 476 (2005) 317.
15. T. Guo, G. Dong, Q. Liu, M. Wang, F. Gao, Q. Chen, H. Yan, and X. Diao, Superlattice. Microstruct. 64 (2009) 552.

16. K. Tao, Y. Sun, H. Cai, D. Zhang, K. Xie, and Y. Wang, Appl. Surf. Sci. 258 (2012) 5943.
17. P. H. Lei, H. M. Wu, and C. M. Hsu, Surf. Coat. 206 (2012) 3258.
18. R. B. Marcia del, J. P. Oscar, P. S. Surinder, A. J. Jose, A. A. Joaquin, and P. H. Samuel, Mater. Sci. Applications 4 (2013) 29.
19. G. B. Williamson, and Smallman, Phios. Mag. 1 (1956) 34
20. B. Cllity, 1978 Elements of X-ray Diffraction (Reading: Addison-Wesley) 102
21. H. Wagata, N. Ohashi, T. Taniguchi, K. Katsumata, K. Okada, and N. Matsushita, Cryst. Growth Des. 10 (2010) 4968.
22. J. Tauc, 1974 Amorphous and Liquid Semiconductors Plenum.
23. E. A. David, and N. F. Mott, Philos. Mag. 22 (1970) 903.
24. H. Wagata, N. Ohashi, K. Katsumata, H. Seagawa, Y. Wada, H. Yoshikawa, S. Ueda, K. Okada, and N. Matsushita, J. Mater. Chem. 22 (2012) 20706.
25. J. B. Lee, H. J. Kim, S. G. Kim, C. S. Hwang, S. H. Hong, Y. H. Shin, and N. H. Lee: Thin Solid Films 435 (2003) 179.

Chapter 6

Fabrication of Heterostructured Ferrite / ZnO film by Aqueous Solution Process

Heterostructured α-Fe_2O_3 / ZnO film and Fe_3O_4 / ZnO film were fabricated by using spin-spray method and properties of each layer and heterostructured α-Fe_2O_3 / ZnO film and Fe_3O_4 / ZnO film were investigated. First, as-deposited ZnO layer on glass substrate exhibited high transmittance of above 80 % in visible range and a low resistivity of ~ 10^{-2} Ω·cm. The formation of α-Fe_2O_3 layer and Fe_3O_4 layer on glass substrate was confirmed by XRD. These α-Fe_2O_3 and Fe_3O_4 layer were successively deposited on ZnO layer and it was confirmed that heterostructured α-Fe_2O_3 / ZnO and Fe_3O_4 / ZnO double layered films could be fabricated by aqueous solution process.

6.1 Introduction

Ferrite films have been used for various applications such as tunneling magnetoresistive (TMR) devices, giant magnetoresistive (GMR) devices, and gas sensor, semiconductor electrode [1-3].

Among the various ferrite films, the hematite (α-Fe_2O_3) has been studied as a semiconductor usable for gas sensor and semiconductor electrode. The α-Fe_2O_3 is semiconductor material having band gap energy of 2.2 eV [4]. Also, α-Fe_2O_3 film can be applied for environmental purification due to their properties such as water splitting and photodecomposition [5-7]. Especially in case of water splitting, it can be applied as a photo electrode to generate hydrogen from the water. Although sputtering and chemical vapor deposition method has been used for the deposition method of α-Fe_2O_3 film, this method required high process temperature, and they are not suitable to apply to transparent

electrodes that require a low heat resistance. Because of these reasons, solution process has been receiving attention as an alternative fabrication method.

And magnetite (Fe_3O_4) has been also receiving attention and is promising material for spin injection into semiconductors due to its high Curie temperature of ~860 K and half metallic properties at room temperature [8-9]. Also, epitaxial growth of Fe_3O_4 based on metallic film seems very important for TMR and GMR devices as a polarized spin injector. Among the various fabrication methods, the sputtering process is the most representative one. Fe_3O_4 layer deposited on ZnO (00n) layers by sputtering likely to have their preferential orientation along the (nnn) plane [10-13]. However, the multilayer films by sputtering process would require a high substrate temperature and/or additional heating process in vacuum system. These high temperature processes cause the change in properties of under layer such as ZnO, MgO, and Si. Therefore low temperature process is required.

In this chapter, heterostructured ferrite / ZnO films such as α-Fe_2O_3 / ZnO, and Fe_3O_4 / ZnO films were deposited by spin-spray method As mentioned before (in chapter 1), spin-spray method is low temperature solution process to fabricate both of transparent conductive oxide film and ferrite film. And their crystallographic properties were investigated.

6.2 Experimental Procedure

6.2.1 Deposition of Double layered Iron Oxide / ZnO

▪ **Deposition of ZnO layer**

First of all, ZnO layers were deposited on plasma treated glass substrate. The source solution was prepared by dissolving 10 mM $Zn(NO_3)_2 \cdot 6H_2O$ (Zinc nitrate hexahydrate, Wako Pure Chemical Industries, Ltd., Japan, 99.0 %) and the reaction solution was prepared by dissolving NH_3 (Ammonia solution, Wako Pure Chemical Industries, Ltd., Japan, 28.0%) and 2 and 0~10 mM $Na_3C_6H_5O_7$ (Trisodium citrate, Wako Pure Chemical Industries, Ltd., Japan,

97.0%) in same amount of de-ionized water. ZnO layers were deposited by spraying these solutions for 10 minutes. And then, as-deposited ZnO layers were subjected to UV irradiation with BLB lamp to decompose citrate incorporated in the deposited films.

▪ **Deposition of α-Fe_2O_3 and Fe_3O_4 layers**

The α-Fe_2O_3 layer was deposited for 30 min on glass substrate and as-deposited ZnO layers. The source solution of 10 mM $FeCl_2 \cdot 4H_2O$ (Iron chloride tetrahydrate Wako Pure Chemical Industries, Ltd., Japan, 99.0 %) and the reaction solution of 20 mM $NaNO_2$ (Sodium nitrite, Wako Pure Chemical Industries, Ltd., Japan, 98.5 %) in same amount of de-ionized water were used for the deposition of α-Fe_2O_3 layer.

And the Fe_3O_4 layers were deposited on as-sprayed these ZnO layers. The source solution of 20mM $FeCl_2 \cdot 4H_2O$ in 2.0L of D.I.Water and the reaction solution of 5mM $NaNO_2$ and 65mM CH_3COONa in same amount of D.I.Water were used for the fabrication of Fe_3O_4 layers.

6.2.2 Characterization

The electrical and optical properties were measured by Hall Effect measurement system (HMS-3000, ECOPIA) and Lambda 35 spectrometer (Perkin Elmer Japan Co., Ltd.), respectively. The surface properties of as-deposited layers were observed by scanning electron microscopy operated at 15 kV (SEM, S4000, Hitachi, Ltd.) and crystallographic properties were analyzed by using X-ray diffraction (XRD, Rint2000, Rigaku Corp.).

6.3 Results and Discussion

6.3.1 α-Fe_2O_3 / ZnO film

Figure 6-1 shows SEM images of as-deposited ZnO layers at citrate concentration of 2 and 10 mM. Both of as-deposited ZnO layers shows dense and smooth surface. Thickness of ZnO layers decreased from 1.4 to 1.2 μm with increasing of citrate concentration from 2 to

10 mM. This result is related to the function of citrate ion to the growth of ZnO crystallites in solutions. As-deposited ZnO layer without citrate indicated rod array structure with (002) preferred orientation [14]. However, ZnO layer deposited using citrate in solution had continuous structure because citrate ions were absorbed to (0001) plane and it suppressed the anisotropic growth along the (001) direction [15-16]. Since this growth control suppressed the growth speed of ZnO columnar, the thickness was decreased with increasing citrate concentration.

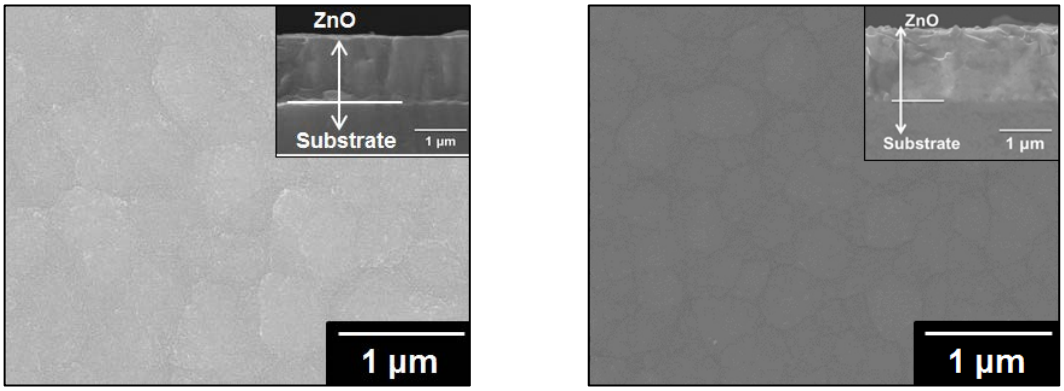

(a) Citrate 2 mM **(b)** Citrate 10 mM

Figure 6-1 SEM images of as-deposited ZnO layers.

Figure 6-2 shows XRD patterns of ZnO films fabricated by spin-spray method at citrate concentration of (a) 2 mM and (b) 10 mM. The ZnO films are in hexagonal crystallographic phase (JCPDS 36-1451). Variation of the full width at half maximum (FWHM) which is one of the criteria of crystallinity was observed. FWHM of (101) peak decreased from 0.18 to 0.16^{o} with increasing citrate concentration from 2 to 10 mM, these result indicates improved crystallinity, and it also contribute to change of crystallite size. Crystallite size calculated by Scherrer's equation also increased from 46.4 to 51.9 nm.

All as-deposited ZnO films were UV illuminated under Black-Light-Blue (BLB) lamp (Wavelength: 300 ~ 400 nm, Intensity ≒ 0.6 mW/cm^2) to obtain conductivity. Resistivity of ZnO layers were changed by UV illumination time, as shown in Figure 6-3.

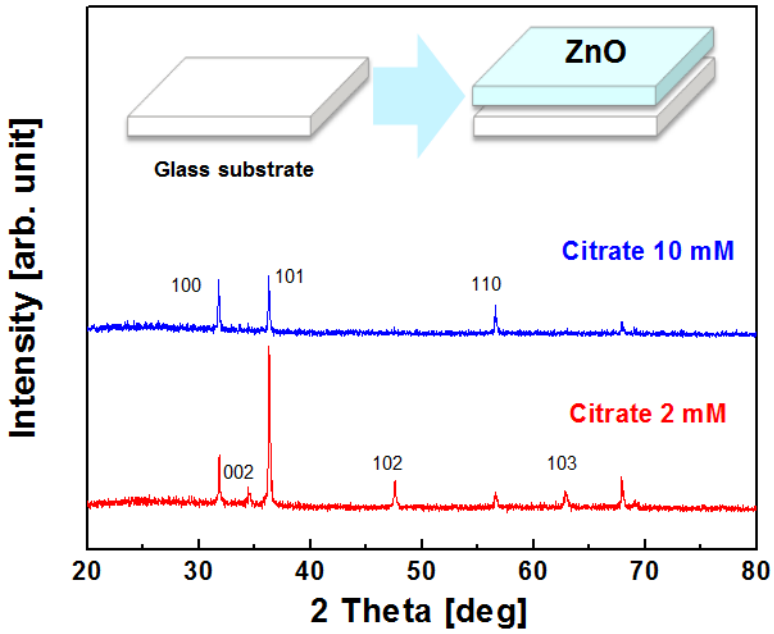

Figure 6-2 XRD patterns of as-deposited ZnO layers.

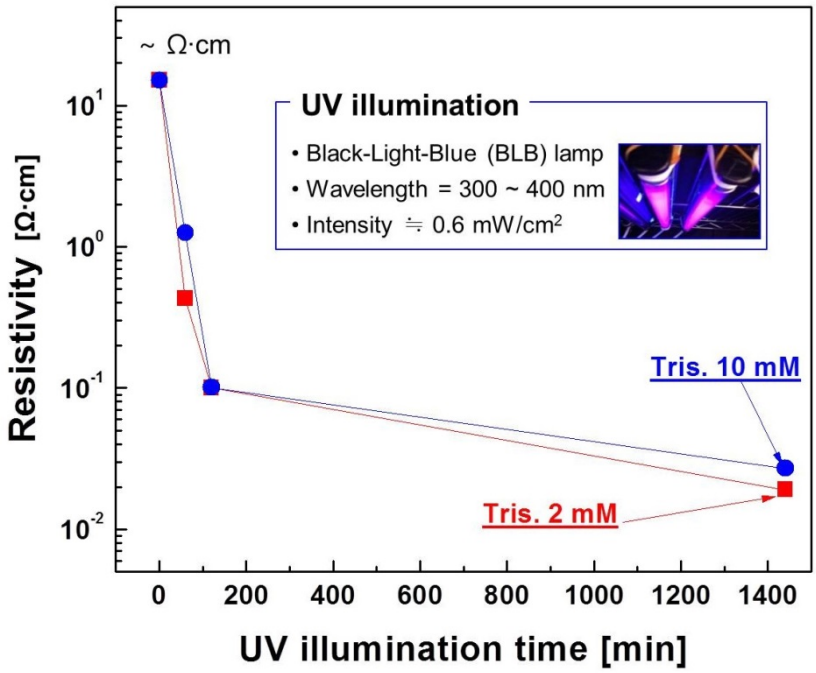

Figure 6-3 Change in resistivity by UV irradiation.

Before UV illumination, ZnO layer had low conductivity (~ several hundred Ω·cm), however, the resistivity was dramatically decreased due to the decomposition of organic

substance in ZnO crystallite by photocatalytic reaction of ZnO under UV illumination condition [16-17]. As a result, the lowest resistivity of 1.8 x 10^{-2} Ω·cm was attained at citrate concentration of 2 mM (2.7 x 10^{-2} Ω·cm at 10 mM). Both of ZnO layers showed high transmittance above 80 % and optical band gap energy of approximately 3.6 eV, as shown in Figure 6-4.

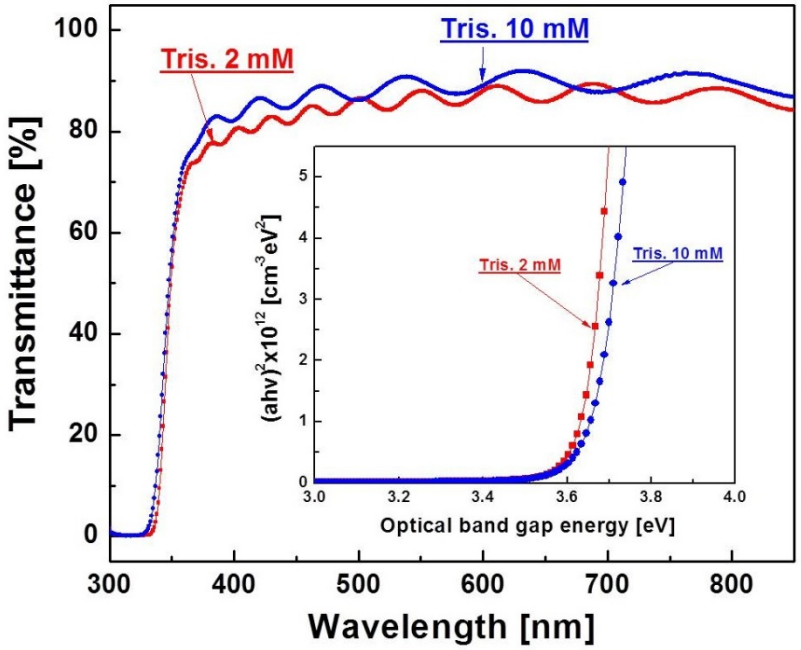

Figure 6-4 Optical properties of ZnO layers after UV irradiation.

Figure 6-5 shows XRD pattern and SEM image of α-Fe_2O_3 film deposited on glass substrate by spin-spray method. All of diffraction peaks were confirmed as α-Fe_2O_3 phase, and other peaks were not found (JCPDS 33-0664). As-deposited α-Fe_2O_3 film had thickness of 320 nm and rough surface.

After evaluation of α-Fe_2O_3 layer fabricated on glass substrate, α-Fe_2O_3 layer was deposited on ZnO layers. Figure 6-6 shows SEM images of as-fabricated heterostructured α-Fe_2O_3 / ZnO double-layered film deposited at different citrate concentrations during ZnO layer deposition. It was confirmed the α-Fe_2O_3 layer deposited on as-deposited ZnO layers and heterostructured α-Fe_2O_3 / ZnO double-layered film had indicated dense surface. More details of structural properties were investigated by XRD, as shown in Figure 6-7.

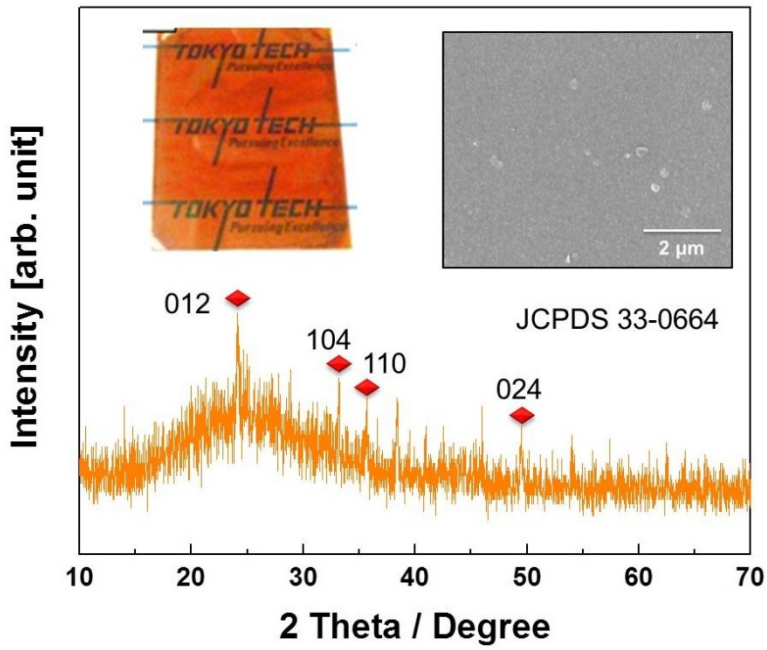

Figure 6-5 XRD patterns and SEM image of α-Fe_2O_3 layer.

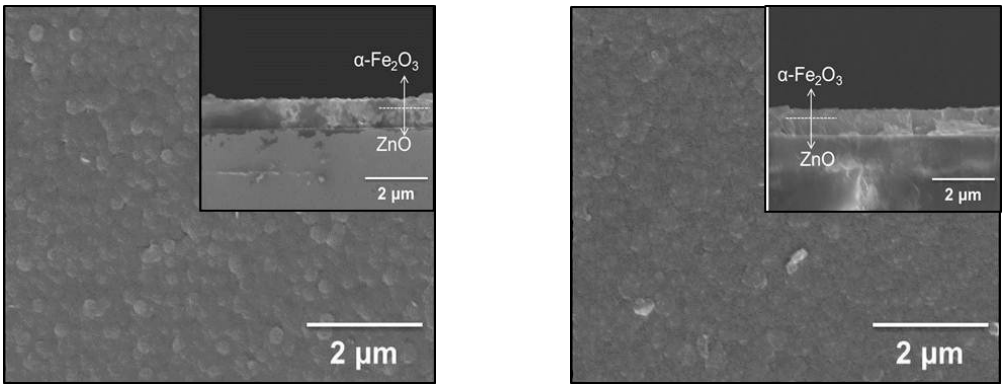

(a) Citrate 2 mM **(b)** Citrate 10 mM

Figure 6-6 SEM images of heterostructured α-Fe_2O_3 / ZnO films.

Figure 6-7 shows XRD patterns of heterostructured α-Fe_2O_3 / ZnO double-layered films fabricated by spin-spray method. All peaks corresponded to ZnO and α-Fe_2O_3 phase, and no other peaks were found. From the XRD result, we could confirm that the change of structural properties with increasing of citrate concentration. Crystallinities were degraded and thickness of α-Fe_2O_3 / ZnO layer was also decreased by increasing citrate concentration.

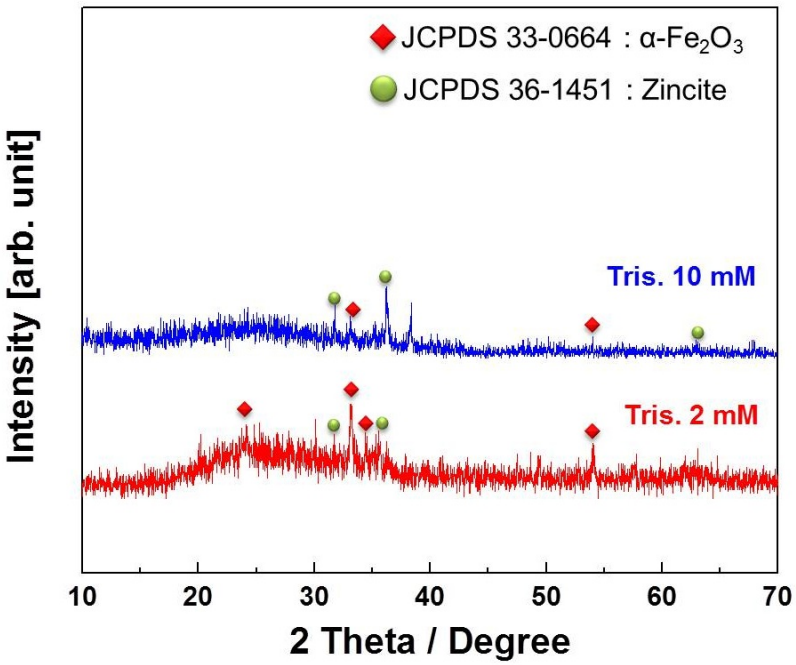

Figure 6-7 XRD patterns of heterostructured α-Fe_2O_3 / ZnO films.

6.3.2 Fe_3O_4 / ZnO film

Figure 6-8 indicated the SEM images of ZnO layer surface morphology deposited at different citrate concentrations. As mentioned before (at Chapter 2), surface morphologies of ZnO layers were gradually changed to dense surface by adding citrate in reaction solution, ZnO layers have dense surface at above 5 mM of citrate concentration.

These changed surface morphologies also affect to their transmittance, as shown in Figure 6-9. ZnO layer deposited without citrate has low transmittance due to the scattering caused by rod structure. However it was increased by adding citrate ions in reaction solution, as a result, ZnO layers deposited at above 5 mM of citrate concentration indicated high transmittance of 80%.

In case of resistivity, as-deposited ZnO layers were decreased by UV irradiation, as-shown in Figure 6-10. ZnO layers deposited at above 5 mM of citrate concentration has low resistivity of ~10^{-2} Ω·cm (1.6 x 10^{-2} Ω·cm at 5mM, and 2.7 x 10^{-2} Ω·cm at 10 mM). However,

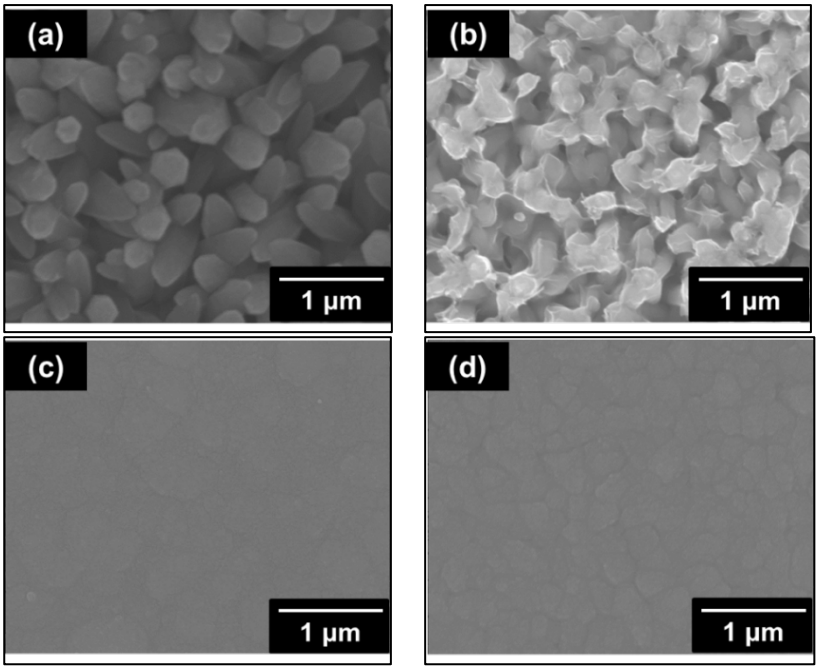

Figure 6-8 SEM images of ZnO layers; (a) citrate none, (b) Citrate 0.05 mM, (c) Citrate 5 mM, and (d) citrate 10 mM.

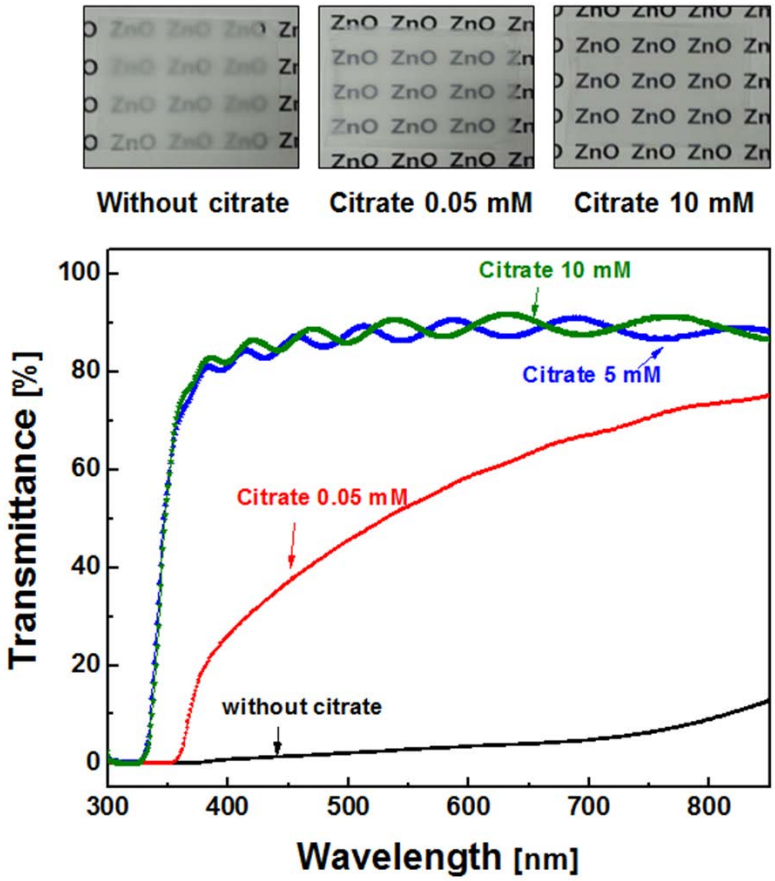

Figure 6-9 Change in transmittance by citarte concentration.

ZnO layer deposited at 0.05 mM has high resistivity approximately 4 Ω·cm due to their rough surface. Additionally, low amount of absorbed citrate ions in ZnO layers are also one of the reasons for the low resistivity. ZnO film prepared by spin-spray method could be

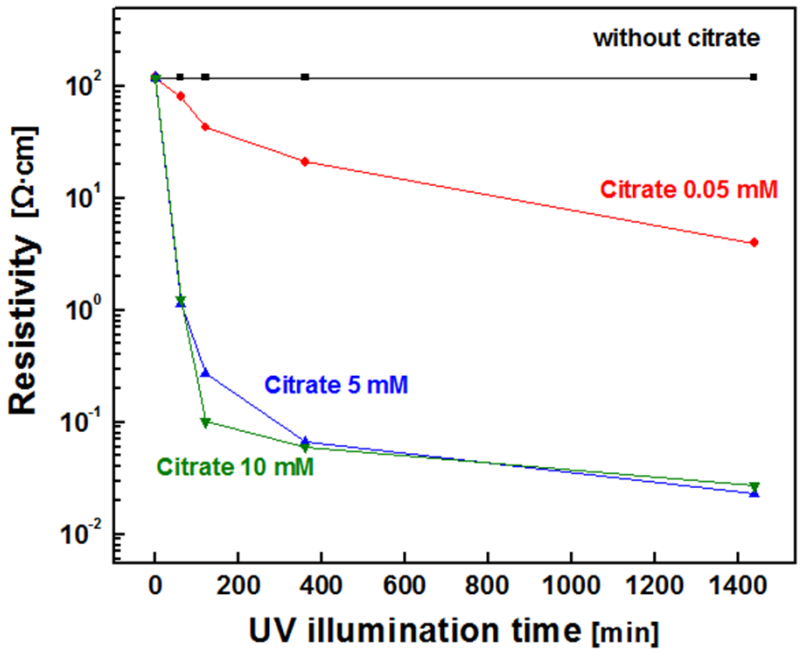

Figure 6-10 Variation of resistivity by UV irradiation.

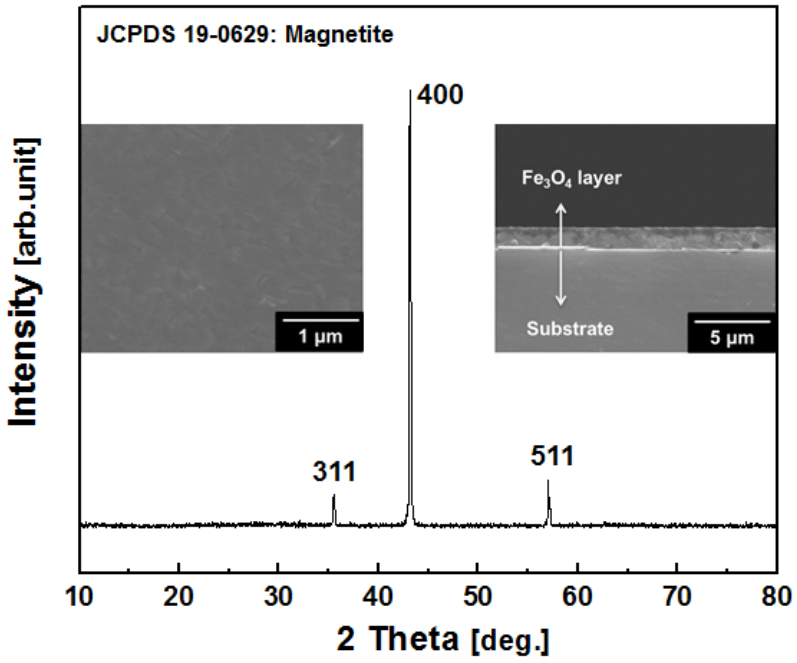

Figure 6-11 XRD pattern and SEM image of as-deposited Fe_3O_4 layer.

attained the conductivity caused by decomposition of organic substance such as citrate ions under UV illumination. Here, amount of citrate ion in the film is important factor, and it was already confirmed at Chapter 4.

Figure 6-11 shows the XRD pattern and SEM images of as-deposited Fe_3O_4 layer. There are three dominant peaks were observed corresponding (311), (400), and (511) at 35.5, 43.1, and 57.0^o, respectively. These peaks were confirmed as magnetite phase and another impurity peak was not observed. Fe_3O_4 layer indicated smooth surface and confirmed thickness from cross-sectional SEM image was 1.4 μm. And then, heterostructured Fe_3O_4 / ZnO was prepared by using Fe_3O_4 layer and ZnO layer.

Figure 6-12 shows the change of surface morphology of as-prepared Fe_3O_4 / ZnO films at various citrate concentrations. As-prepared Fe_3O_4 / ZnO film without citrate indicated the rough surface morphorogy, while it was gradually changed to smooth surface. Especially, in case of as-prepared Fe_3O_4 / ZnO film at citrate concentration of 10 mM, it had cubic shape, as shown in Figure 6-13. To cofirm the more details, as-prepared Fe_3O_4 / ZnO films were anlaized by XRD. Figure 6-14 shows the XRD patterns of as-prepared Fe_3O_4 / ZnO films at various citarte concentrations. All diffraction peaks were confirmed as a ZnO and magnetite by using JCPDS 36-1451 (Zincite) and JCPDS 19-0629 (Magnetite) and another impurity peaks such as hydroxide was not observed. And preferential orientation along the (nnn) plane was also confirmed. As shown in Figure 6-14, (111), (222), and (333) peaks were observed at 18.3, 37.1, and 57.0^o, these results are very close to the results of the standard magnetite crystal. Generally, these preferential orientations along the (nnn) plane are observed in Fe_3O_4 layer deposited on ZnO (00n) layers by sputtering. However, heterostructured Fe_3O_4 / ZnO film by sputtering process would require a high substrate temperature and/or additional heating process in vacuum system. In contrast, heterostructured Fe_3O_4 / ZnO film which has preferential orientations along the (nnn) planes such as (111), (222), and (333) peaks were simply fabricated by solution process at low

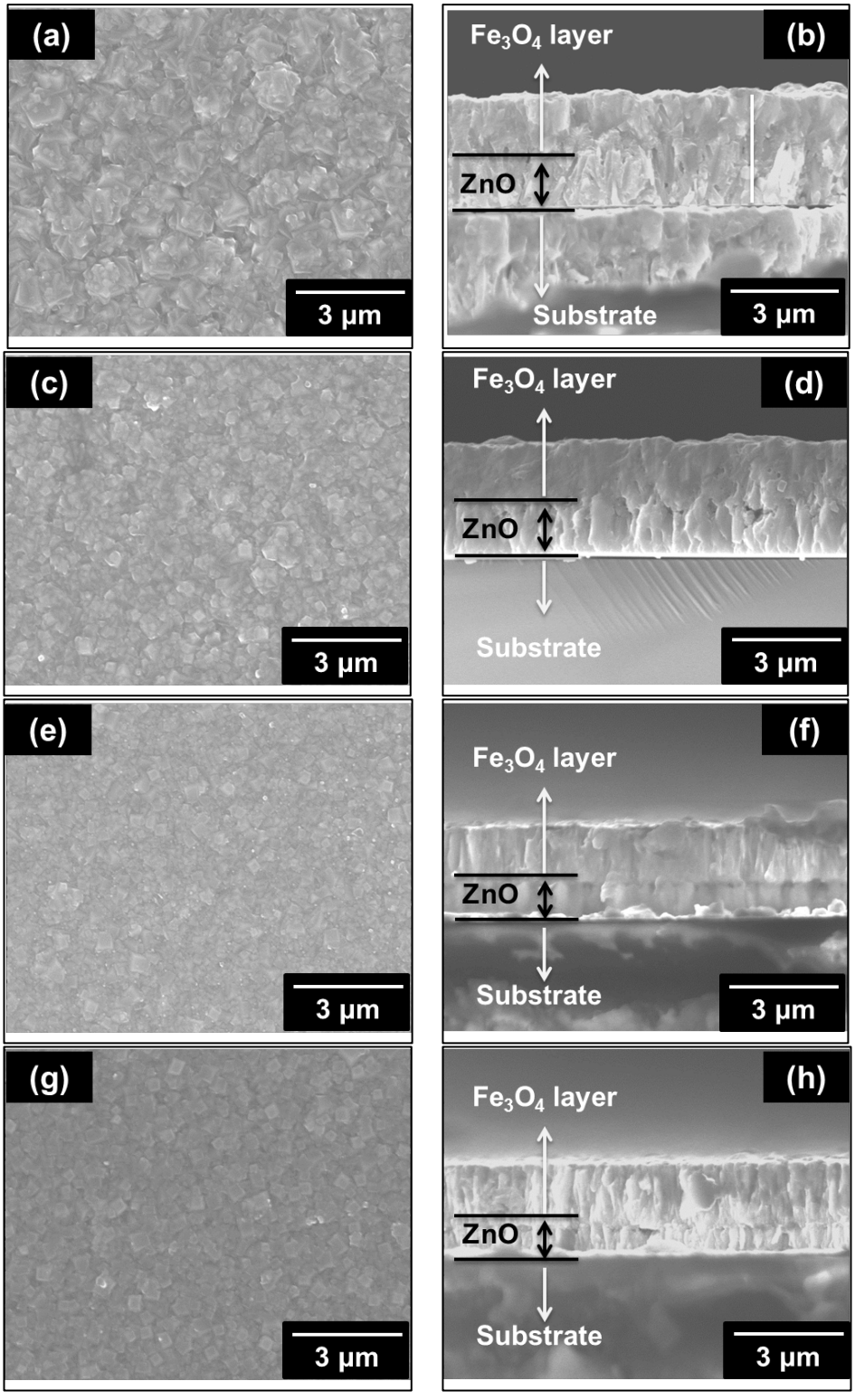

Figure 6-12 SEM image of as-prepared Fe_3O_4 / ZnO films at various citrate concentration; Surface morphology (a) none, (c) 0.05 mM, (e) 5 mM, and (g) 10mM, Cross-sectional image (a) none, (c) 0.05 mM, (e) 5 mM, and (g) 10mM.

substrate temperature without post-annealing process. It suggests that solution process is also one of the possible ways for applying to TMR (tunneling magnetoresistive) and GMR (giant magnetoresistive) devices as a polarized spin injector.

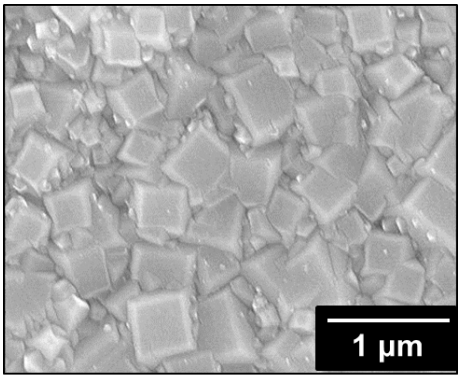

Figure 6-13 Surface morphology of as-prepared Fe_3O_4 / ZnO films at citarate concentration of 10 mM.

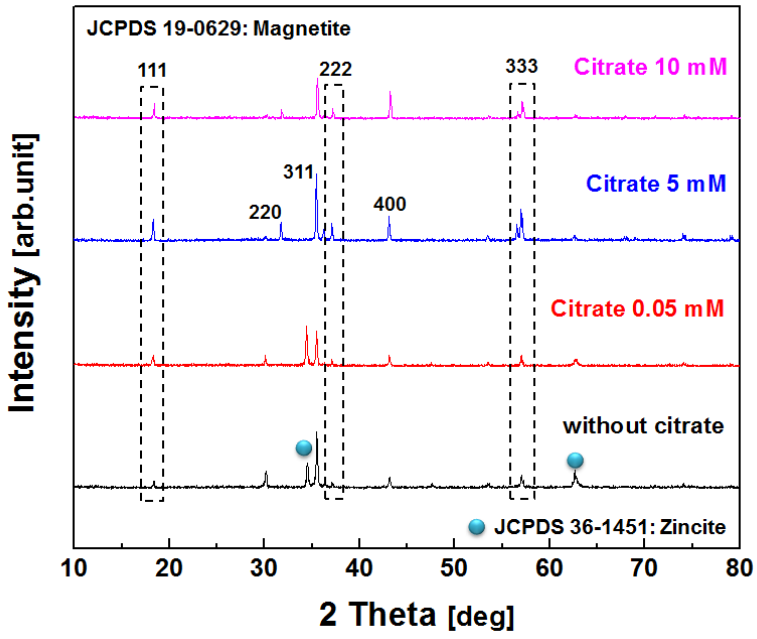

Figure 6-14 XRD patterns of as-prepared Fe_3O_4 / ZnO films.

6.4 Summary

In this study, heterostructured α-Fe_2O_3 / ZnO and Fe_3O_4 / ZnO films were fabricated by spin-spray method and their structural, crystallographic, and electrical properties were investigated.

First, α-Fe_2O_3 and ZnO films and the double-layered of them were deposited on glass substrate As-deposited ZnO films showed high transmittance above 80 % and improved crystallinity was also confirmed through the decreasing of FWHM values from 0.18 to 0.16^{o}. The lowest resistivity of 1.8 x 10^{-2} Ω·cm was attained at citrate concentration of 2 mM after UV irradiation with BLB lamp. Heterostructured α-Fe_2O_3 / ZnO double-layered films were fabricated by deposition of α-Fe_2O_3 layer on ZnO layer. Formation of Heterostructured α-Fe_2O_3 / ZnO films were verified by XRD, and dense surface properties confirmed by SEM. From these results, we could confirm the successive deposition of ZnO and α-Fe_2O_3 layers are possible by solution method.

And Fe_3O_4 and ZnO films and the double-layered of them were deposited on glass substrate. Surface morphologies of as-deposited ZnO were changed by adding citrate ion in reaction solution, and ZnO had dense structure at above 5 mM of citrate concentration. Transmittance was also increased to above 80 % with changing surface morphology and, the lowest resistivity was 1.6 x 10^{-2} Ω·cm at 5mM. In case of Fe_3O_4/ZnO film, Fe_3O_4 film had preferential orientation along the (nnn) plane, while other peaks which identified Fe_3O_4 were also confirmed. The SEM images for as-fabricated Fe_3O_4/ZnO film revealed that formed crystallites had cubic phase.

Reference

1. K. Song, Q. Wang, Q. Liu, H. Zhang, and Y. Cheng, Sensors 11 (2011) 485.
2. F. Qin, Y. Nozaki, and K. Matsuyama, J. Mag. Mag. Mater. 272-276 (2004) e1835.
3. X. Wu, and S. B. Kim, Electrochem. Solid-State Lett. 2 (1999) 184.
4. F. L. Souza, K. P. Lopes, E. Longo, and E. R. Leite, Phys. Chem. Chem. Phys. 11 (2009).
5. G. Rahman, and O. S. Joo, Int. J. Hydro. Ener. 37 (2012) 13989.
6. Y. S. Hu, A. Kleimna-Shwarsctein, A. J. Forman, D. Hazen, J. N. Park, and E. W. McFarland, Chem. Mater. 20 (2008) 3803.
7. C. D. Bohn, A. K. Agrawal, E. C. Walter, M. D. Vaudin, A. A. Herzing, P. M. Haney, A. A. Talin, and V. A. Szalai, J. Phys. Chem. C 116 (2012) 15290.
8. A. Nielsen, A. Brandlmaier, M. Althammer, W. Kaiser, M. Opel, J. Simon, W. Mader, S. T. B. Goennenwein, and R. Gross, Appl. Phys. Lett. 93 (2008) 162510.
9. H. Xiang, F. Shi, M. S. Rzchowski, P. M. Voyles, and Y. A. Chang, Appl. Phys. Lett. 97 (2010) 092508.
10. P. Li, B. L. Guo, and H. L. Bai, J. Appl. Phys. 109 (2011) 013908.
11. M. Paul, D. Kufer, A. Müller, S. Brück, E. Goering, M. Kamp, J. Verbeeck, H. Tian, G. Van Tendeloo, N. J. C. Ingle, M. Sing, and R. Claessen, Appl. Phys. Lett. 98 (2011) 012512.
12. P. Li, C. Jin, W. Mi, and H. Bai, Chin. Phys. B 22 (2013) 047505.
13. H. su, J. Dai, Y. Liao, Y. Wu, J. C. A. Huang, and C. Lee, Thin Solid Films, 518 (2010) 7275.
14. H. Wagata, N. Ohashi, T. Taniguchi, A. K. Subramani, K. Katsumata, K. Okada, and N. Matsushita, Cryst. Growth Des. 10 (2010) 3502.
15. H. Wagata, N. Ohashi, T. Taniguchi, K. Katsumata, K. Okada, and N. Matsushita, Cryst. Growth Des. 10 (2010) 4968.

16. J. S. Hong, H. Wagata, K. Katsumata, K. Okada, and N. Matsushita, Jpn. J. Appl. Phys. 52 (2013) 110108
17. H. Wagata, N. Ohashi, K. Katsumata, H. Seagawa, Y. Wada, H. Yoshikawa, S. Ueda, K. Okada, and N. Matsushita, J. Mater. Chem. 22 (2012) 20706.

Chapter 7

Future Prospects

ZnO is promising material to apply to various electronic devices, and aqueous solution process named spin-spray method is the most simple and cost effective method for fabricating ZnO films.

• Spin-spray method

It is well known that solution process is more cost-effective and simpler than dry processes. And among the solution processes, spin-spray is the most unique equipment for fabricating film due to their advantages such as low substrate temperature, crystallization without post-annealing, and good adhesion without seed layer [1-3]. And spin-spray method has a wide range of application because it can fabricate the various kinds of film such as ZnO, Fe_3O_4, and α-Fe_2O_3 film [4-7]. These films can be applied to electronic devices and electromagnetic devices.

Additionally, other materials having photocatalytic property such as titanium dioxide (TiO_2) also can be fabricated by spin-spray method [8-10]. As-fabricated film by spin-spray method uses photocatalytic reaction to decompose the organic substance in the film, and it causes the positive result such as high conductivity (ZnO film) [11-12]. Thus, TiO_2 film could be fabricated by spin-spray method, and it can be applied to self-cleaning glass.

• ZnO films having various structures

As-fabricated ZnO films by spin-spray method have various forms such as rod array, flower-like, and sphere-like structure. They can be applying to dye-sensitized solar cell as a

photoelectrode due to their high specific surface area. And ZnO films having dense structure and high transparency can be easily obtained by adding citrate ions in reaction solution. These films can be applying to displays, OLEDs, and thin film transistor as a transparent electrode.

• Transparent conductive ZnO films

ZnO films having high conductivity are achieved by UV irradiation and hydrogen treatment. These films indicated n-type semiconductor property with high carrier concentration (10^{19}~10^{20} cm^{-3}). These films can be used as a transparent electrode to various applications such as OLED and solar cell. Additionally, ZnO films having amorphous structure can be simply fabricated by spin-spray method, and reported ZnO film having high mobility with p-type semiconductor property [13-15]. These films can be used to thin film transistor as a channel layer. Additionally, these two types ZnO films are can be applying to p-n junction diodes. Generally, the fabrication process of p-n junction diodes by dry process is very complicated. In contrast, n-type and p-type ZnO films can be easily obtained by spin-spray method. It means that p-n junction diodes can be fabricated by one step process using spin-spray method.

• ZnO film on flexible substrate

Rod array structure and transparent conductive ZnO films on flexible substrates were successfully deposited on PES substrate. These films can be applying to flexible devices such as e-paper, wearable devices.

And universal solution process requires high substrate and post-annealing temperature, and it became the problem in fabrication of flexible devices. However, spin-spray method is

low temperature process, and it means that spin-spray method can be one of the methods for fabricating flexible devices. Additionally, spray process is applicable to mass production by roll-to-roll (R2R). Generally, R2R has been used in dry process for fabricating film on flexible substrates, while it is unsuitable for conventional solution process due to the post-annealing process for crystallization. However, spray process can fabricate the crystallized ZnO film on flexible substrate without post-annealing process, and it is the possible reason for mass production by spin-spray method. As a result, it is thought that spray process with R2R can be achieved the cost reduction for fabricating devices.

Reference

1. H. Wagata, N. Ohashi, T. Taniguchi, A. K. Subramani, K. Katsumata, K. Okada, and N. Matsushita, Cryst. Growth Des. 10 (2010) 3502.
2. H. Wagata, N. Ohashi, T. Taniguchi, K. Katsumata, K. Okada, and N. Matsushita, Cryst. Growth Des. 10 (2010) 4968.
3. H. Wagata, K. Katsumata, N. Ohashi, M. Sakai, A. Nakajima, A. Fujishima, K. Okada, and N. Matsushita, Photochem. Photobio. 87 (2011) 1009.
4. J. Miyasaka, M. Tada, M. Abe, and N. Matsushita, J. Appl. Phys. 99 (2006) 08M916.
5. Y. Xing, J. Myers, O. Obi, N. X. Sun, and Y. Zhang, J. Appl. Phys. 111 (2012) 707A512.
6. J. S. Hong, H. Wagata, K. Katsumata, K. Okada, and N. Matsushita, J. Jpn. Soc. Powder and Powder Metallurgy 61 (2014) S324.
7. E. E. Carpenter, V. Cestone, G. Landry, and V. G. Harris, Chem. Mater. 15 (2003) 1235.
8. K. Hashimoto, H. Irie, and A. Fujishima, Jpn. J. Appl. Phys. 44 (2005) 8269.
9. K. Nakata, and A. Fujishima, J. Photochem. Photobio. 13 (2012) 169.
10. A. L. Lisebigler, G. Lu, and J. T. Yates, Chem. Rev. 95 (1995) 753.
11. J. S. Hong, H. Wagata, K. Katsumata, K. Okada, and N. Matsushita, Jpn. J. Appl. Phys. 52 (2013) 110108.
12. H. Wagata, N. Ohashi, K. Katsumata, H. Seagawa, Y. Wada, H. Yoshikawa, S. Ueda, K. Okada, and N. Matsushita, J. Mater. Chem. 22 (2012) 20706.
13. H. Hsieh, and C. Wu, Appl. Phys. Lett. 91 (2007) 013502.
14. B. Kumar, H. Gong, and R. Akkipeddi, J. Appl. Phys. 98 (2005) 073703.
15. C. Wang, X. Liu, X. Xiao, Y. Liu, W. Chen, J. Li, G. Shen, and L. Liao, IEEE Electron Device Lett. 34 (2013) 72

Chapter 8

Conclusion

In this thesis, solution-processed ZnO films were discussed.

First, the spin-spray method is attractive fabrication method for preparing ZnO film. It is environmentally friendly, and construction is simple. The spin-spray method can fabricate the high quality ZnO film at low substrate temperature below 100^{o}C. Furthermore, deposition process is also very simple. Two kinds of solution such as source and reaction solution are sprayed on rotating and heated substrates, and then film is formed on substrate surface. Although, deposition process is simple, however, as-deposited films by spin-spray method have high transparency and crystallized without seed layer.

ZnO films which has various forms such as rod array, dense, and flower-like structure were obtained by change of solution conditions. Rod array structure changed to dense structure by adding trisodium citrate in reaction solution, and flower-like structured ZnO film was simply obtained by change of *p*H adjusted from ammonia solution to sodium hydroxide. These various 1 dimensional and dense structures of ZnO films have various functional properties and they are expected to apply for various applications such as nano-generators, sensors, organic light emitting diodes, thin film transistors and solar cells.

High carrier concentration (~10^{20} cm^{-3}) of ZnO films were achieved by UV irradiation. Under UV irradiation, organic substance in the ZnO films is decomposed by photocatalytic reaction of ZnO, C, and /or H doping into ZnO. As a result, many carriers are generated by ions doping. Additionally, it is also confirmed that UV condition having wide wavelength is more effective to decompose the organic substance in the film, and it resulted lower resistivity.

Effect of thermal treatment on solution-processed ZnO films was also investigated, in this thesis. Because, ZnO films fabricated spin-spray method contains organic substances in the film, and they may affect to their properties such as conductivity and crystallinity. Thermally treated (at 100^{o}C) and UV irradiated ZnO films had the lowest resistivity of 1.6 x 10^{-2} Ω·cm with high carrier concentration and relatively higher mobility than other samples. However, in case of mobility, it is still too lower than that of films deposited by sputtering method. To improve the electron mobility, hydrogen treatment was used before UV irradiation. Hydrogen treated and UV irradiated ZnO film has the lowest resistivity of 1.8 × 10^{-3} Ω·cm with high carrier concentration (1.5 × 10^{20} cm^{-3}), in case of moility, it increased 10 times from 1.2 to 11.2 $cm^{2}V^{-1}s^{-1}$. Reasons for low resistivity are estimated two kinds of phenomenon. First is generating carrier by UV irradiation. And second is decomposition of negatively charged oxygen species on grain boundary by hydrogen treatment. This result suppose that pure ZnO film without metal ions doping such as aluminum and gallium can be applied to various applications as a transparent electrode due to their high conductivity.

Finally, ZnO films were deposited by spin-spray method on flexible substrates at low substrate temperature of 85^{o}C. As I mentioned before, flexible devices are receiving attention as a future technology, and simple and low temperature process for film fabrication on flexile substrates are intensively studied. However, solution processes generally use the annealing process for crystallization and high substrate temperature is required for removing organic substance in the film. On the other hand, spin-spray method is solution process however it can fabricate crystallized ZnO film without post-annealing process at low substrate temperature. ZnO films on flexible substrate which has low resistivity and high transmittance was obtained by spin-spray method, it is one of the good examples for using the advantage of spin-spray method.

List of Publications

Publication related to this thesis

1 **JeongSoo Hong**, Hajime Wagata, Ken-ichi Katsumata, Kiyoshi Okada, and Nobuhiro Matsushita
"Effects of Thermal Treatment on Crystallographic and Electrical Properties of Transparent Conductive ZnO Films Deposited by Spin-Spray Method"
Japanese Journal of Applied Physics-Selected Topics in Applied physics 52 **(2013)** 110108

2 **JeongSoo Hong**, Hajime Wagata, Ken-ichi Katsumata, Kiyoshi Okada, and Nobuhiro Matsushita
"Fabrication of Heterostructured α-Fe_2O_3 / ZnO Film for Photoelectrode by Aqueous Solution Process"
Journal of the Japan Society of Powder and Powder Metallurgy 61 **(2014)** S324

Other publication

1 **JeongSoo Hong**, Nobuhiro Matsushita, KyungHwan Kim
"Investigation of the effects of oxygen gas on properties of GAZO thin films fabricated by facing targets sputtering system"
Semiconductor Science and Technology 29 **(2014)** 075007

2 **JeongSoo Hong**, Nobuhiro Matsushita, KyungHwan Kim
"Effect of dopants and thermal treatment on properties of Ga-Al-ZnO thin films fabricated by hetero targets sputtering system"
Thin Solid Films 531 **(2013)** 238

3 **JeongSoo Hong**, SangMo Kim, KyungHwan Kim
"Preparation of SiO_2 Passivation Thin Film for Improved the Organic Light-Emitting Device Life Time"
Japanese Journal of Applied Physics 50 **(2011)** 08KE02-1

4 **JeongSoo Hong**, KyungWook Jang, YongSeo Park, HyungWook Choi, KyungHwan Kim
"Preparation of ZnO based thin films for OLED anode by facing targets sputtering system"
Molecular Crystals and Liquid Crystals 538 **(2011)** 103

5 **JeongSoo Hong**, KyungHwan Kim
"Characteristic of Al-In-Sn-ZnO Thin Film Prepared by FTS System with Hetero Targets Sputtering System"
Transactions on Electrical and Electronic Materials 12 **(2011)** 76

6 **JeongSoo Hong**, YongSeo Park, KyungHwan Kim
"Preparation of Transparent Conductive Oxide cathode for Top-Emission Organic Light-Emitting Device by FTS system and RF system"
Journal of the Semiconductor & Display Technology 9 **(2010)** 23

7 **JeongSoo Hong**, SangMo Kim, SangJoon Park, HyungWook Choi, KyungHwan Kim
"Preparation of In_2O_3-ZnO (IZO) Thin Film on Glass Substrate for Organic Light Emitting Device (OLED)"
Molecular Crystals and Liquid Crystals 520 **(2010)** 19

Presentation at International Conference

1 (Poster) **JeongSoo Hong**, Hajime Wagata, Naoki Ohashi, Ken-ichi Katsumata, Kiyoshi Okada, and Nobuhiro Matsushita
"Effects of UV illumination and thermal treatment in hydrogen on electrical conductivity of solution processed ZnO film"
Materials Research Society (MRS) 2014 Spring Meeting, San-francisco, USA, (2014)

2 (Poster) **JeongSoo Hong**, Hajime Wagata, Naoki Ohashi, Ken-ichi Katsumata, Kiyoshi Okada, and Nobuhiro Matsushita
"High Conductivity of Thermally-Treated ZnO Films at Various Gas Atmospheres"
The 30th Japan-Korea International Seminar on Ceramics, Kitakyushu, Japan, (2013)

3 (Poster) **JeongSoo Hong**, Nobuhiro Matsushita, and KyungHwan Kim
"Influence of Oxygen on the Properties of Transparent Ga-Al-ZnO Thin Film"
2013 The 2nd International Conference on Advanced Electromaterials, Jeju, Korea, (2013)

4 (Poster) **JeongSoo Hong**, Hajime Wagata, Ken-ichi Katsumata, Kiyoshi Okada, and Nobuhiro Matsushita
"Solution-Processed ZnO Films on Flexible Substrate"
European Materials Research Society (EMRS) 2013 Fall Meeting, Warsaw, Poland, (2013)

5 (Poster) **JeongSoo Hong**, Hajime Wagata, Naoki Ohashi, Ken-ichi Katsumata, Kiyoshi Okada, and Nobuhiro Matsushita
"Influence of Thermal Treatment on Crystallographic and Electrical Properties of Solution-Processed ZnO Films"
7th International Conference on Science and Technology of Advanced Ceramics (STAC-7), Yokohama, Japan, (2013)

6 (Poster) **JeongSoo Hong**, Hajime Wagata, Naoki Ohashi, Ken-ichi Katsumata, Kiyoshi Okada, and Nobuhiro Matsushita
"Fabrication of Heterostructured a-Fe_2O_3/ZnO Film for Photoelectrode by Aqueous Solution Process"
The 11th International Conference on Ferrite (ICF 11), Okinawa, Japan, (2013)

7 (Poster) **JeongSoo Hong**, Hajime Wagata, Naoki Ohashi, Ken-ichi Katsumata, Kiyoshi Okada, and Nobuhiro Matsushita
"The Crystallographic Property of Fe_3O_4 Layer Deposited Successively on ZnO Layer by Spin-Spray Method"
The 11th International Conference on Ferrite (ICF 11), Okinawa, Japan, (2013)

8 (Poster) **JeongSoo Hong**, Hajime Wagata, Naoki Ohashi, Ken-ichi Katsumata, Kiyoshi Okada, and Nobuhiro Matsushita
"Fabrication of 1 Dimension Ga doped ZnO Films by Aqueous Solution Process"
The 11th International Conference on Ferrite (ICF 11), Okinawa, Japan, (2013)

9 (Poster) **JeongSoo Hong**, Hajime Wagata, Naoki Ohashi, Ken-ichi Katsumata, Kiyoshi Okada, and Nobuhiro Matsushita
"Electrical, Optical and Structural Properties of Solution Processed ZnO Films with Various UV Illumination Condition"
The 11th International Conference on Ferrite (ICF 11), Okinawa, Japan, (2013)

10 (Poster) **JeongSoo Hong**, Hajime Wagata, Naoki Ohashi, Ken-ichi Katsumata, Kiyoshi Okada, and Nobuhiro Matsushita
"Al doped ZnO Films Fabricated by Aqueous Solution Process"
Materials Research Society (MRS) 2013 Fall Meeting, Boston, USA, (2012)

11 (Poster) **JeongSoo Hong**, Nobuhiro Matsushita, and KyungHwan Kim
"Flower-like ZnO Fabricated on Spin-Sprayed Film"
International Union of Materials Research Societies-International Conference on Electronic Materials (IUMRS-ICEM) 2012, Yokohama, Japan, (2012)

12 (Poster) **JeongSoo Hong**, Hajime Wagata, Ken-ichi Katsumata, Kiyoshi Okada, and Nobuhiro Matsushita
"Comparison of Crystallographic and Electrical Properties of ZnO Films Fabricated by Dry and Wet Process"
4th International Congress on ceramic (ICC 4), Chicago, USA, (2012)

13 (Poster) **JeongSoo Hong**, Nobuhiro Matsushita, HyungWook choi, and KyungHwan Kim
"Effect of Dopants and Thermal Treatment on Properties of Ga-Al-ZnO Thin Films Fabricated by Hetero Targets Sputtering System"
39th International Conference on Metallugical coating and thin films (ICMCTF), San-diego, USA, (2012)

14 (Oral) **JeongSoo Hong**, Hajime Wagata, Naoki Ohashi, Ken-ichi Katsumata, Kiyoshi Okada, and Nobuhiro Matsushita
"Transparent ZnO Films Fabricated by Solution Process Spin-Spray at Different pH"
Materials Research Society (MRS) 2012 Spring Meeting, San-francisco, USA, (2012)

15 (Poster) **JeongSoo Hong**, Hajime Wagata, Naoki Ohashi, Ken-ichi Katsumata, Kiyoshi Okada, and Nobuhiro Matsushita
"Effect of Citrate Ion to Obtain Flat ZnO Film in Spin-Spray Process"
The 12th International Symposium on Biomimetic Materials Processing, Nagoya, Japan

16 (Poster) **JeongSoo Hong**, and KyungHwan Kim
"Characteristics of GAZO Thin films Fabricated by Hetero Targets Sputtering System"
International Conference on Thin Films (ICTF) 2011, Kyoto, Japan, (2011)

17 (Poster) **JeongSoo Hong**, Hajime Wagata, Naoki Ohashi, Ken-ichi Katsumata, Kiyoshi Okada, and Nobuhiro Matsushita
"Fabrication of Transparent ZnO Film on PET Substrate by Spin-Spray Method"
International Conference on Thin Films (ICTF) 2011, Kyoto, Japan, (2011)

Presentation at Domestic Conference

1 (Oral) **JeongSoo Hong**, Hajime Wagata, Naoki Ohashi, Ken-ichi Katsumata, Kiyoshi Okada, and Nobuhiro Matsushita
"水溶液プロセスを用いて作製した酸化亜鉛膜の窒素雰囲気熱処理の影響"
2013 電気学会, Japan

2 (Poster) **JeongSoo Hong**, Hajime Wagata, Naoki Ohashi, Ken-ichi Katsumata, Kiyoshi Okada, and Nobuhiro Matsushita
"溶液プロセスによる透明 ZnO 膜の堆積と紫外線照射による導電性の変化"
団法人日本セラミックス協会 第 25 回秋季シンポジウム, Japan

3 (Oral) **JeongSoo Hong**, Hajime Wagata, Naoki Ohashi, Ken-ichi Katsumata, Kiyoshi Okada, and Nobuhiro Matsushita
"溶液プロセスによる 鉄酸化物 / ZnO 積層膜の作製"
2012 粉体粉末冶金協会, Japan

Honors and Awards

2013 Yamazaki Yohtaro Memorial Student Award
(The 11th International Conference on Ferrites)

Scholarship

2013 Kato Foundation for promotion of Science Scholarship